Landslide hydrology: the case of the pyroclastic slopes of Campania (Italy)

Roberto Greco roberto.greco@unicampania.it
Dipartimento di Ingegneria

28 Septmber 2023
iRALL School
Chengdu University of Technology

Università degli Studi della Campania *Luigi Vanvitelli*

Scuola Politecnica e delle Scienze di Base
Dipartimento di Ingegneria

Landslide hydrology

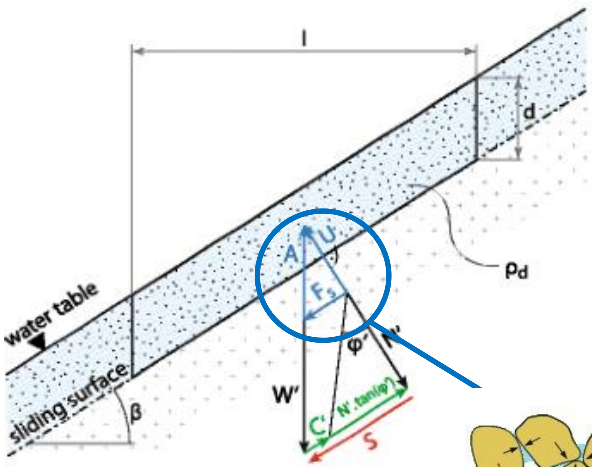

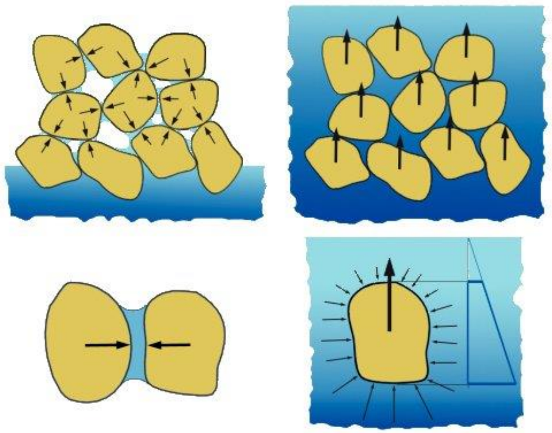

Capillary forces in unsaturated porous media

Water pressure forces in saturated porous media

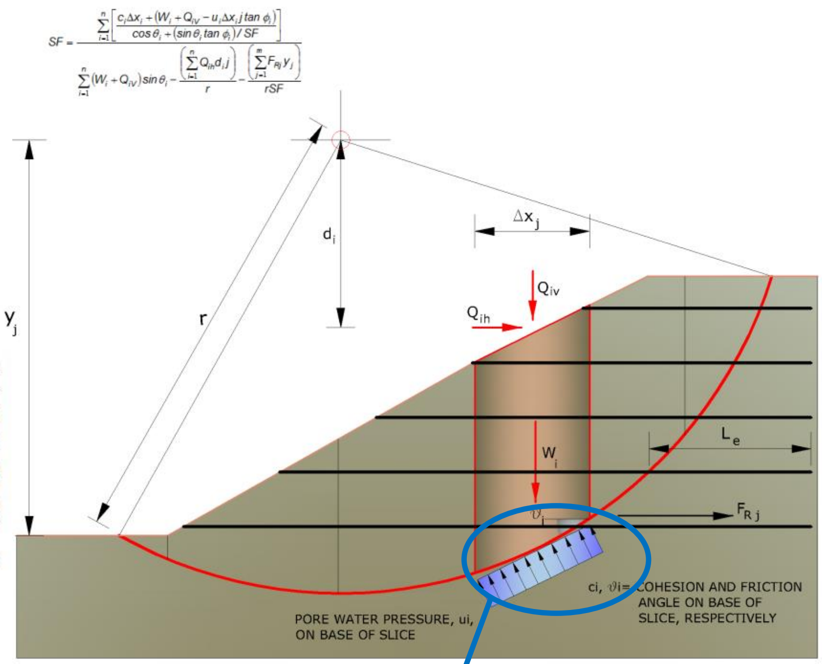

It is well-known that slope equilibrium is affected by water...

Slope Failure

Effects of a deep-seated landslide

Shallow landslide

Slope failure is a local mechanism caused by water accumulation.

But what is the origin of the water accumulating within the slope?

Landslide hydrology

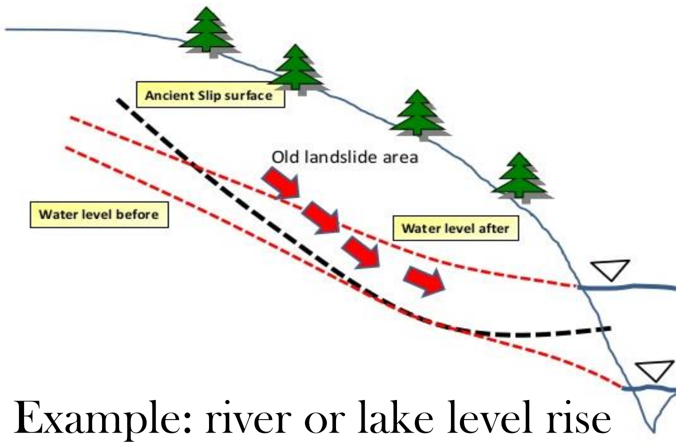

Example: river or lake level rise

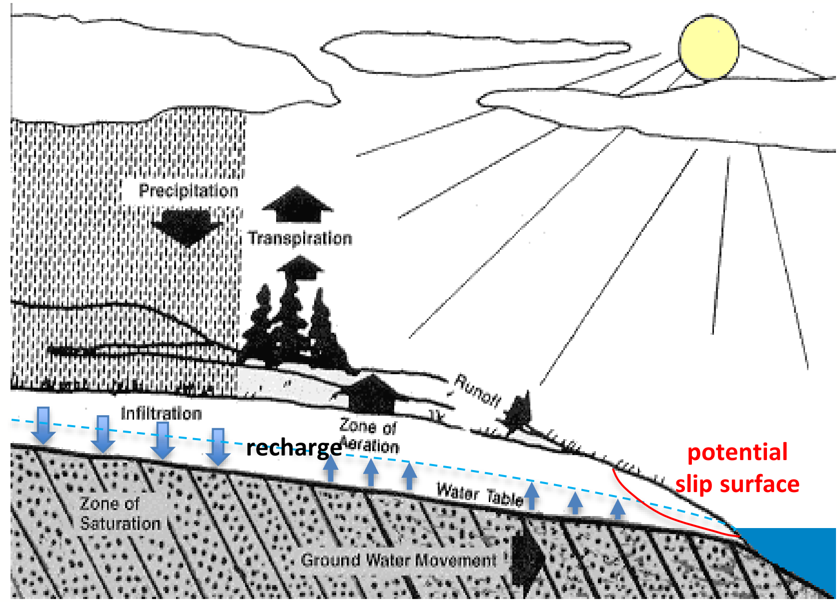

Example: regional groundwater recharge

Deep-seated landslides often activated (or reactivated) by groundwater level rise.

Groundwater level is often linked to processes occurring within a hydrological system larger than the landslide body.

It is important to understand where the water comes from…

Landslide hydrology

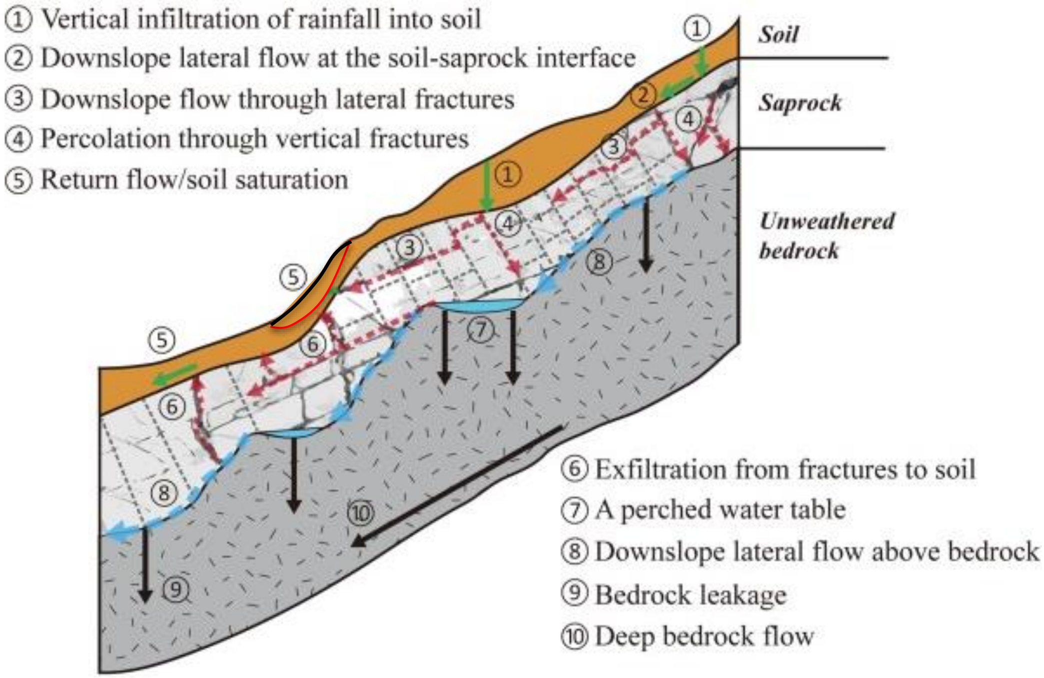

Examples: infiltration, evapotranspiration, interflow, percolation…

Shallow landslides are often triggered in initially unsaturated soil covers by reduction of soil suction. The potentially unstable soil mass belongs to a **hillslope.**

Many hydrological processes favor water exchange between the landslide body and the surrounding systems.

…and where the water goes to…

Slope water balance

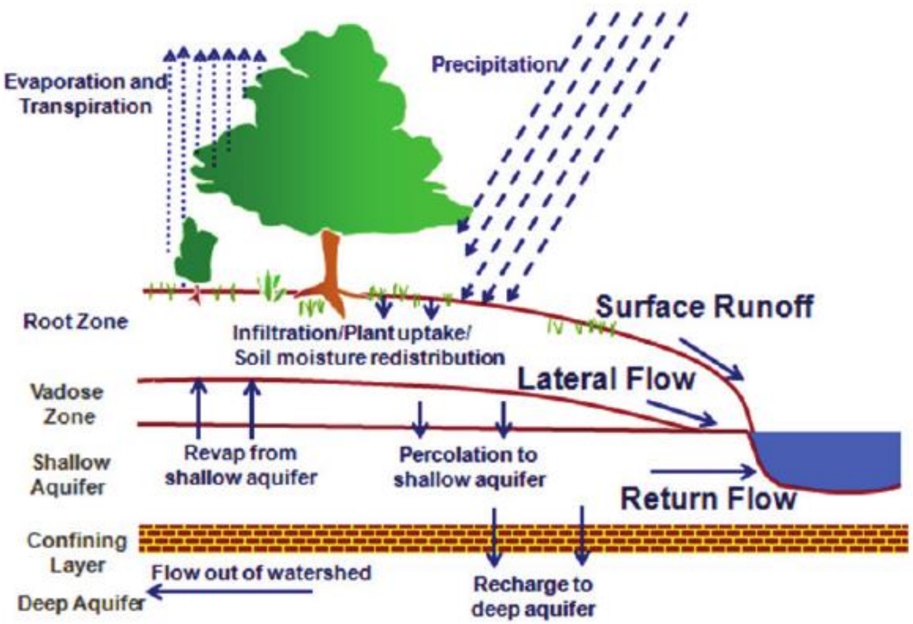

A slope is part of a larger hydrological system, and it **exchanges water** with it.

Water exchanges are controlled by **bottlenecks** along water flow paths, which manifest themselves in the **hydraulic conditions at the boundaries** of the landslide.

The boundary conditions are often **changing in time**, owing to dynamic hydrological processes in the larger system.

To predict the hydrological response of slopes to precipitation, the **water balance** should be assessed.

Filling, storing, draining

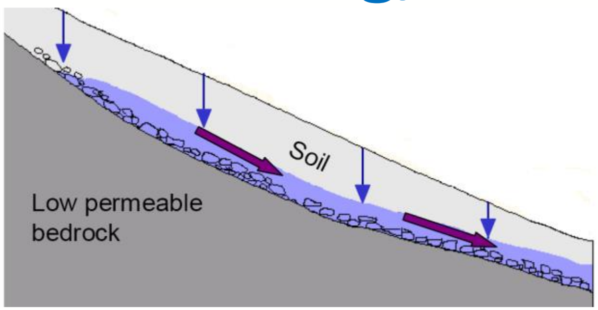

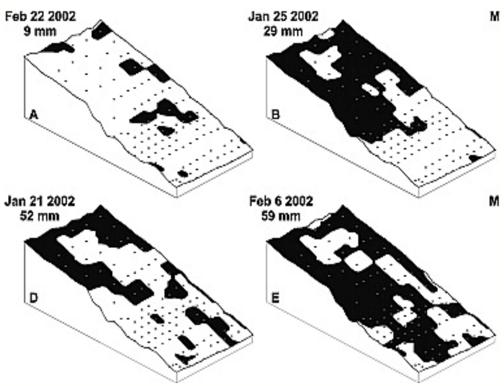

Tromp-van Meerveld and McDonnell, 2006

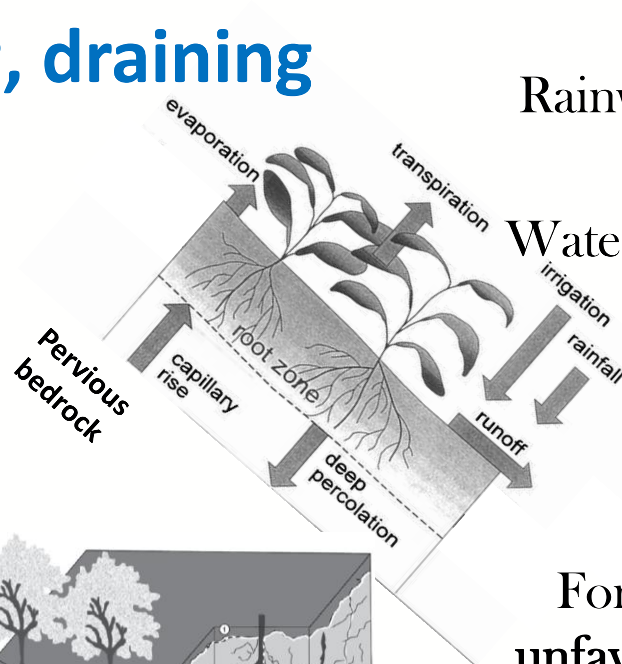

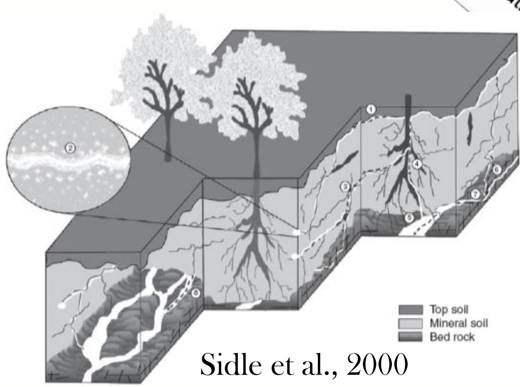

Sidle et al., 2000

Rainwater infiltration **fills** up the system.

Water **storage** is required for pore pressure increase.

Hillslopes develop (non-linear) **drainage** mechanisms.

For landslides to occur, an **unfavorable interplay** should exist between fast and/or prolonged infiltration, and a relatively slow drainage.

This is the timing of landslides, the overlay of hydrological processes with different timescales.

Causes and triggers of landslides

A **triggering event** is the last push for a slope to fail, and it activates a local failure mechanism.

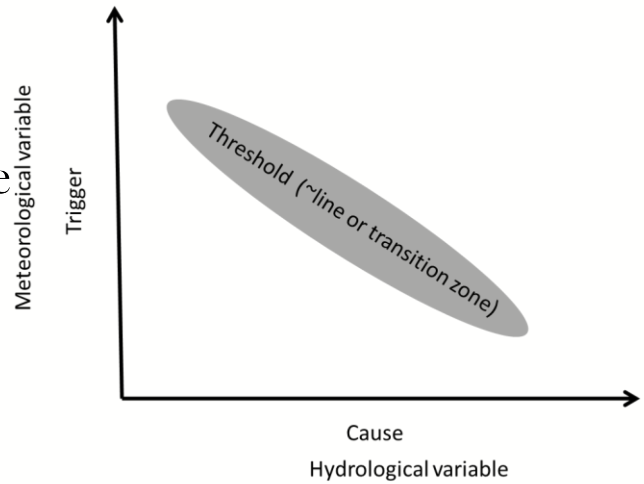

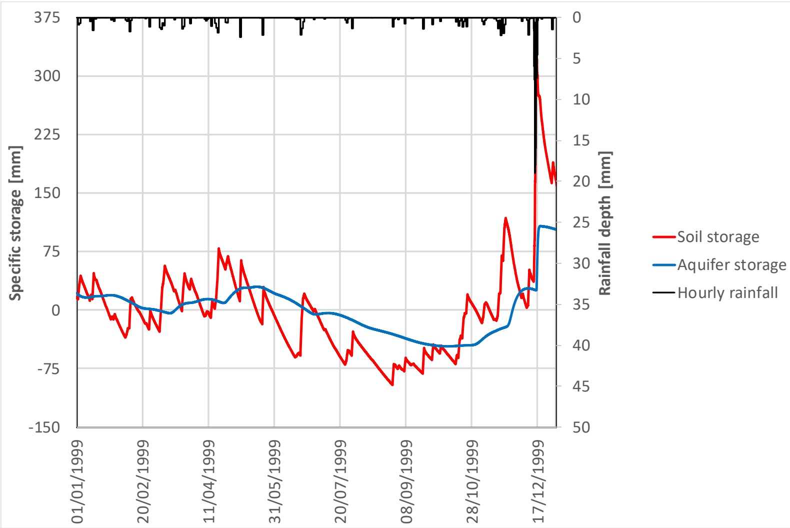

Causal factors depend on large scale (in time and space) processes, related to the hydrology of an area wider than the landslide.

Case-specific variables should be chosen as proxies of the hydrological causes as predisposing conditions to landslides.

The pyroclastic slopes of Campania (Italy)

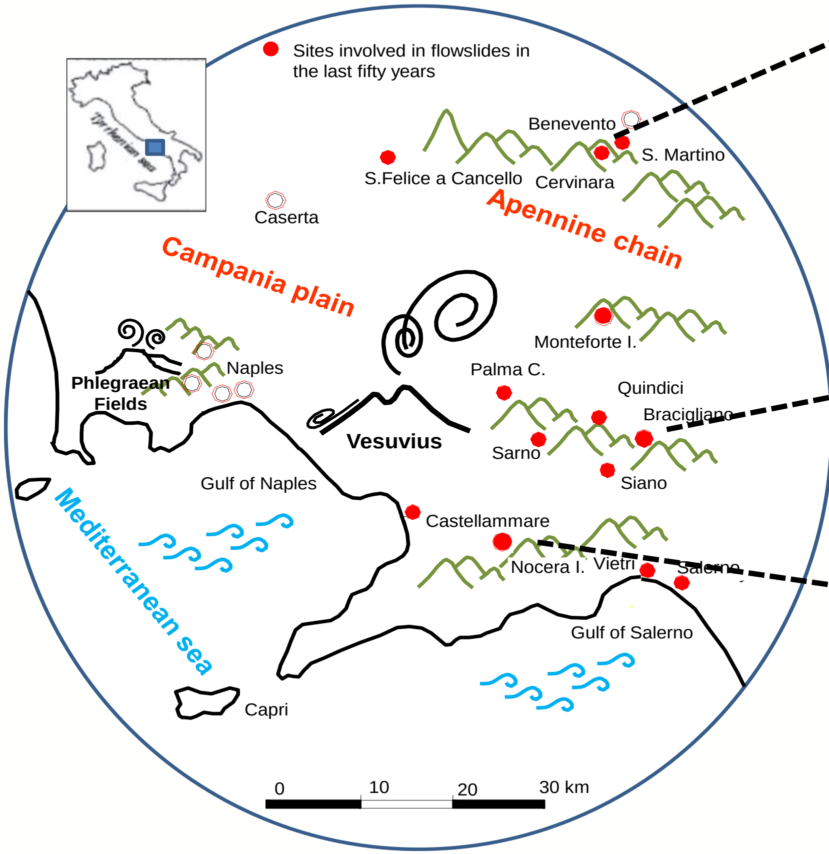

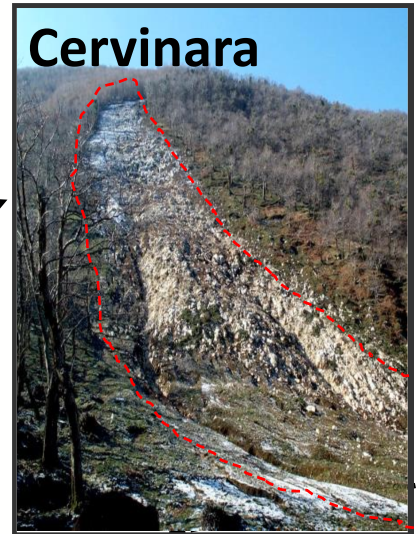

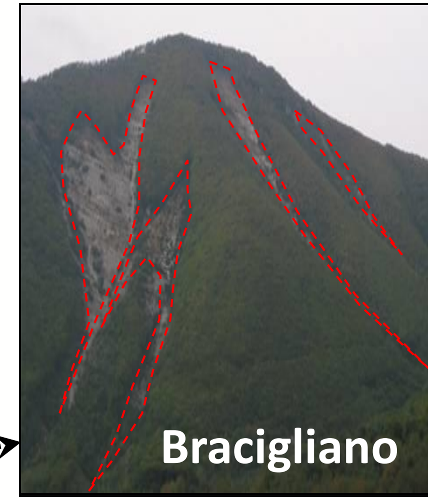

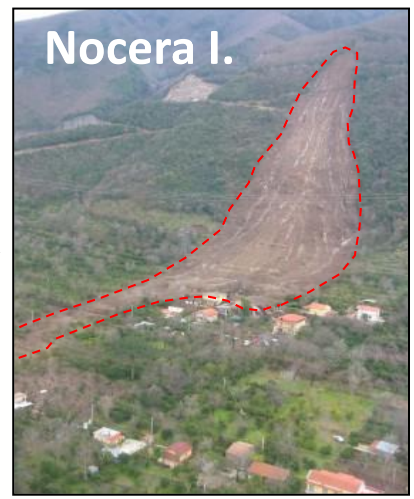

The pyroclastic slopes of Campania (Italy)

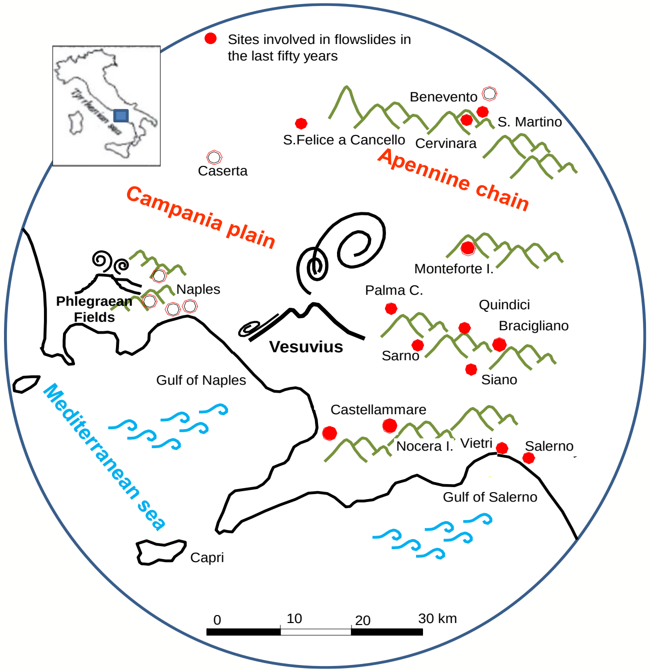

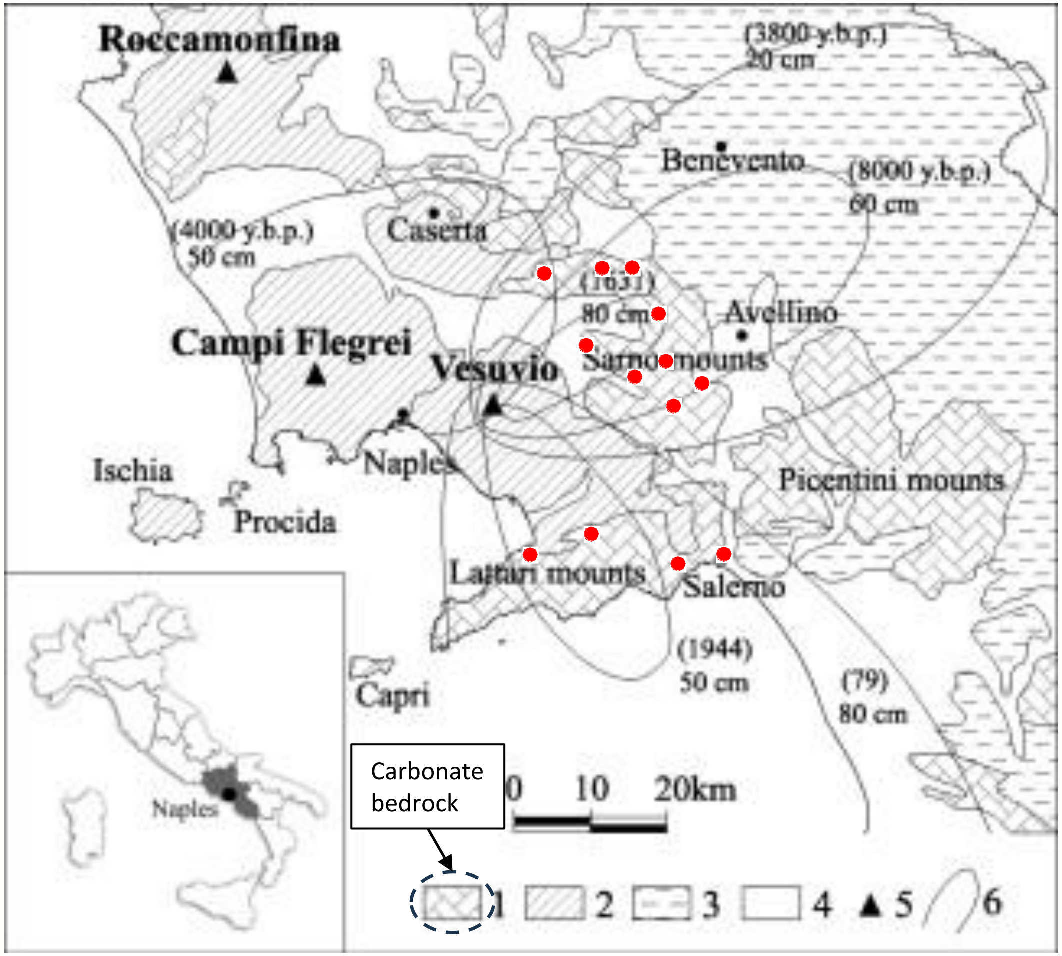

modified after Cascini et al., Eng Geol 2008

The pyroclastic slopes of Campania (Italy)

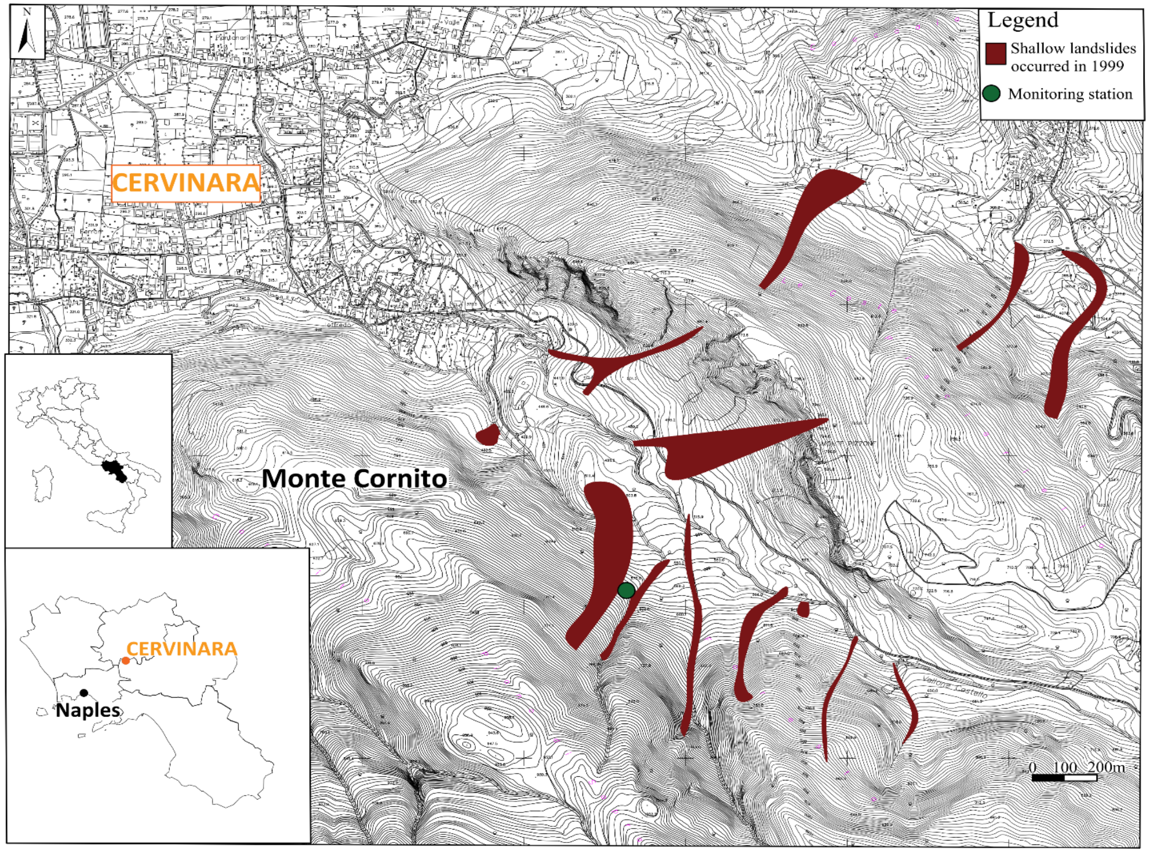

Cervinara – 16 December 1999

The pyroclastic slopes of Campania (Italy)

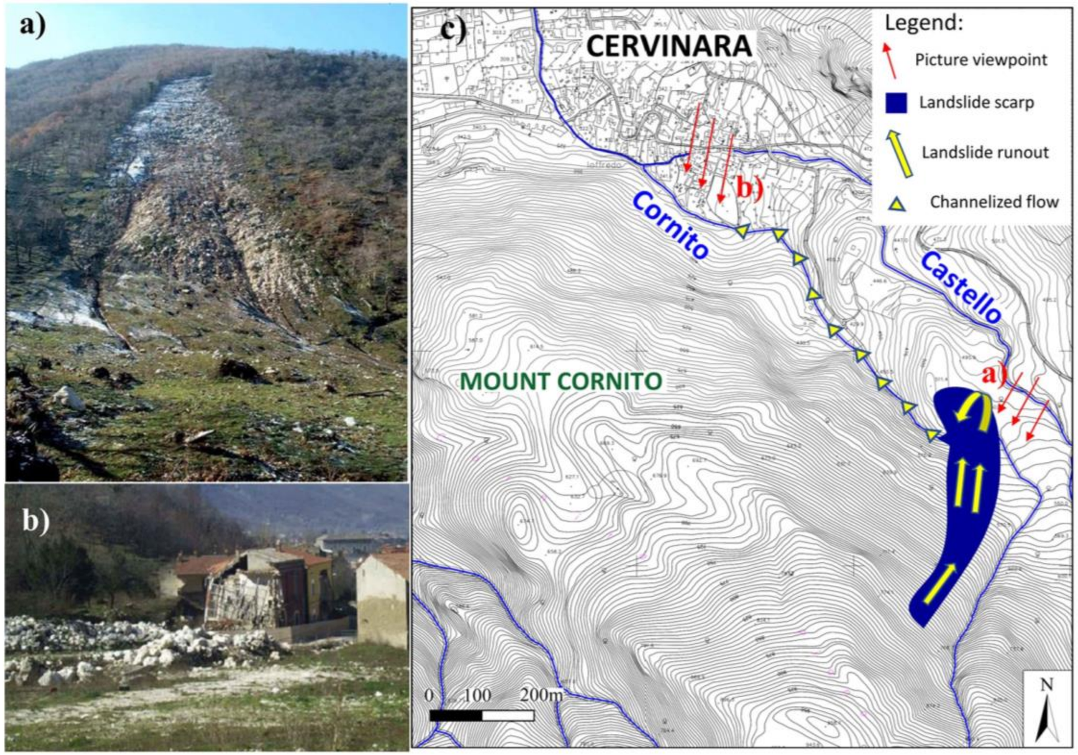

Cervinara – 16 December 1999

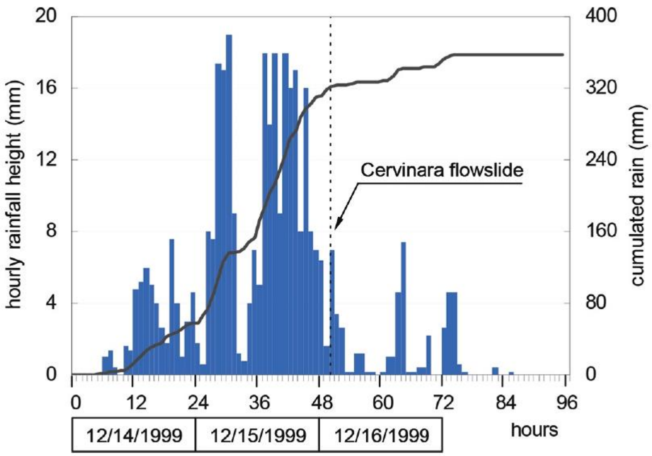

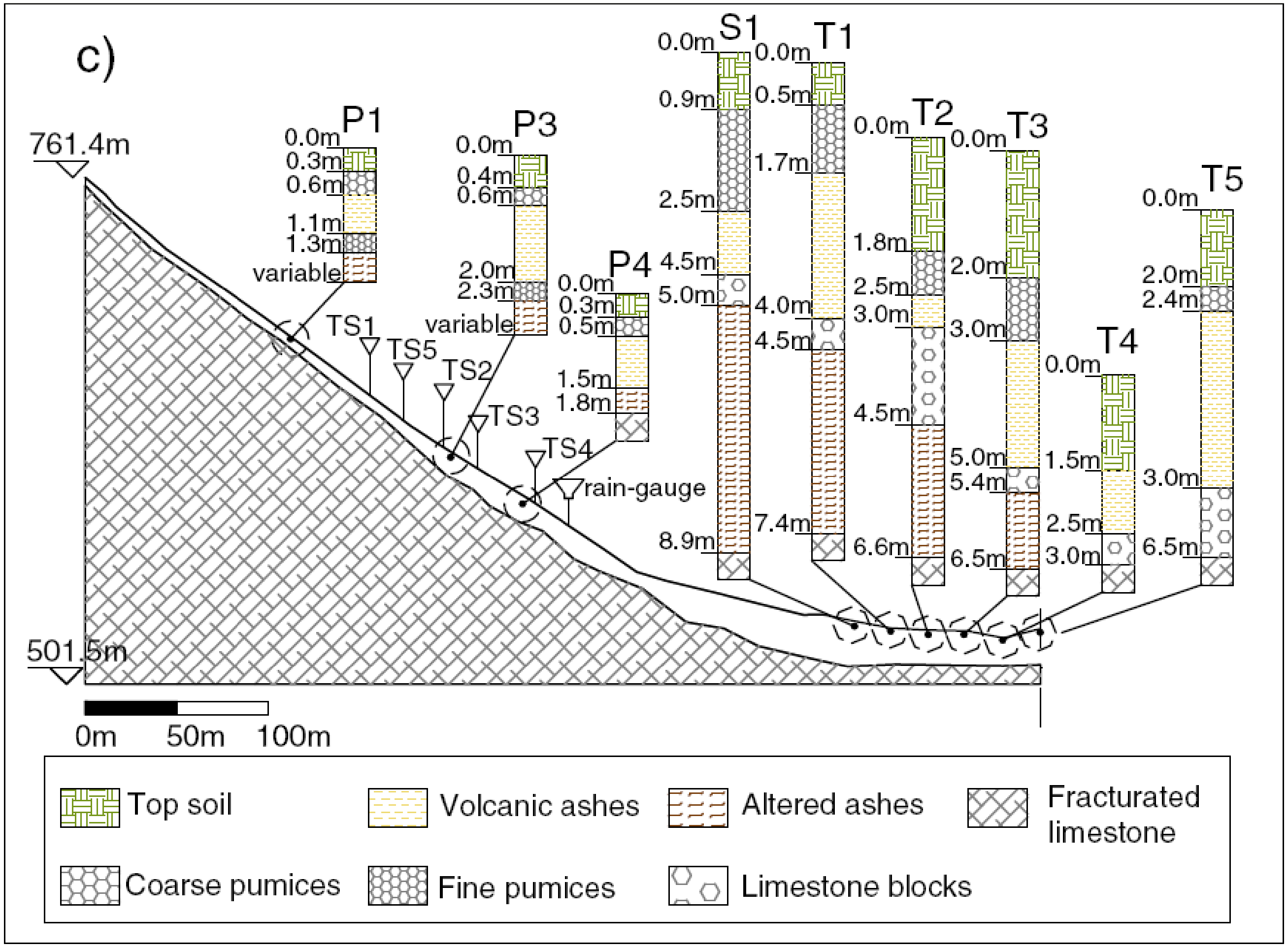

<u>Volcanoclastic soil deposit over fractured carbonate bedrock</u>

Damiano et al., Eng Geol 2013

Altered uppermost limestone bedrock: epikarst

Under pyroclastic soil covers in Mediterranean climate, highly conductive **epikarst**, with thickness up to 10m and high and diffuse porosity (up to 15%) has been observed.

In the upper part of the epikarst, fractures are often filled with the overlying soil.

Tree roots are able to penetrate the fractures of the epikarst.

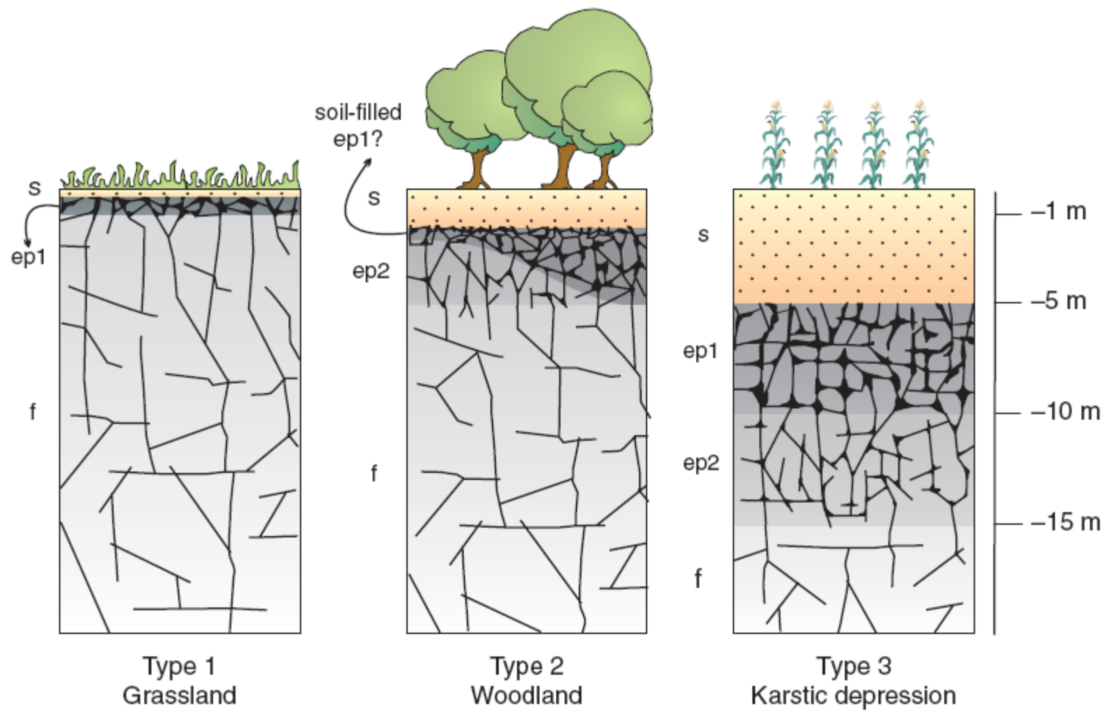

Celico et al., Terra Nova 2010

The hydrological role of epikarst

A shallow (some meters) layer of high porosity and permeability, temporarily storing water, contributing to evapotranspiration, slow deep percolation, and springs.

Often modeled as a dual or triple porosity medium.

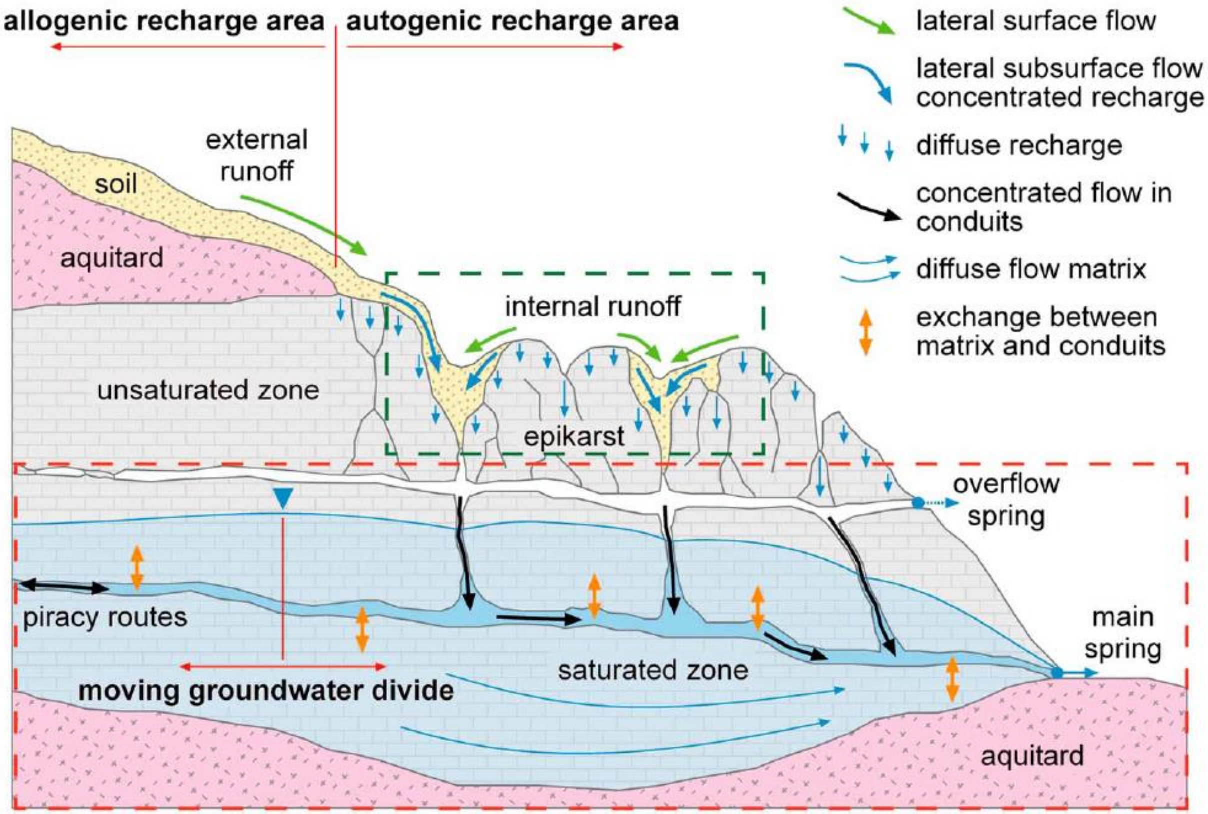

Hydraulic conductivity 10^{-7}–10^{-8} m/s (matrix pores) 10^{-3}–10^{-5} m/s (fractures).

Hartmann et al., Rev Geophys 2014

Groundwater recharge in karst aquifers of southern Apennines

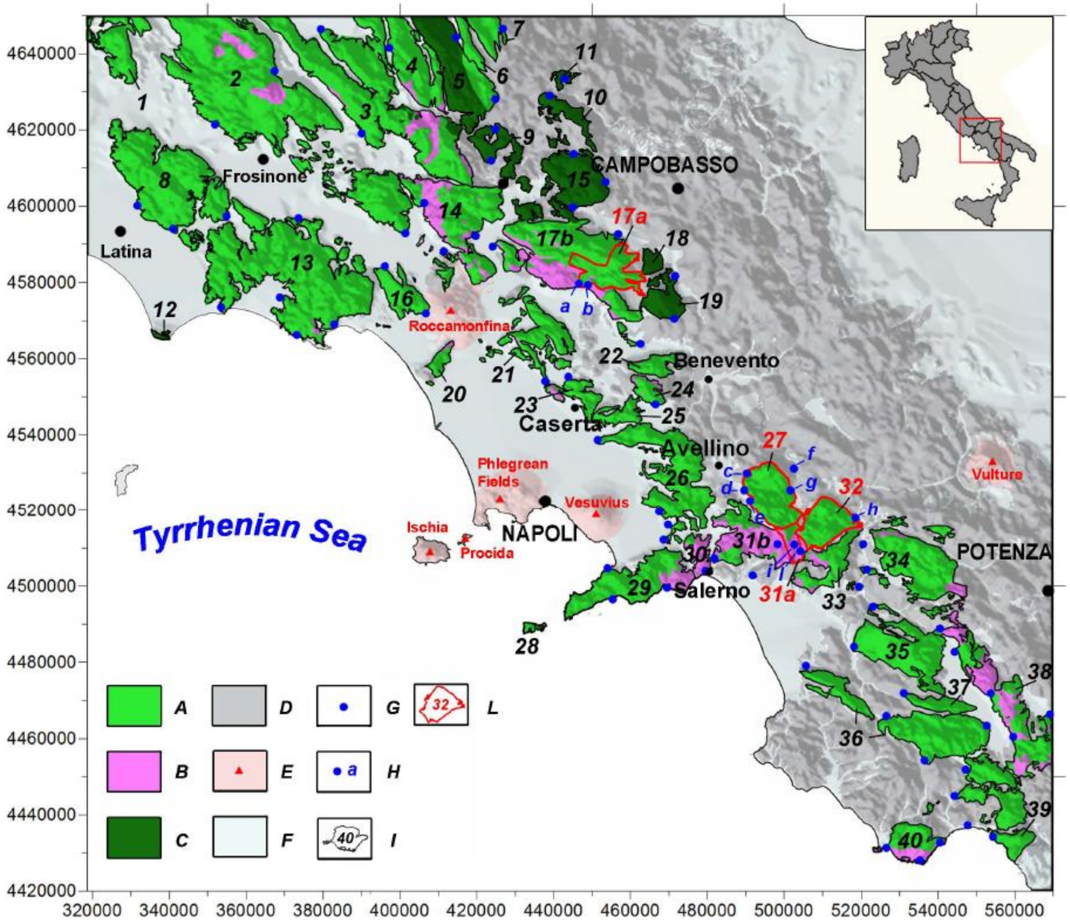

Up to 600mm yearly recharge

100-200mm in the area of Cervinara

21	Maggiore	63.5
22	Camposauro	27.4
23	Tifatini	29.2
24	Taburno	29.8
25	Durazzano	22.7
26	Avella	201.2
27	Terminio	167.4
28	Capri	2.7
29	Lattari	115.2

Allocca et al., HESS 2014

The case study of Cervinara

Volcanoclastic cover laying upon fractured limestone bedrock.

Slope elevation between 500m and 1000m above sea level.

Deciduous chestnut woods with dense understorey in spring and summer

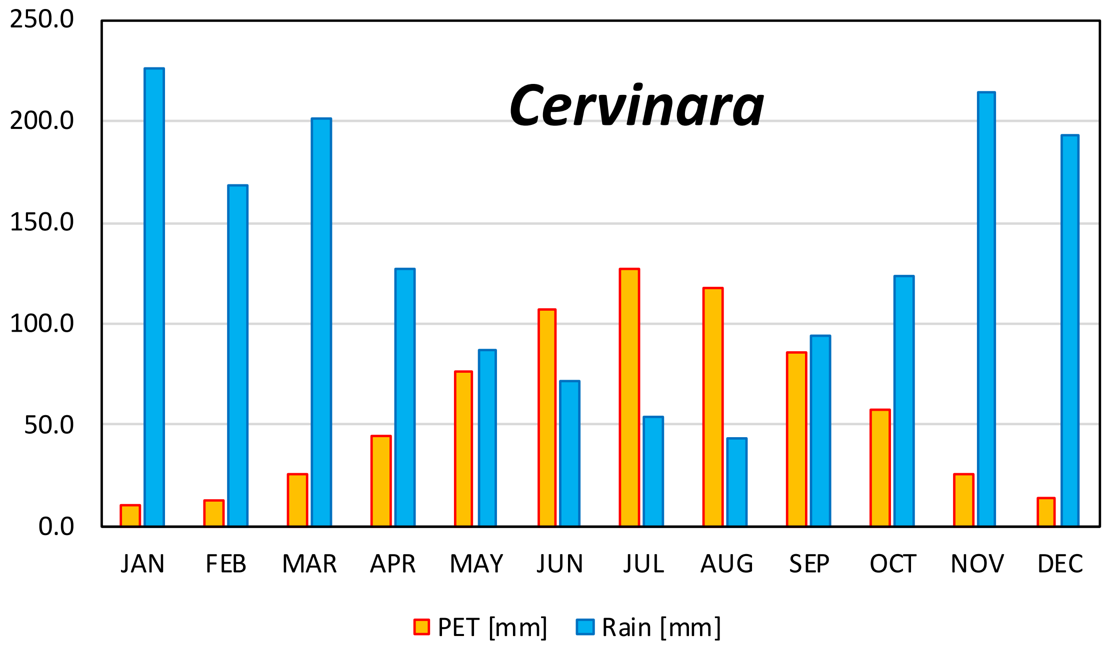

Mean annual rainfall: 1600mm

Mean annual potential evapotranspiration: 750mm

Humid Mediterranean climate

Pyroclastic soil cover

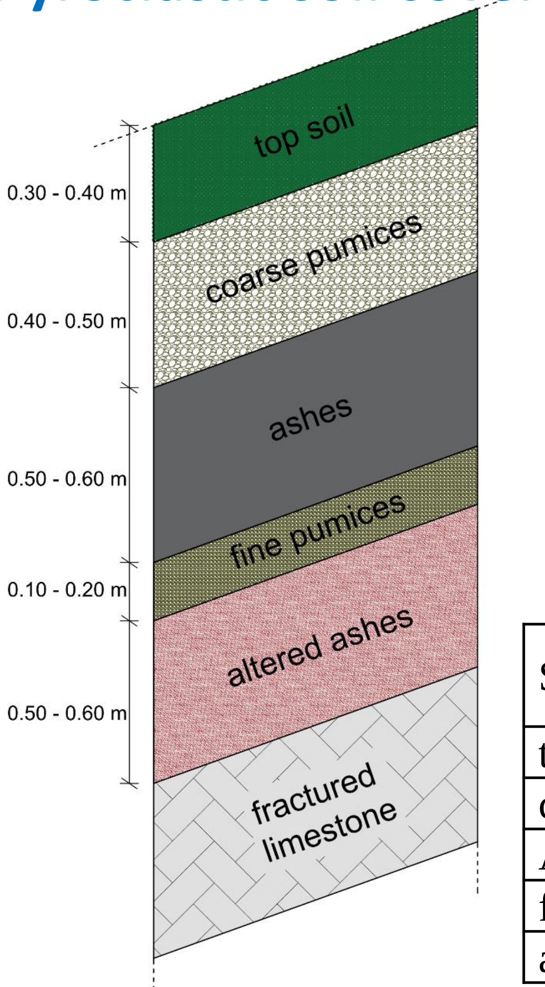

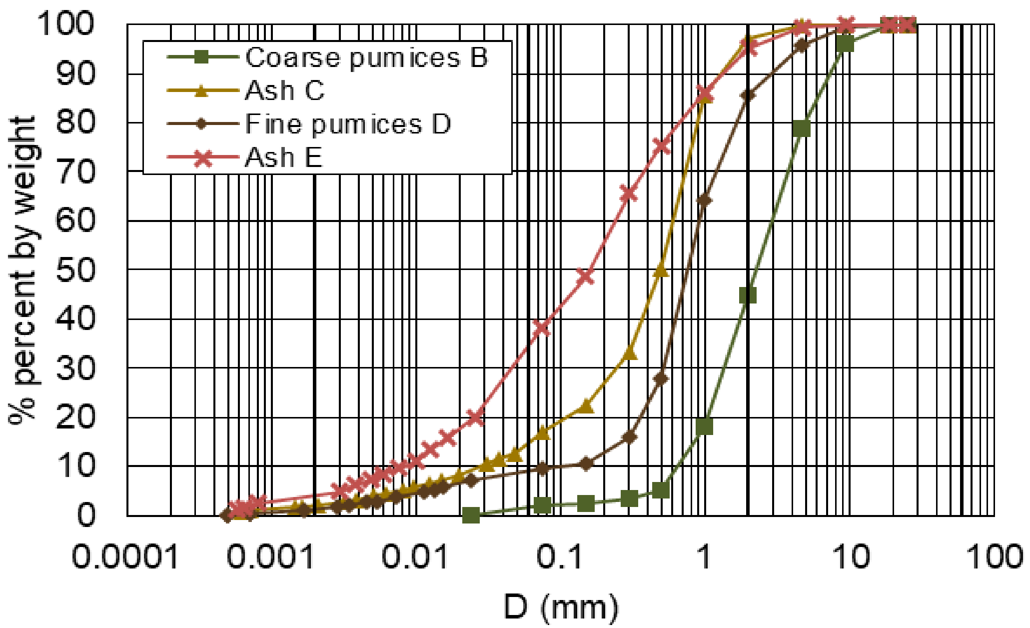

Soil	n [%]	γ_{dry} [kN/m^3]	K_{sat} [m/s]	ϕ' [°]	c' [kPa]
topsoil	-	-	-	-	-
coarse pumices	50	1.3	5×10^{-6}-1×10^{-5}	-	-
Ashes	70-75	0.7-0.8	1×10^{-6}-6×10^{-6}	38	0
fine pumices	50-55	1.2-1.3	-	-	-
altered ashes	60-65	0.9-1.1	8×10^{-7}-1×10^{-6}	31	11

Field monitoring

2017-2020

Stream

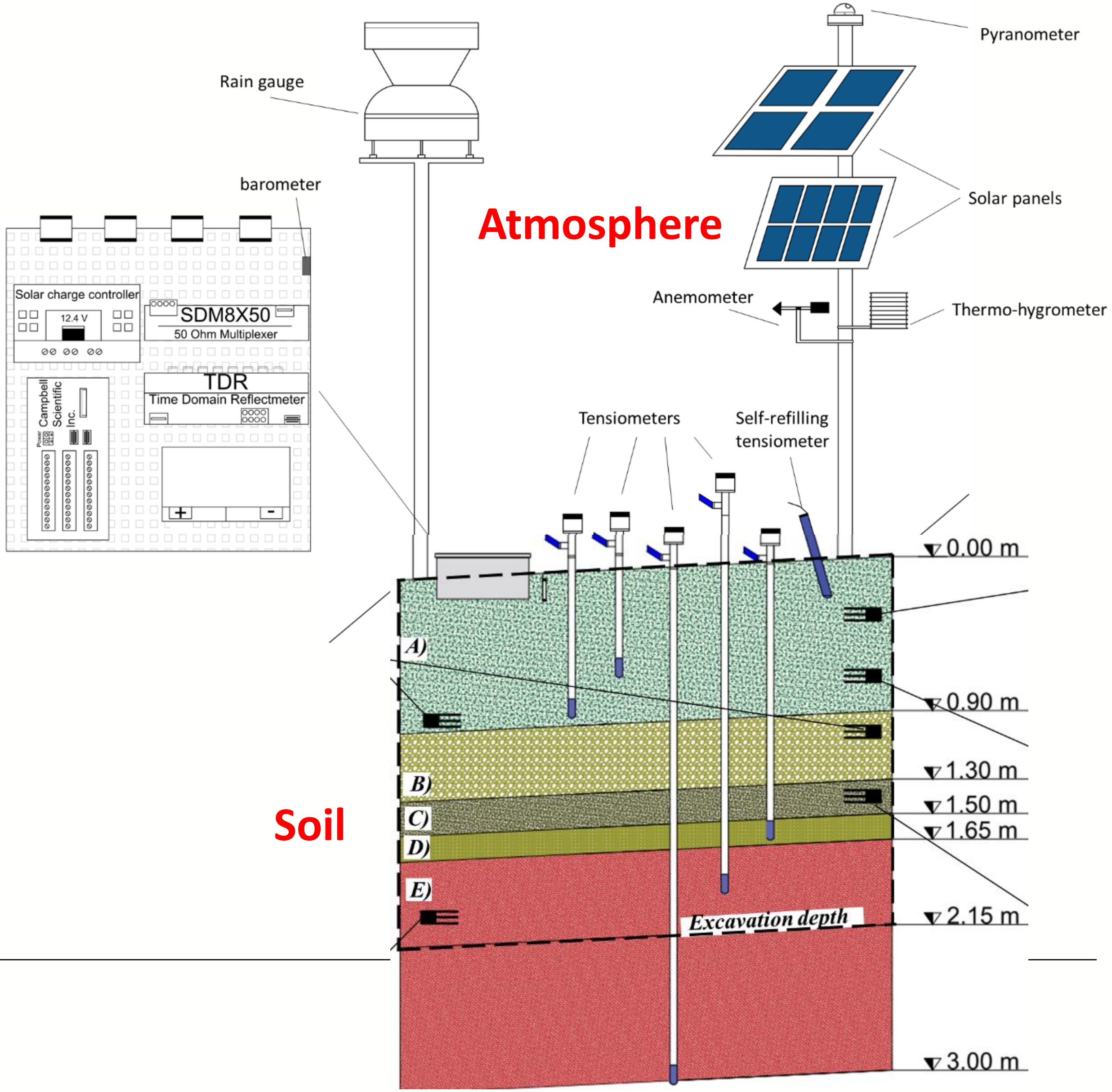

Field monitoring

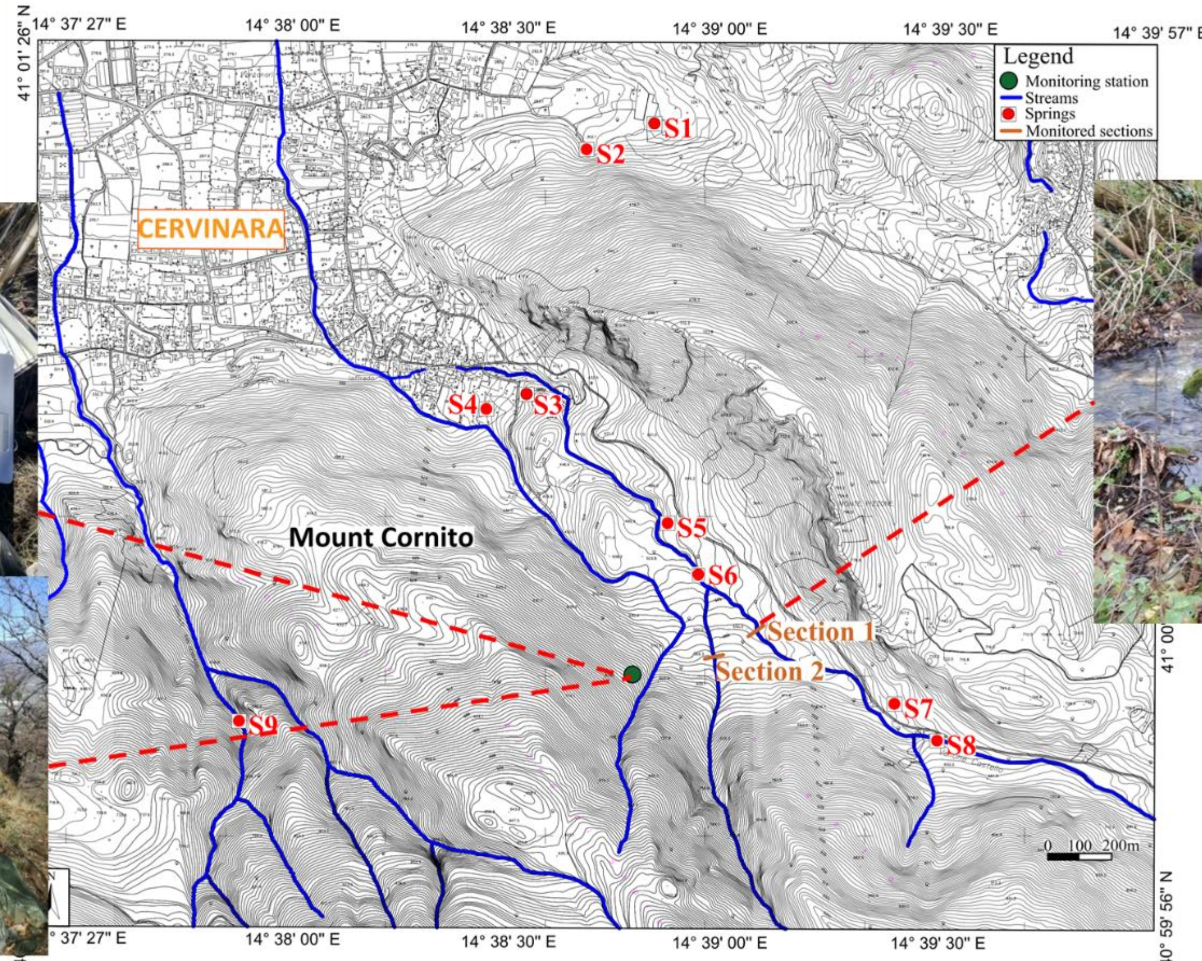

Marino et al., Water 2020

Rainfall

Year	*R* (mm)
2017-2018	1900
2018-2019	1600
2019-2020	1360

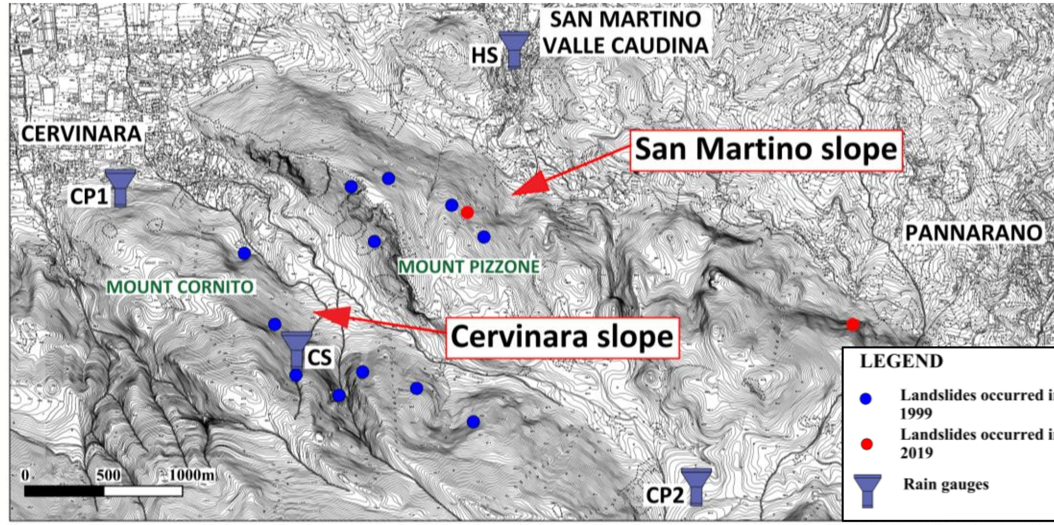

Rainfall at the slope 2017-2020

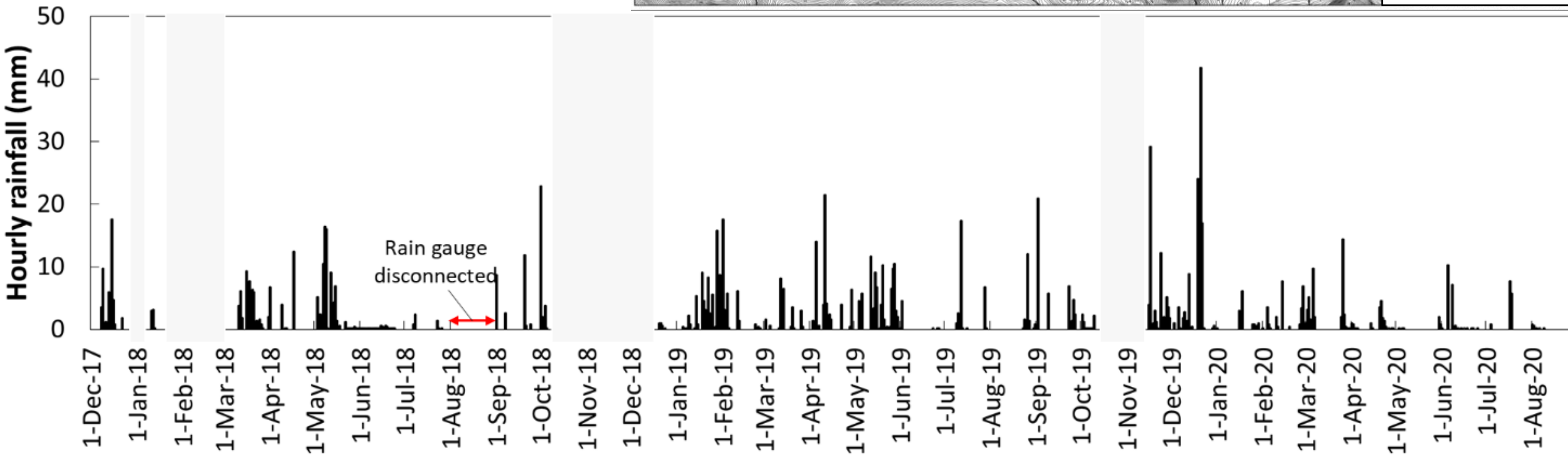

Evapotranspiration

All years warmer than average

ET ≅ 80% ET_0

Year	ET_0 (mm)	ET (mm)
2017-2018	911.3	734.3
2018-2019	1000.3	781.0
2019-2020	1021.6	793.2

Potential evapotranspiration 2017-2020

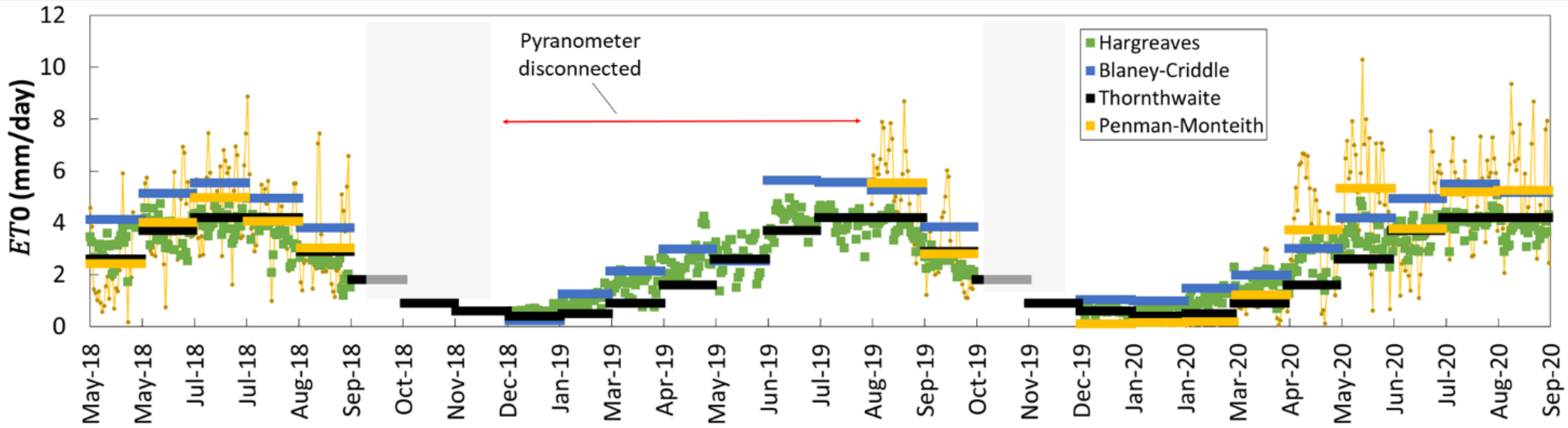

Soil suction and water content

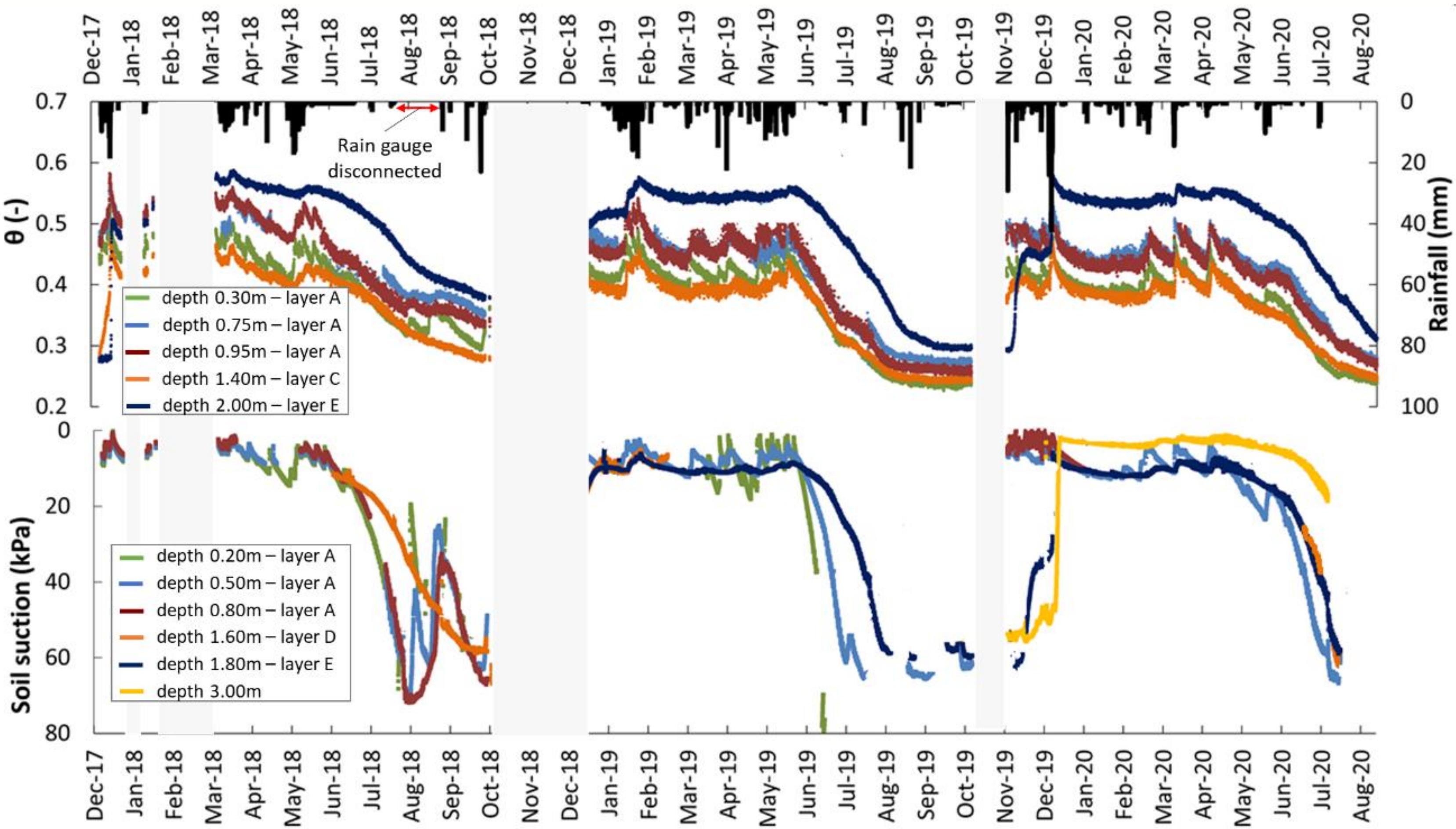

Università degli Studi della Campania *Luigi Vanvitelli*

Soil always far from saturation

Soil suction and water content

Seasonally recurrent water content and suction profiles

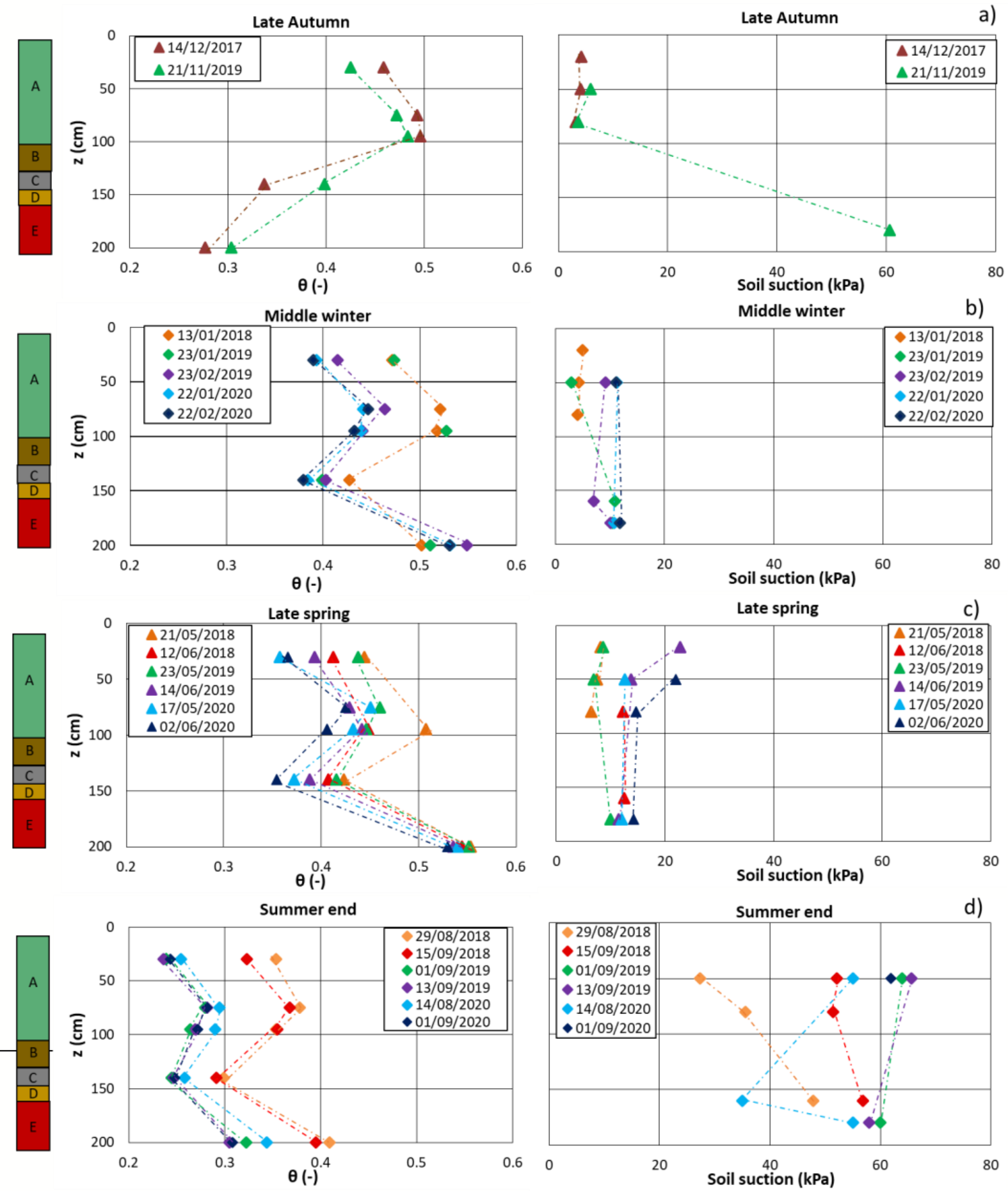

Soil water content and suction

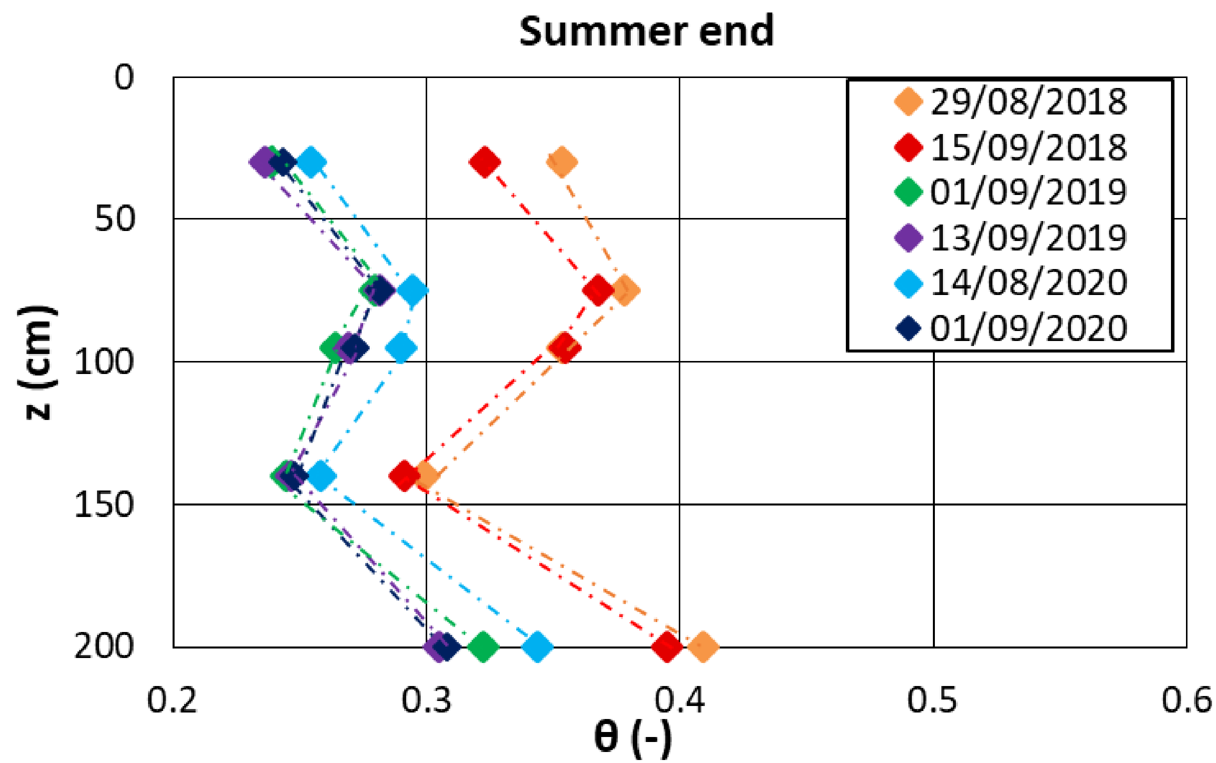

Typical late summer water content profile

Soil water content

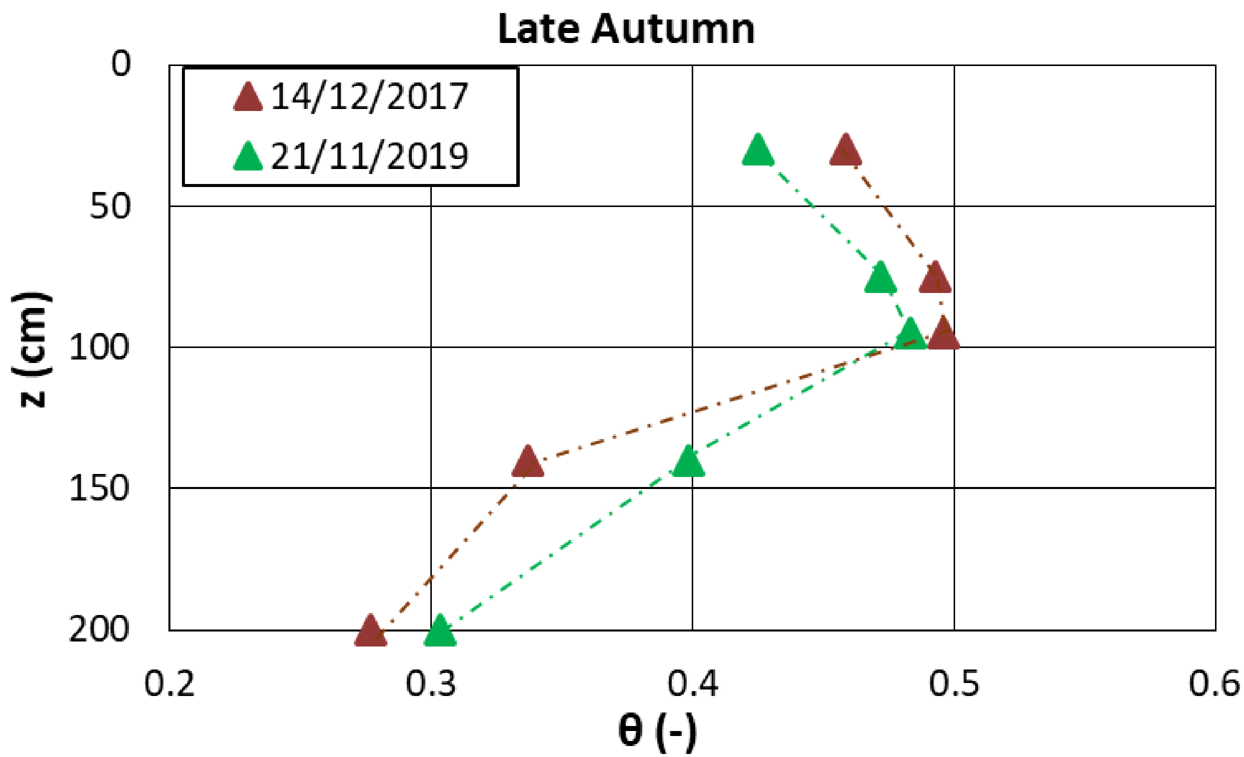

Typical late autumn water content profile

Soil suction and water content

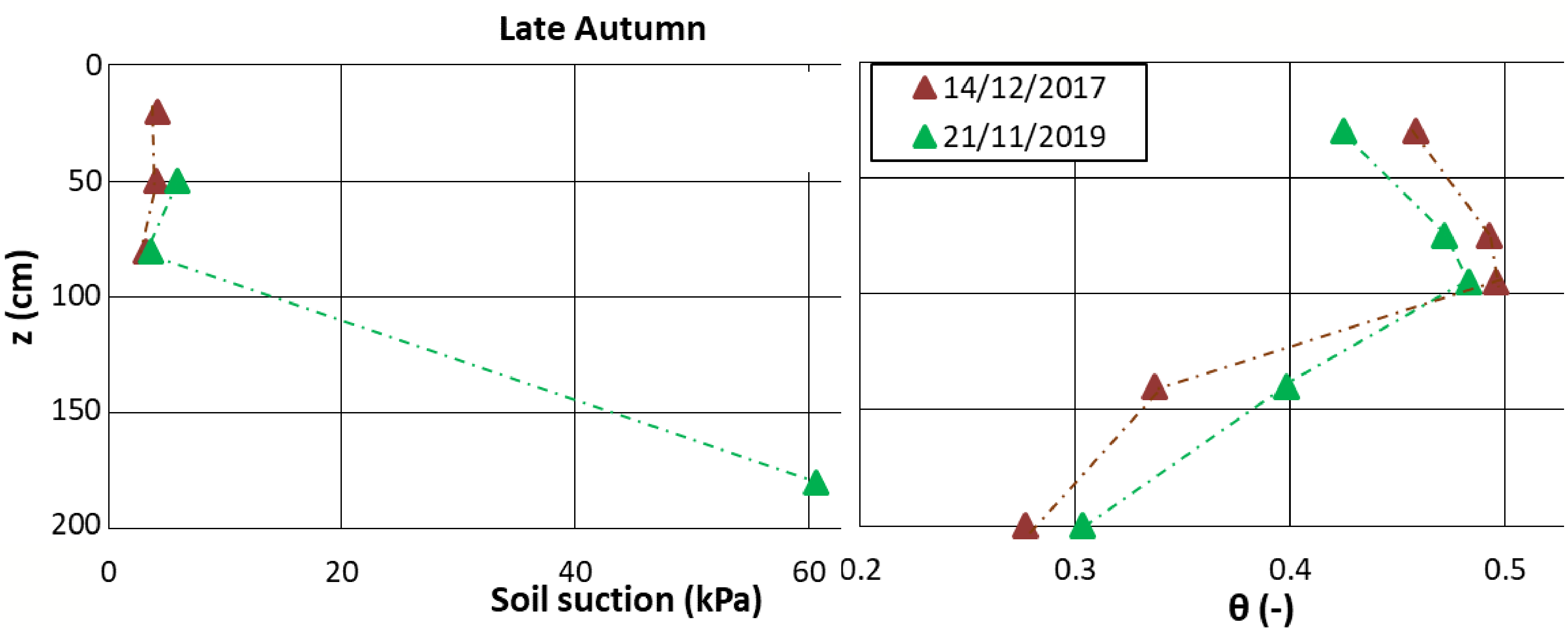

Typical late autumn suction and water content profiles

Soil water content

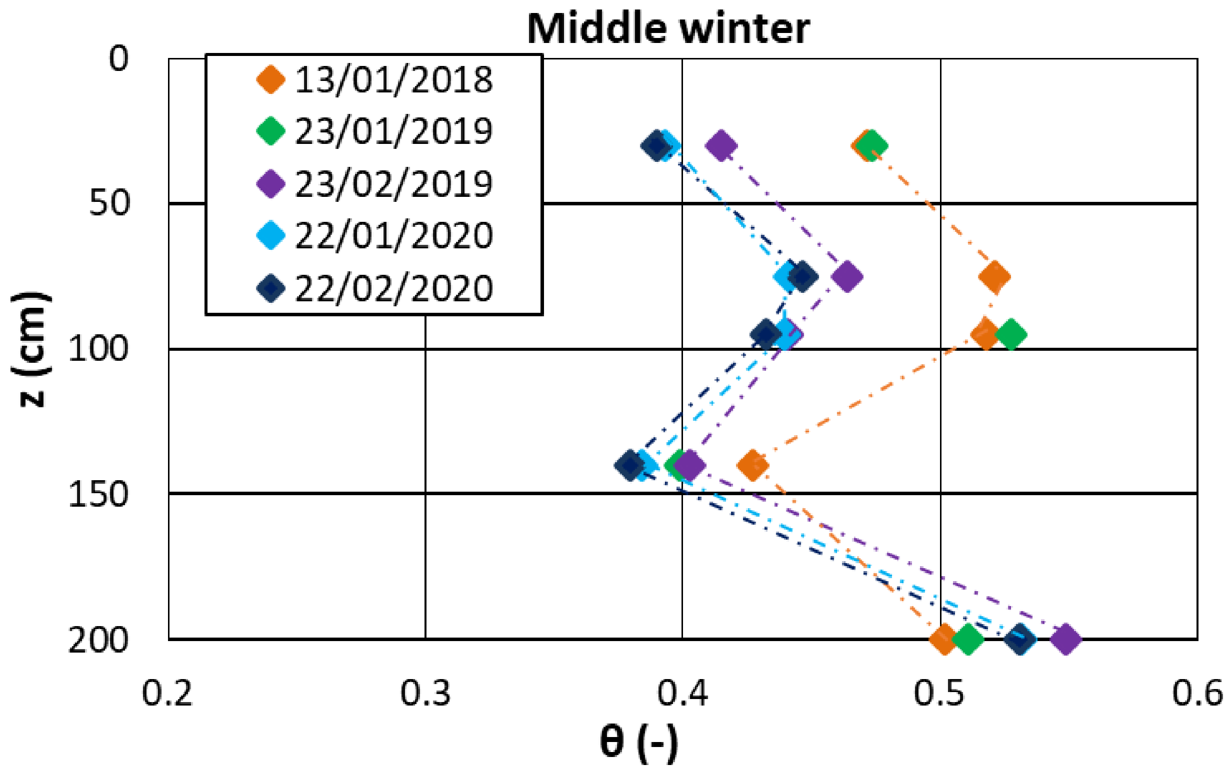

Typical middle winter water content profile

Soil suction and water content

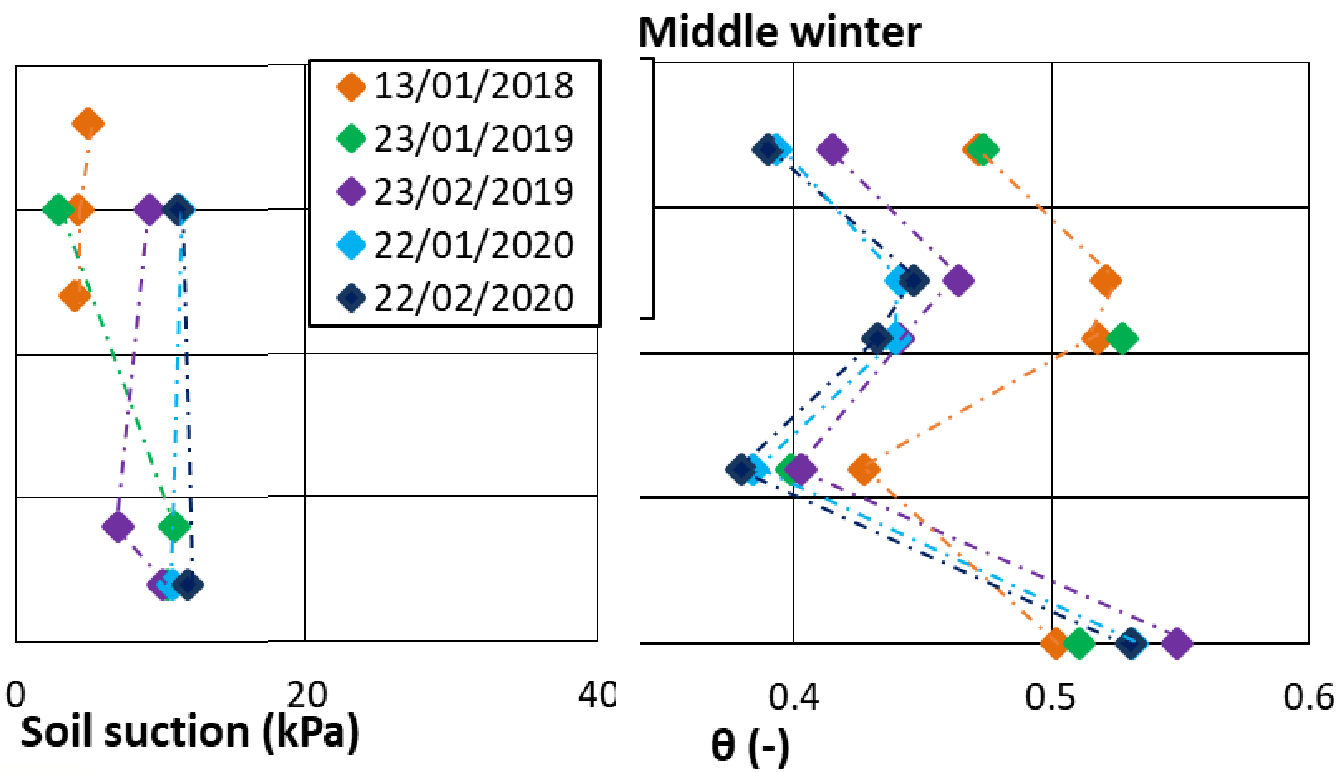

Typical middle winter suction and water content profiles

Stream discharge

Slow response to precipitations ➡ **Baseflow**

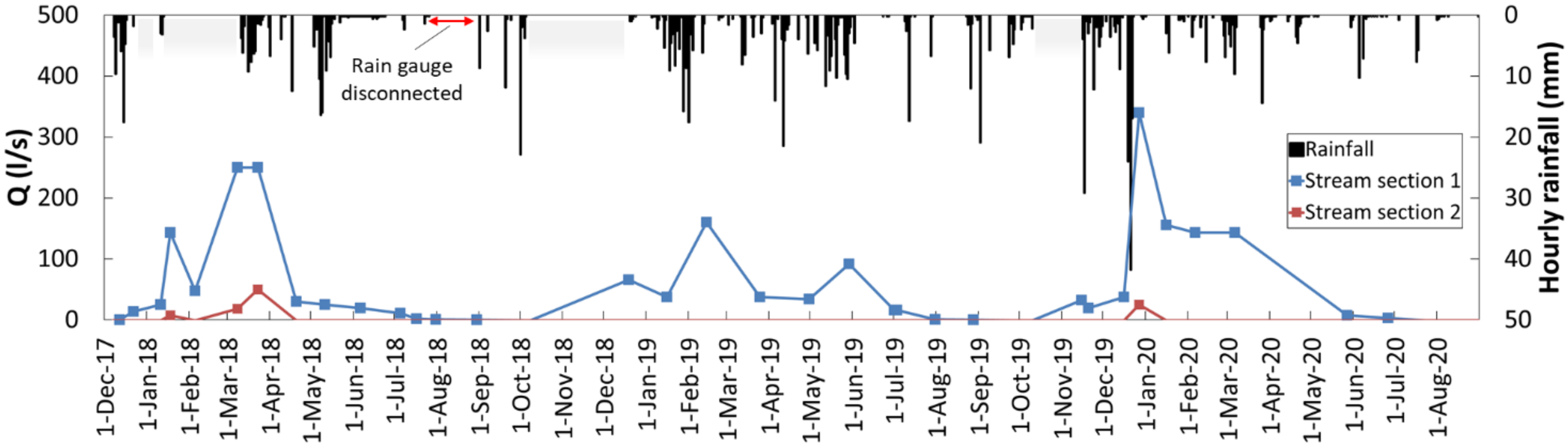

Stream water level and electrical conductivity

High EC

⬇

Baseflow

Small EC reduction during rainfall

⬇

Small flood runoff

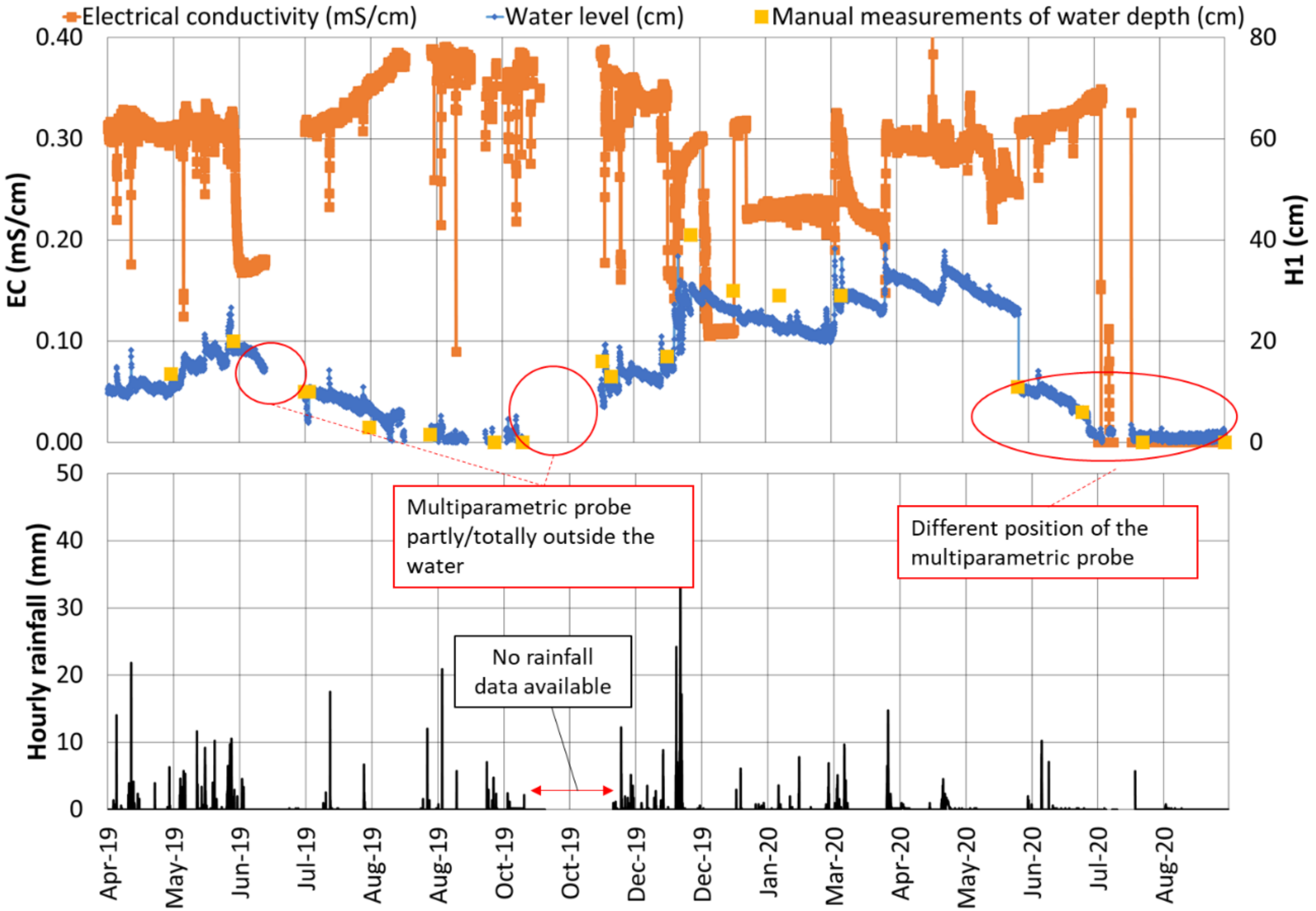

Flood runoff and baseflow

Date	Precipitation depth (mm)	Specific flood runoff (mm)	Runoff coeff. (%)
15 May 2019	45.1	0.487	1.08
27 May 2019	25.6	0.253	0.98
24 November 2019	34.5	0.217	0.63
13 December 2019	35.3	0.197	0.56
19 December 2019	102.2	1.038	1.02

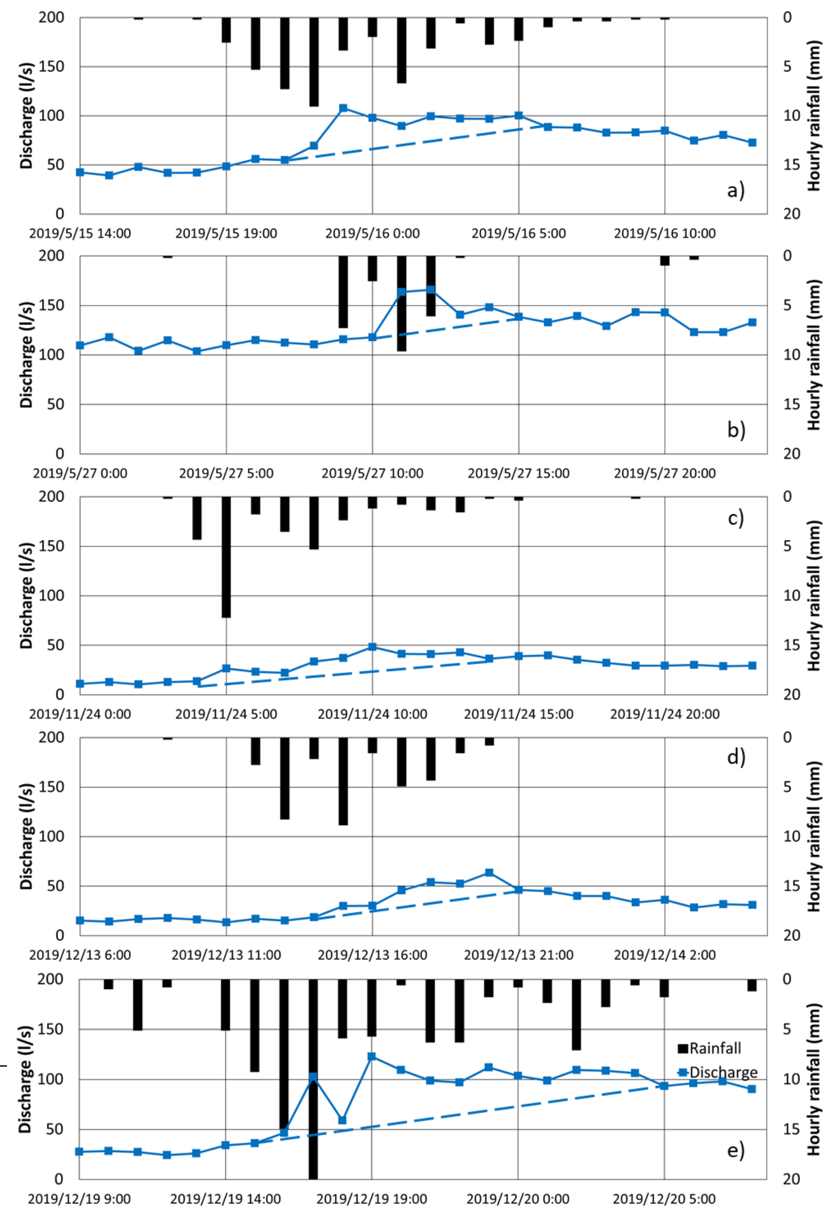

Flood runoff ≈ 1% Rainfall

Flood runoff and baseflow

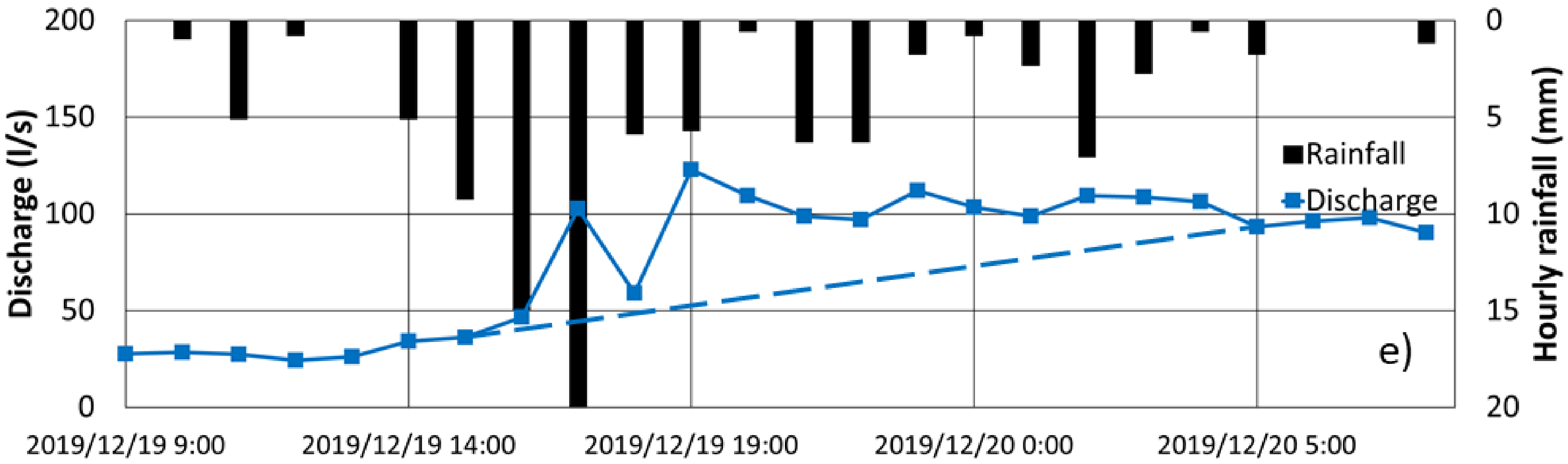

Slow and stable discharge growth ➡ Baseflow

Slope water balance

Rainfall (measured)

$$\int_0^t (R - ET - q_s)\, dt = V_s + V_b$$

Slope water balance

Rainfall (measured)

Evapotranspiration (measured)

$$\int_0^t (R - ET - q_s)\, dt = V_s + V_b$$

Slope water balance

Rainfall (measured)

Evapotranspiration (measured)

$$\int_0^t (R - ET - q_s)\, dt = V_s + V_b$$

Stream discharge (measured)

Slope water balance

Rainfall (measured)

Evapotranspiration (measured)

Soil storage (measured)

$$\int_0^t (R - ET - q_s)\, dt = V_s + V_b$$

Stream discharge (measured)

Slope water balance

Rainfall (measured)

Evapotranspiration (measured)

Soil storage (measured)

$$\int_0^t (R - ET - q_s)\, dt = V_s + V_b$$

Stream discharge (measured)

Bedrock storage: epikarst + groundwater (calculated)

Slope water balance

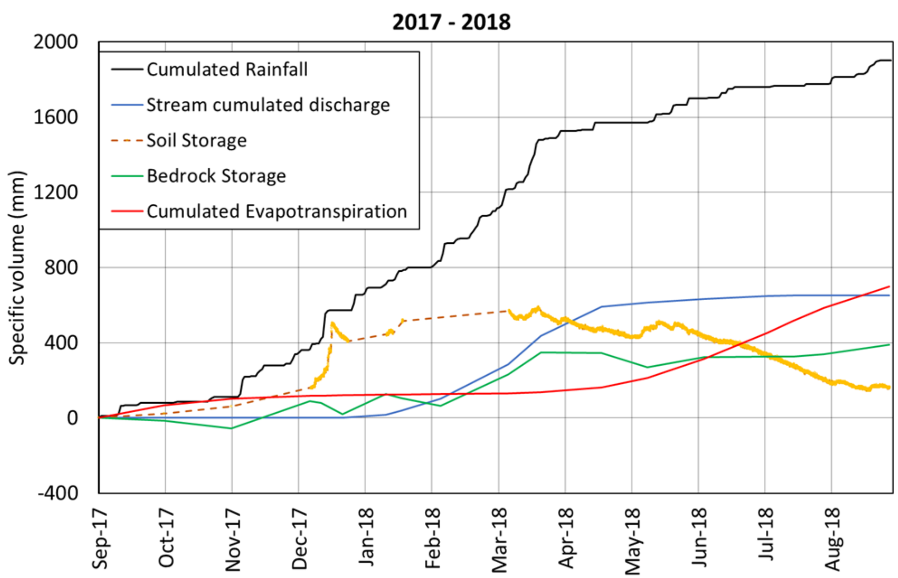

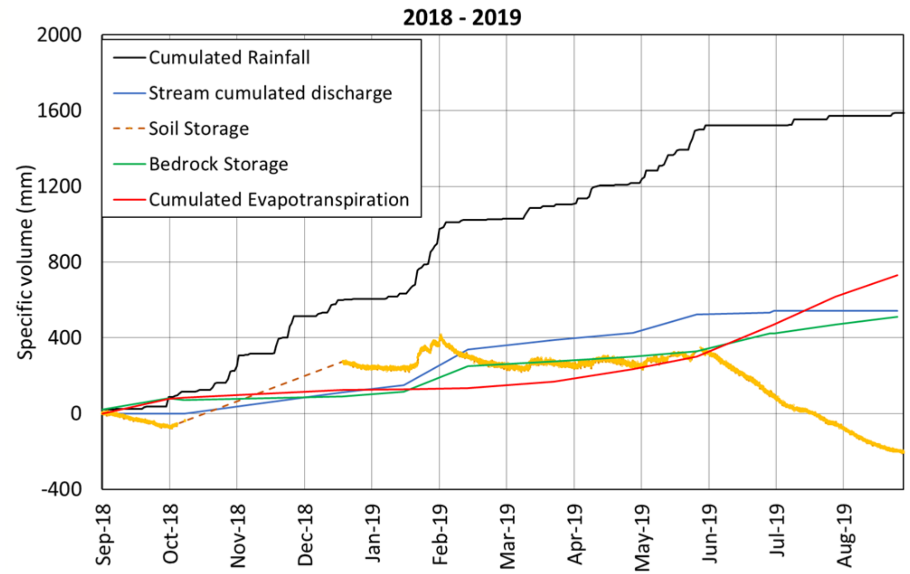

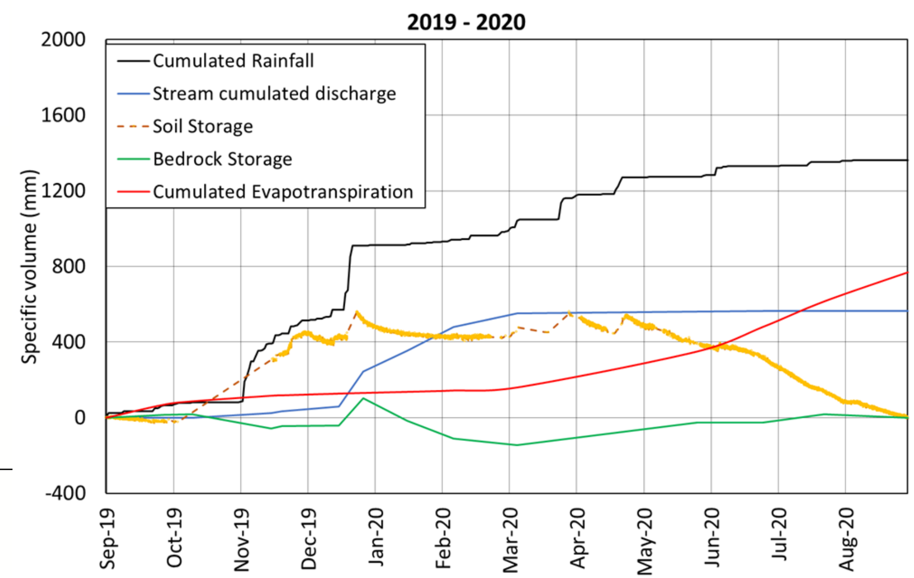

$$\int_0^t (R - ET - q_s)\, dt = V_s + V_b$$

Slope water balance

Rainfall above average
(1900 mm > 1600 mm)

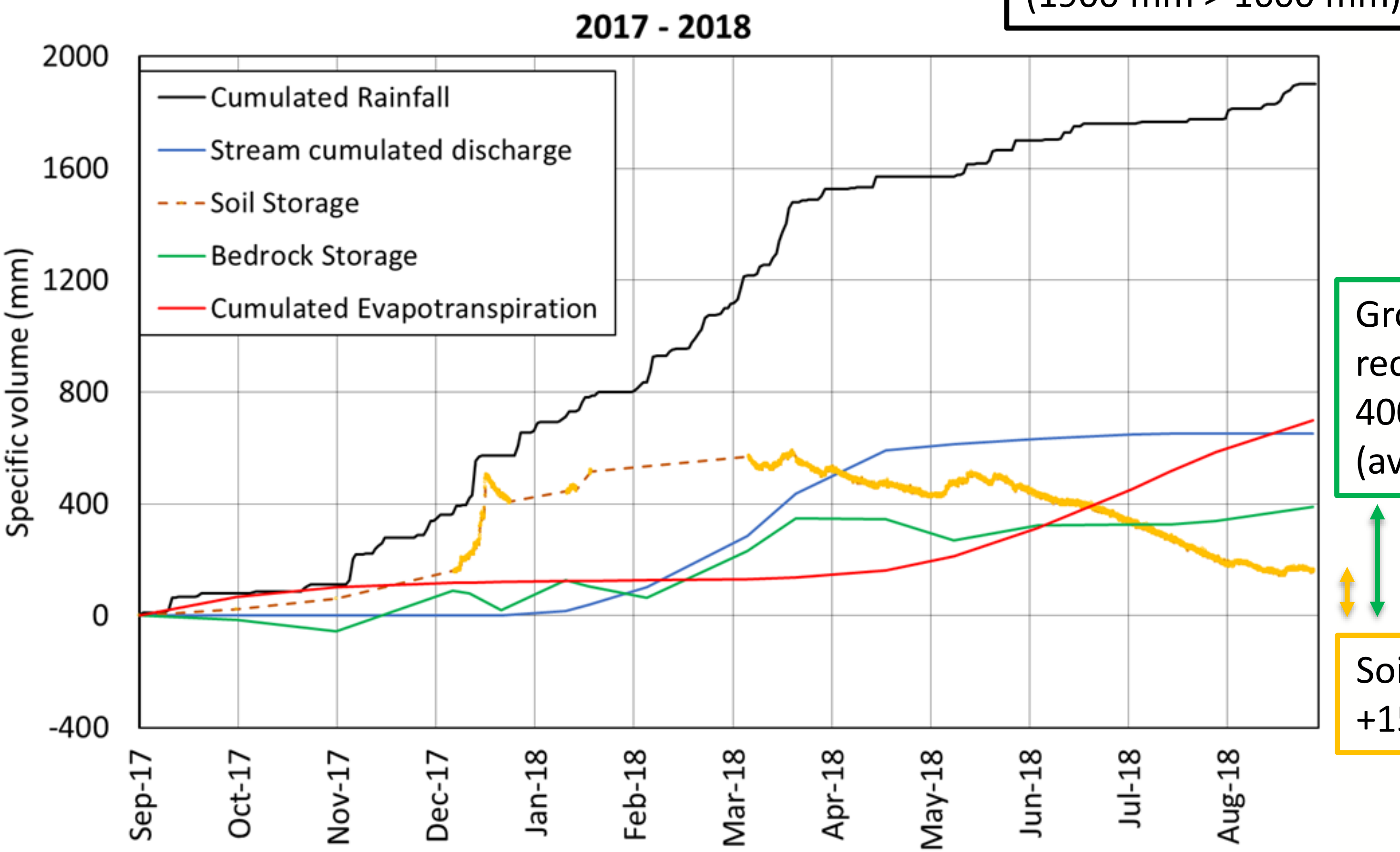

Groundwater recharge
400 mm
(average 200 mm)

Soil storage
+150mm

Slope water balance

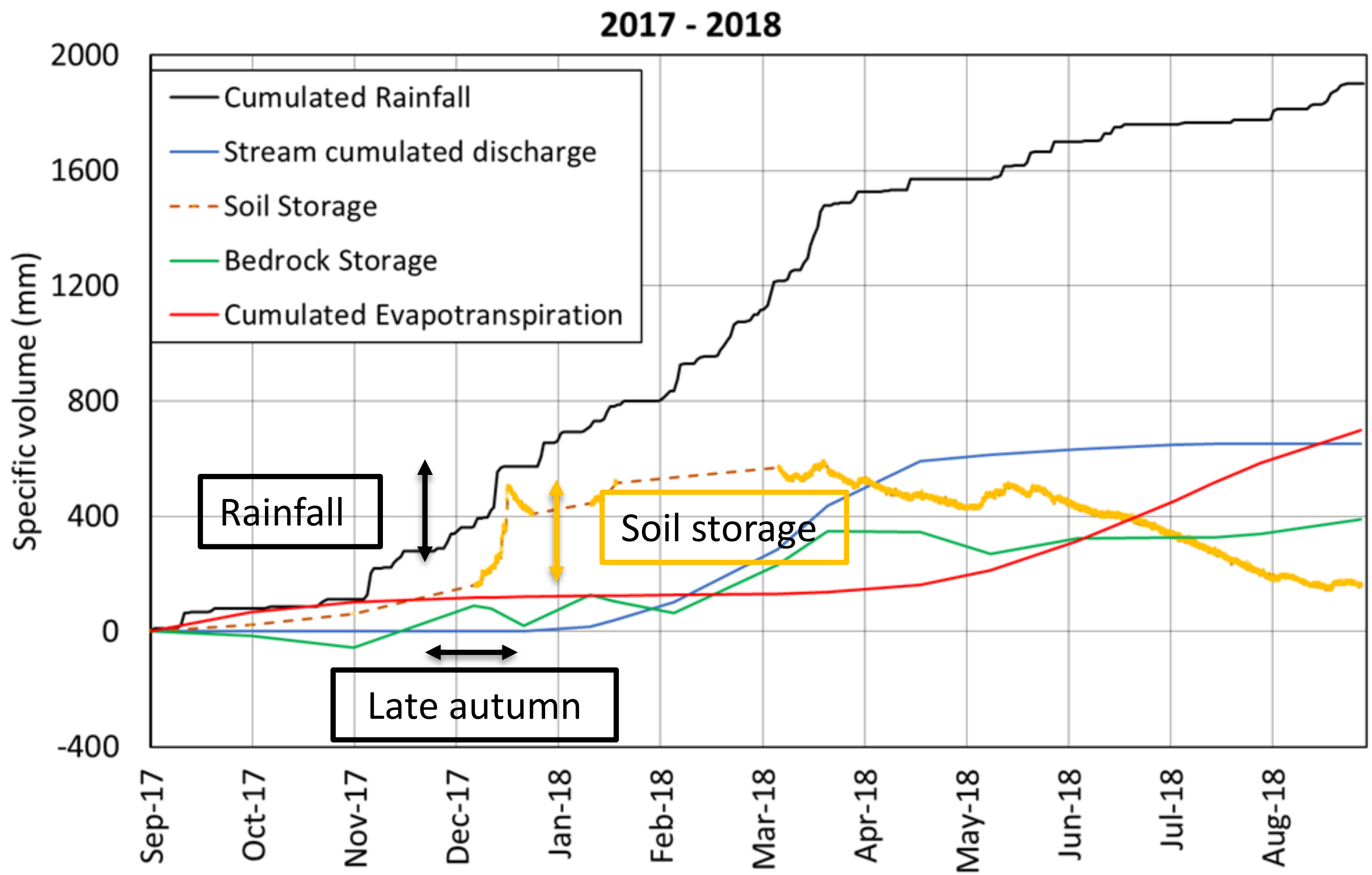

Slope water balance

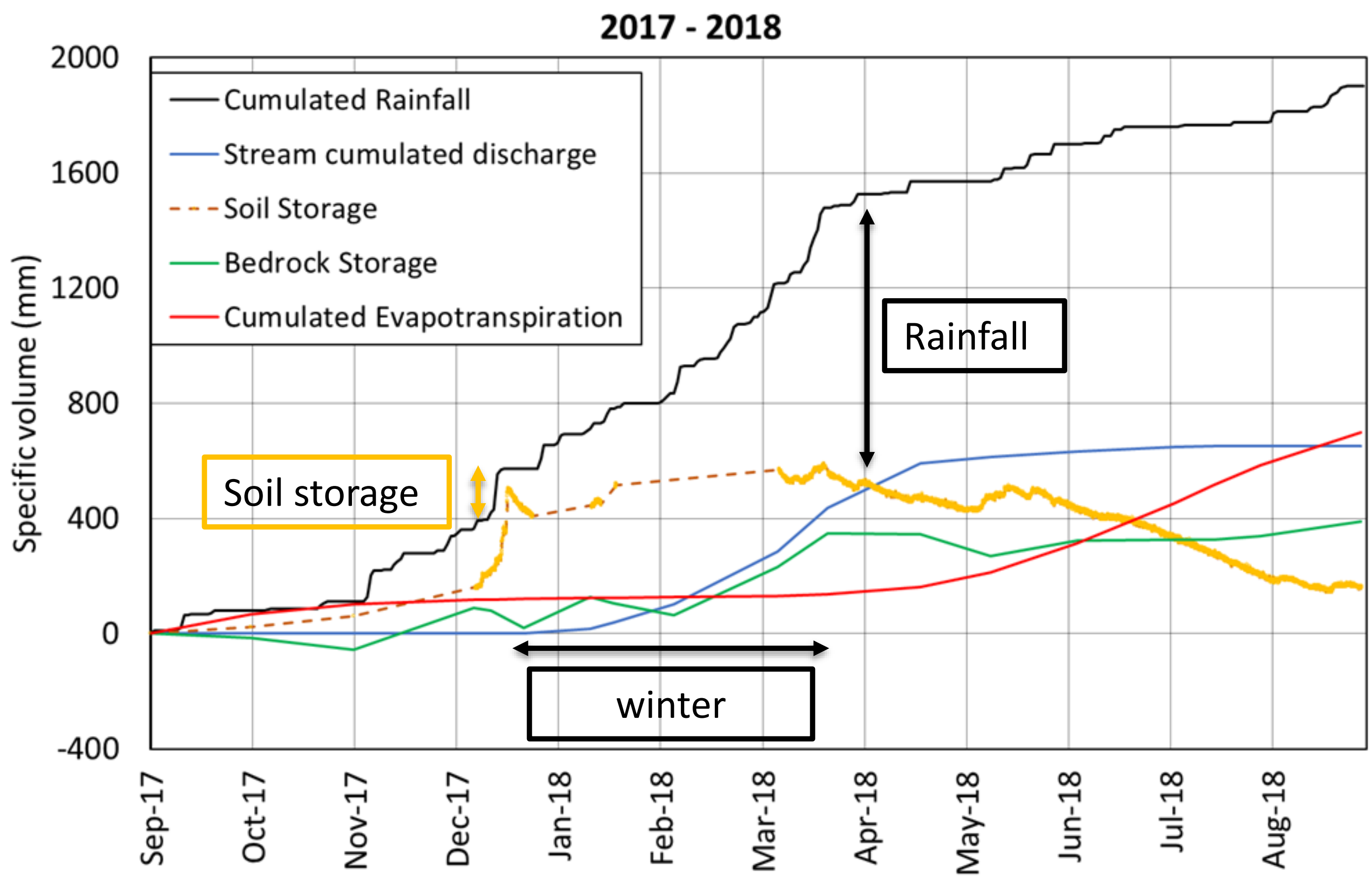

Slope water balance

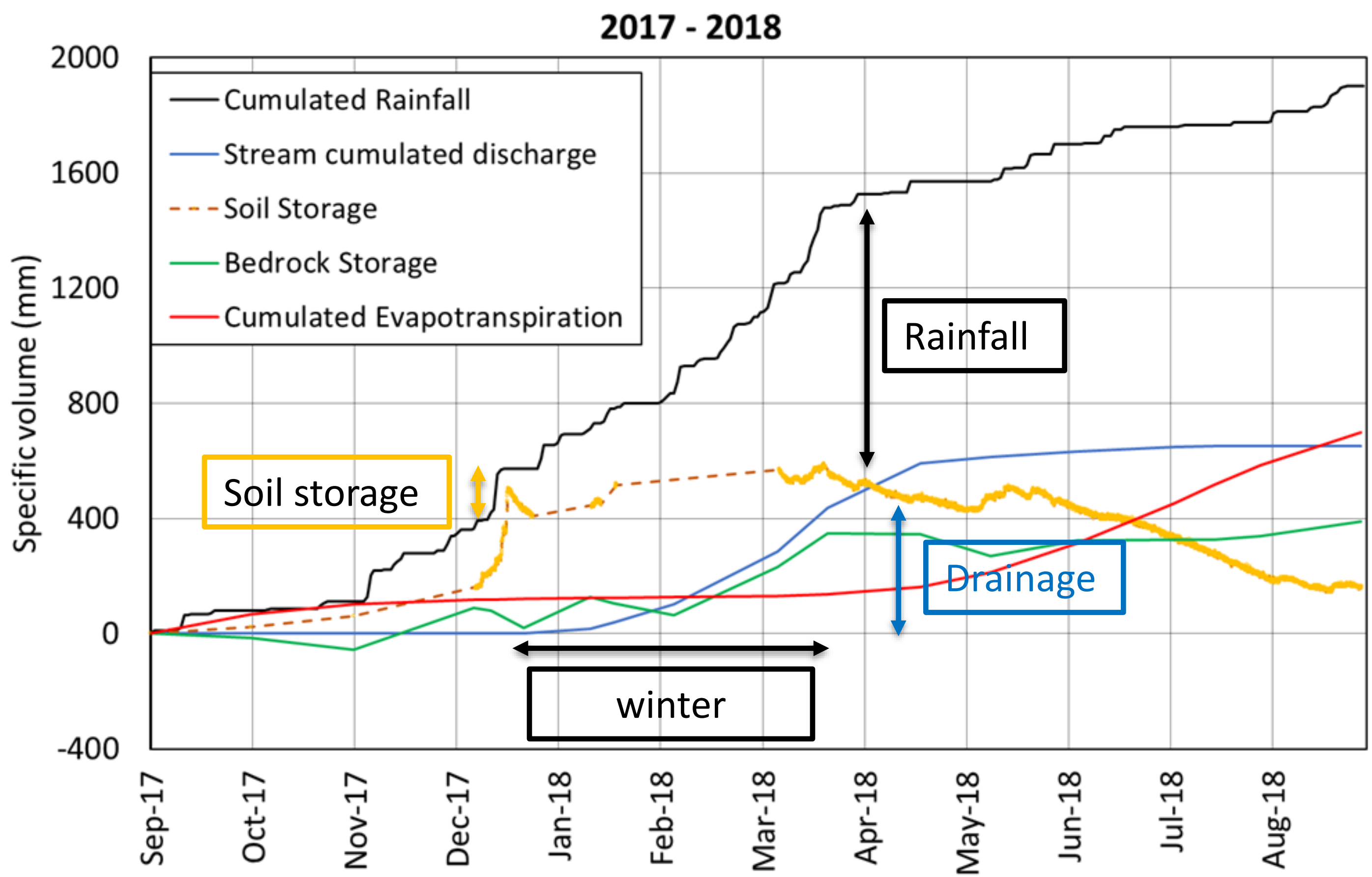

Slope water balance

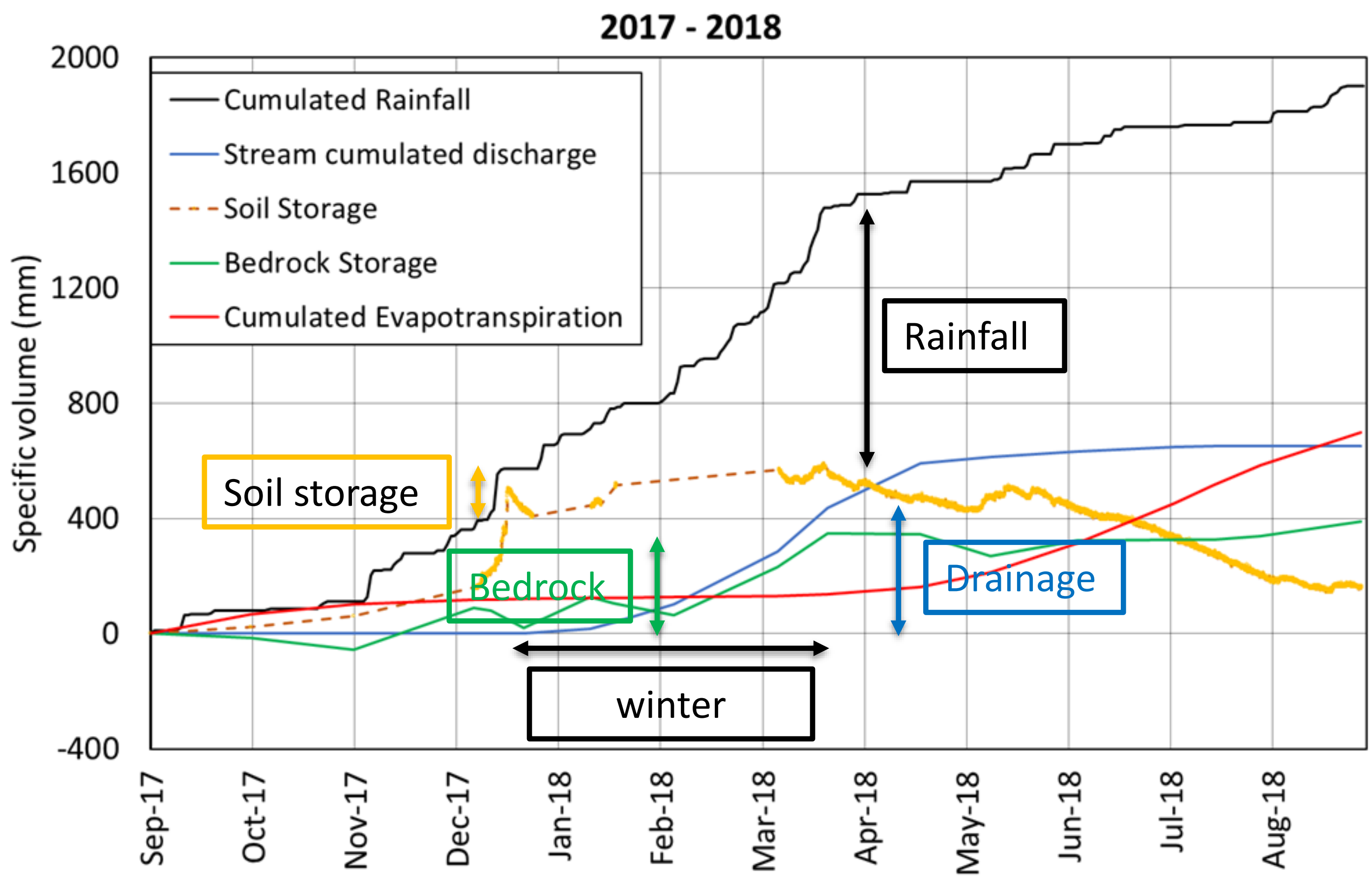

Slope water balance

Rainfall below average
(1360 mm < 1600 mm)

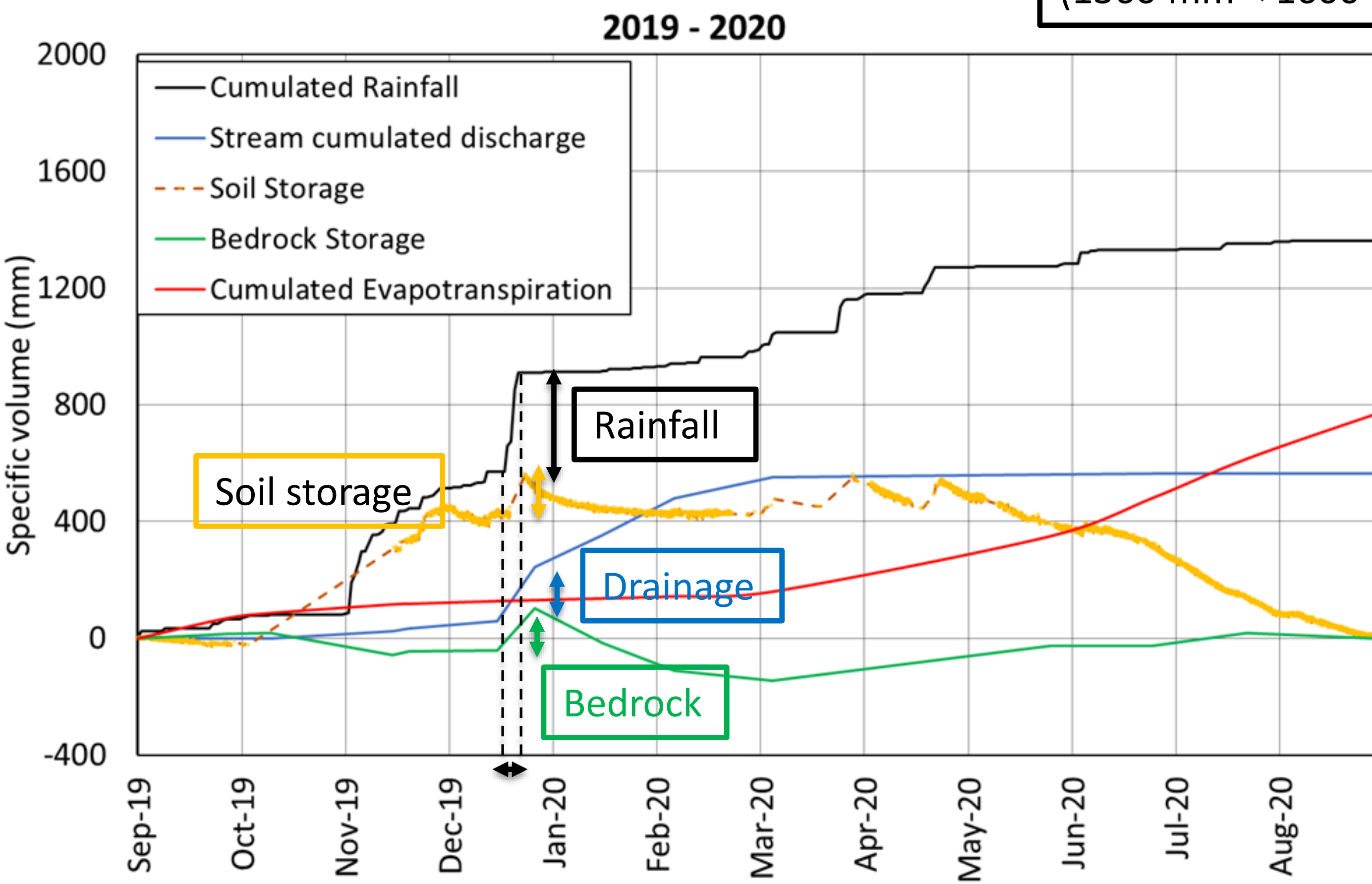

No groundwater recharge (average 200 mm)

Stable soil storage

Building a physically based mathematical model

$$\frac{d\theta}{d\psi}\frac{\partial\psi}{\partial t} = \frac{\partial}{\partial s}\left[k(\psi)\left(\cos\alpha + \frac{\partial\psi}{\partial s}\right)\right] +$$

Soil cover: 2D Richards equation

Fractured bedrock
(1D Darcy equation)

$$n_e\frac{\partial h}{\partial t} = \frac{\partial}{\partial s}\left[K_f h\left(\sin\beta + \frac{\partial h}{\partial s}\right)\right] + i_b$$

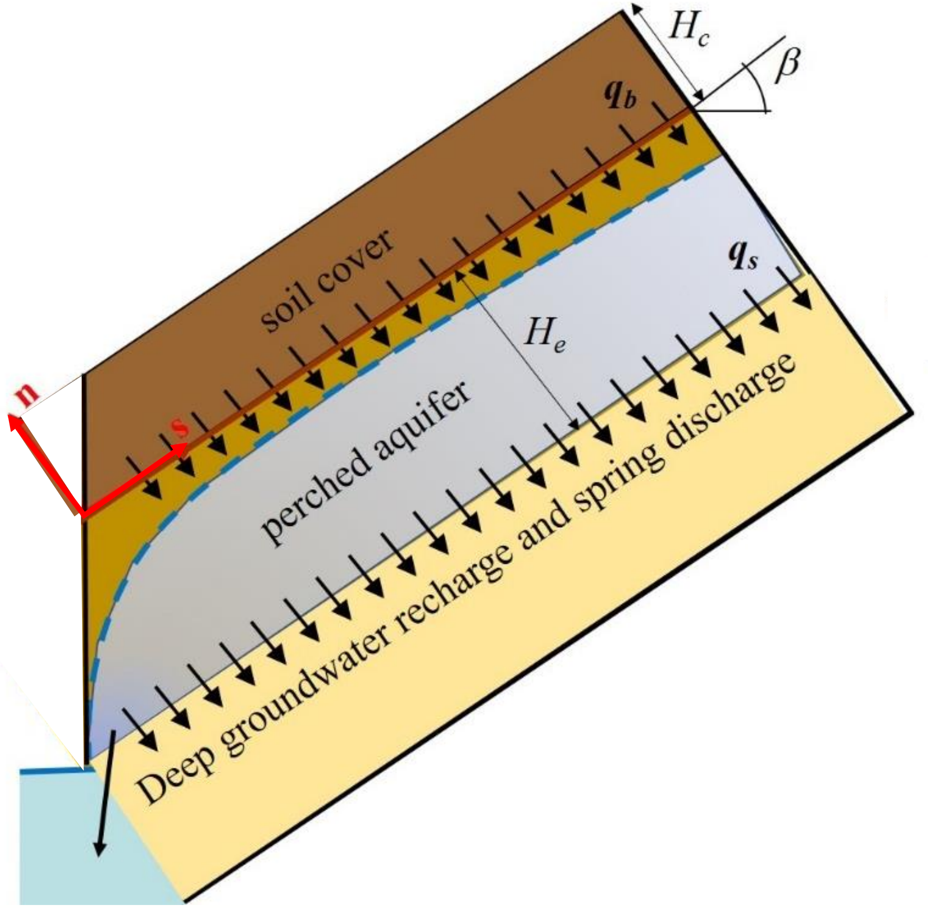

Building a physically based mathematical model

Soil cover parameters have been assigned through back-analysis of field monitoring results carried out with a 1D simplified version of the model.

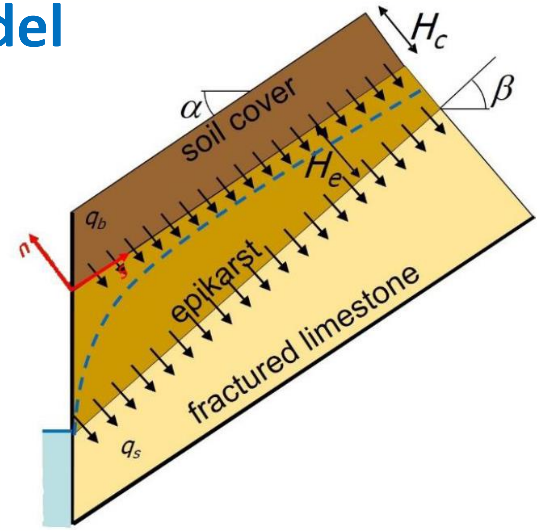

Soil cover	θ_s	0.7
	θ_r	0.01
	α (1/m)	6.0
	n	1.3
	k_s (m/s)	3.0×10^{-5}
	c' (kPa)	0
	ϕ' (°)	38
Epikarst aquifer	n_e	0.015
	K_e (m/s)	1.1×10^{-6}

Epikarst aquifer parameters are derived from literature, and chosen so to ensure long-term equilibrium of the aquifer

Seasonally different slope response to preciptations

A dry condition at the base of the soil cover prevents drainage.

Hence, in late autumn a rainfall of **250mm in 48 hours** can trigger a landslide.

In middle winter, instead, landslides become likely only for rainfall of about **300mm in 48 hours**.

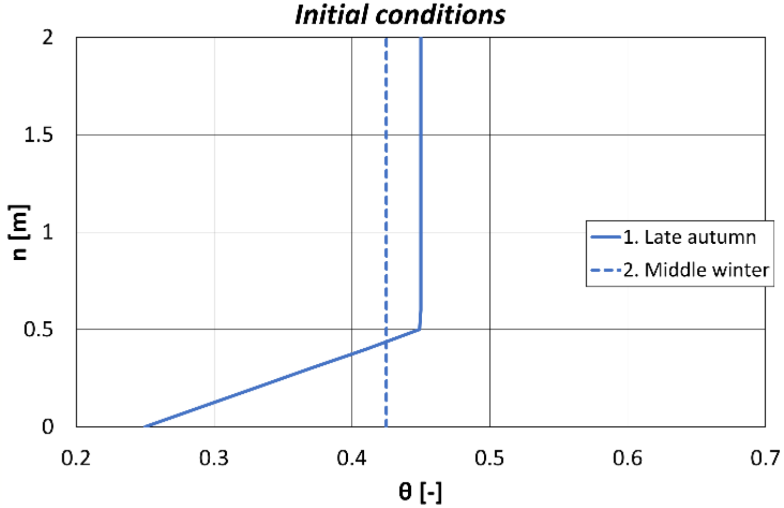

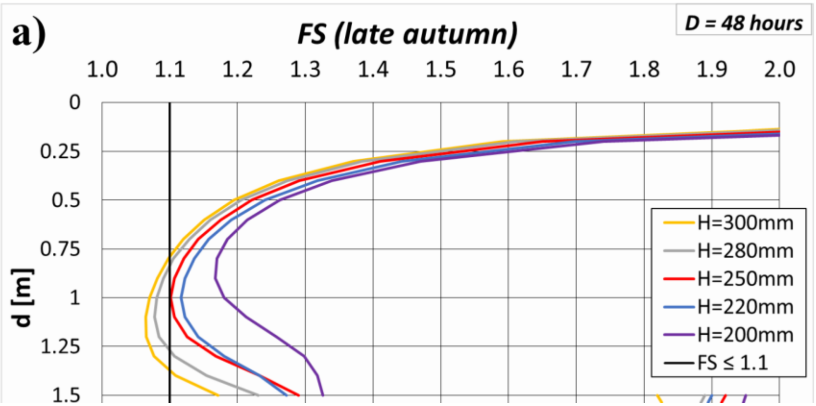

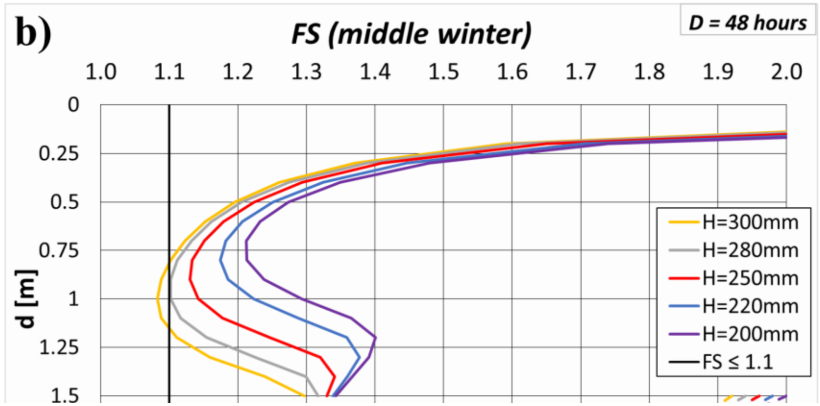

Simulation of the landslide of 1999

At the onset of the triggering event on 15 December 1999, the **water level in the aquifer was still low.**

Hence, the base of the soil cover was still so dry to have low hydraulic conductivity.

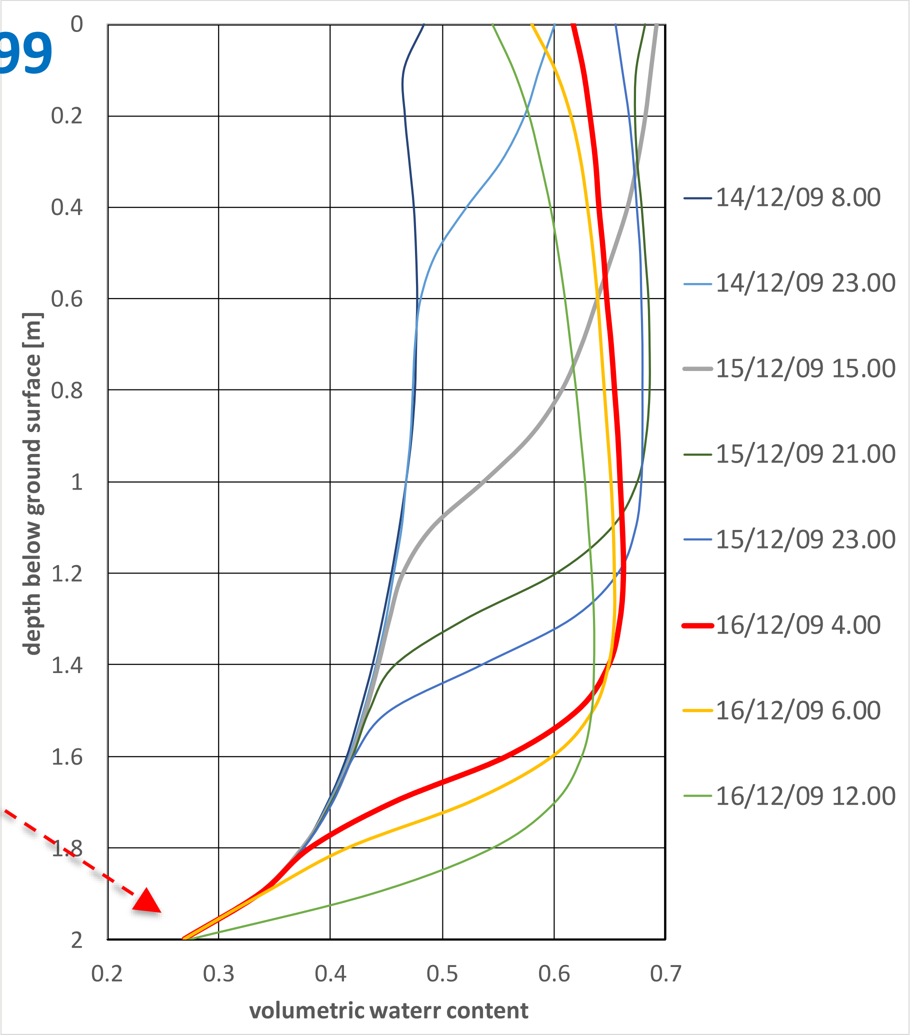

Greco et al., Water 2018

Simulation of the landslide of 1999

At the onset of the triggering event on 15 December 1999, the **water level in the aquifer was still relatively low.**
Hence, the base of the soil cover was still so dry to have low hydraulic conductivity.
The hydraulic gradient, needed to accomodate the intense infiltration rate, caused the accumulation of water in the upper part of the soil profile.

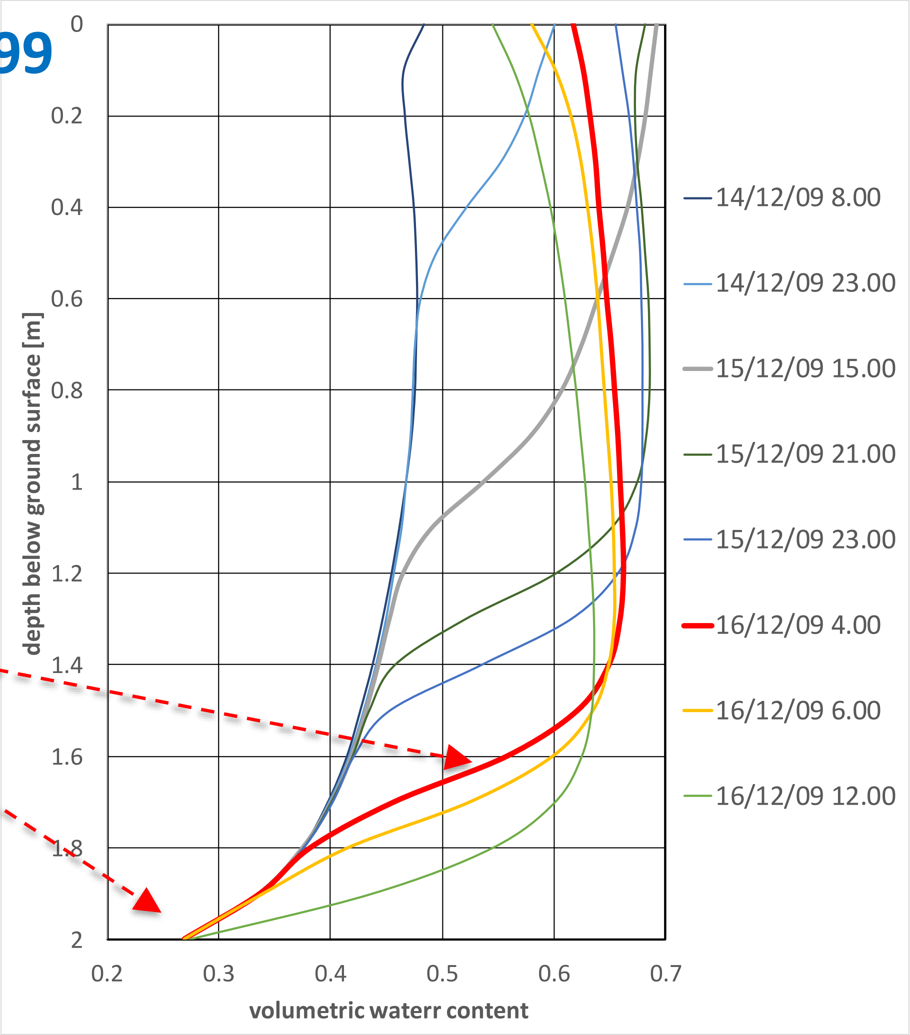

Simulation of the landslide of 1999

At the onset of the triggering event on 15 December 1999, the **water level in the aquifer was still relatively low.**

Hence, the base of the soil cover was still so **dry** to have low hydraulic conductivity.

The **hydraulic gradient** needed to accomodate the intense infiltration rate caused the **accumulation of water** in the upper part of the soil profile.

The drainage of water through the soil-bedrock interface was impeded by the dry conditions in the lower part of the soil cover.

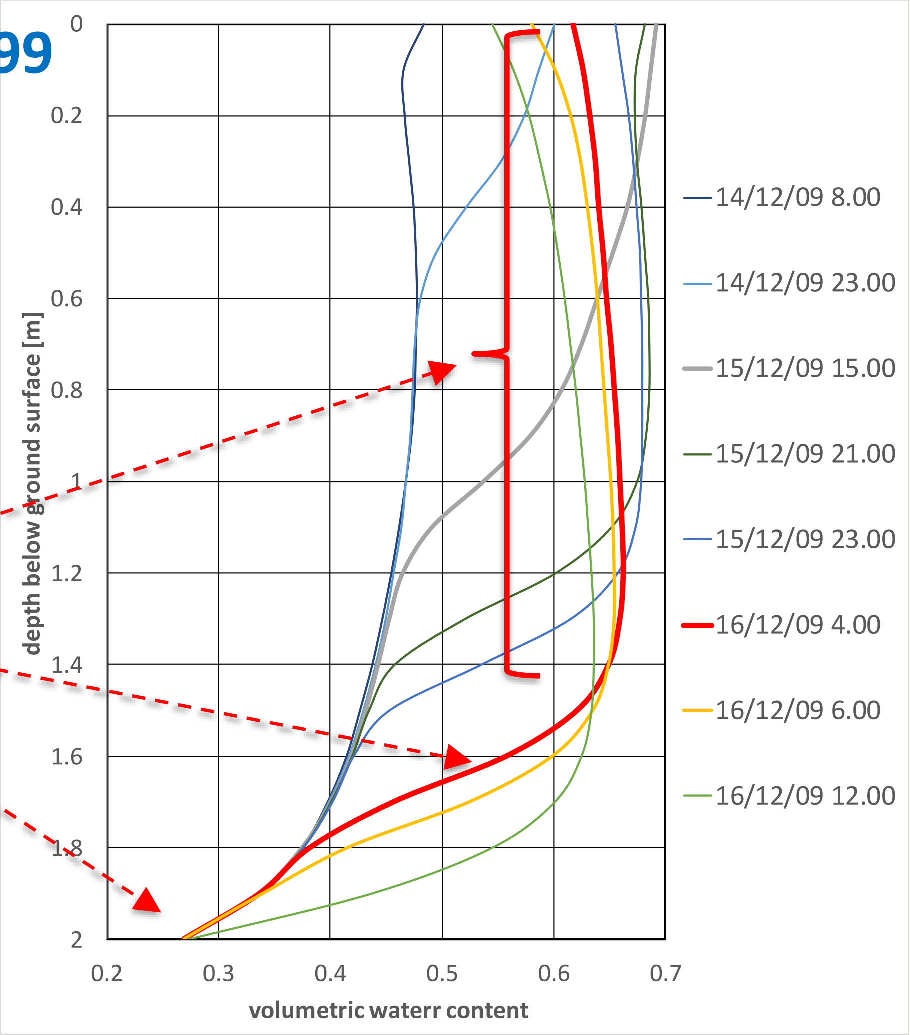

Università degli Studi della Campania *Luigi Vanvitelli*

Greco et al., Water 2018

Hydrometeorological thresholds for landslide early warning

During field monitoring it is ulikely to observe landslide events, inherently rare. In this case, we were *lucky*, as on 21 December 2019 a shallow landslide was triggered at a slope less than 1 km from the monitoring station (with some damages to roads and buildings, but no injuried people).

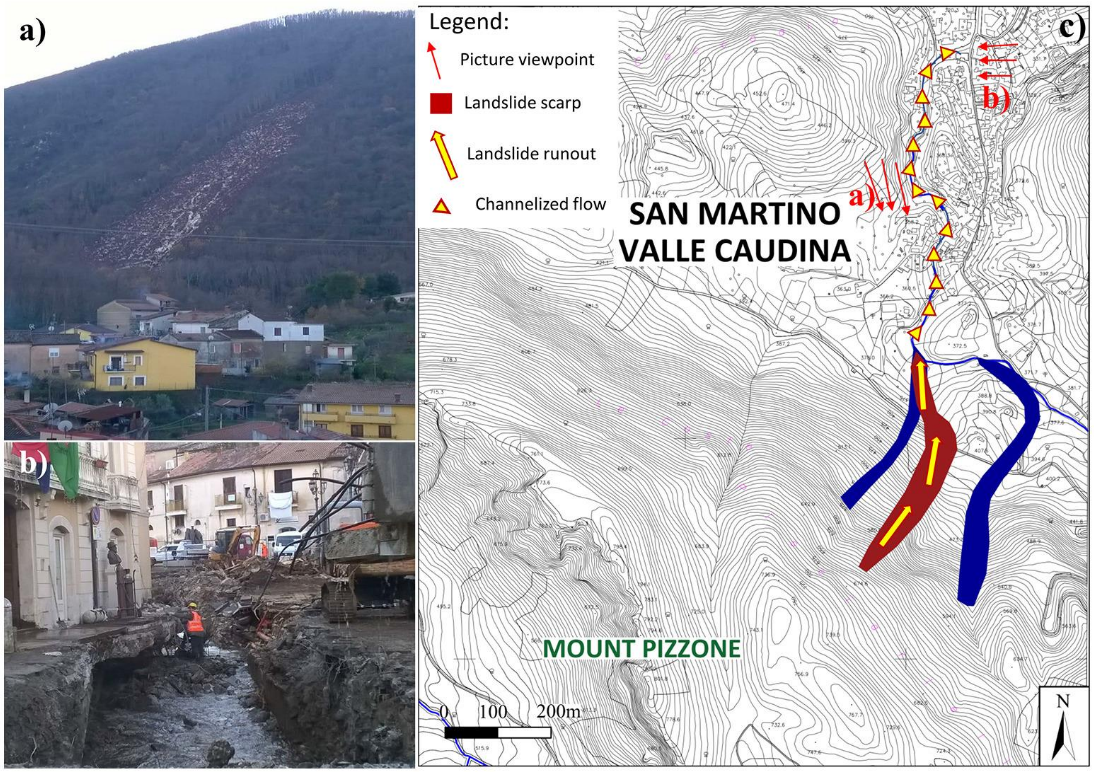

Università
degli Studi
della Campania
Luigi Vanvitelli

Greco et al., Eng Geol 2021

Hydrometeorological thresholds for landslide early warning

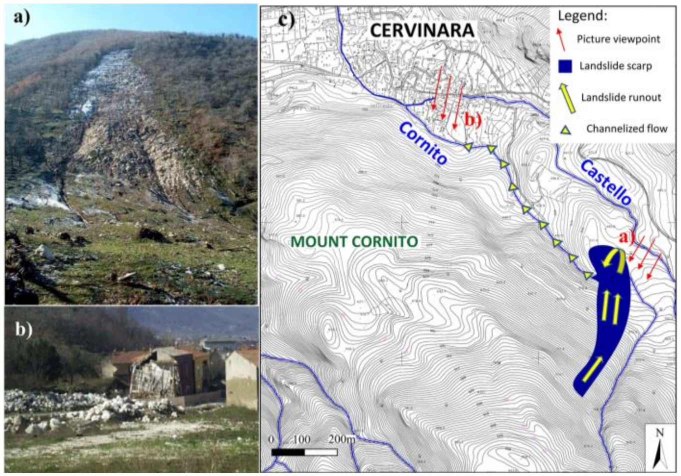

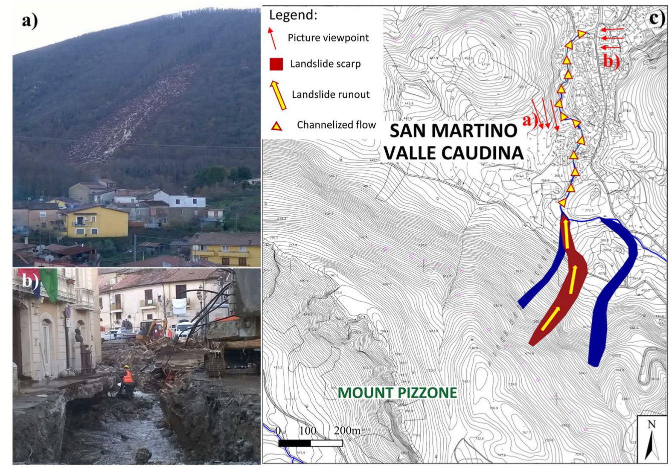

The rainfall of 2019 was characterized by longer duration and smaller depth: only one large landslide was triggered.

Event	H (mm)	D (h)	I (mm/h)
1999	309	46	6.7
2019	280	58	4.8

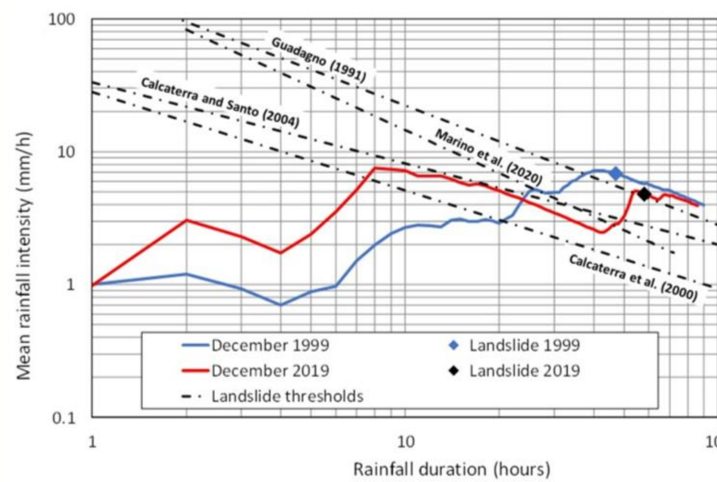

Simulation of the landslides of 1999

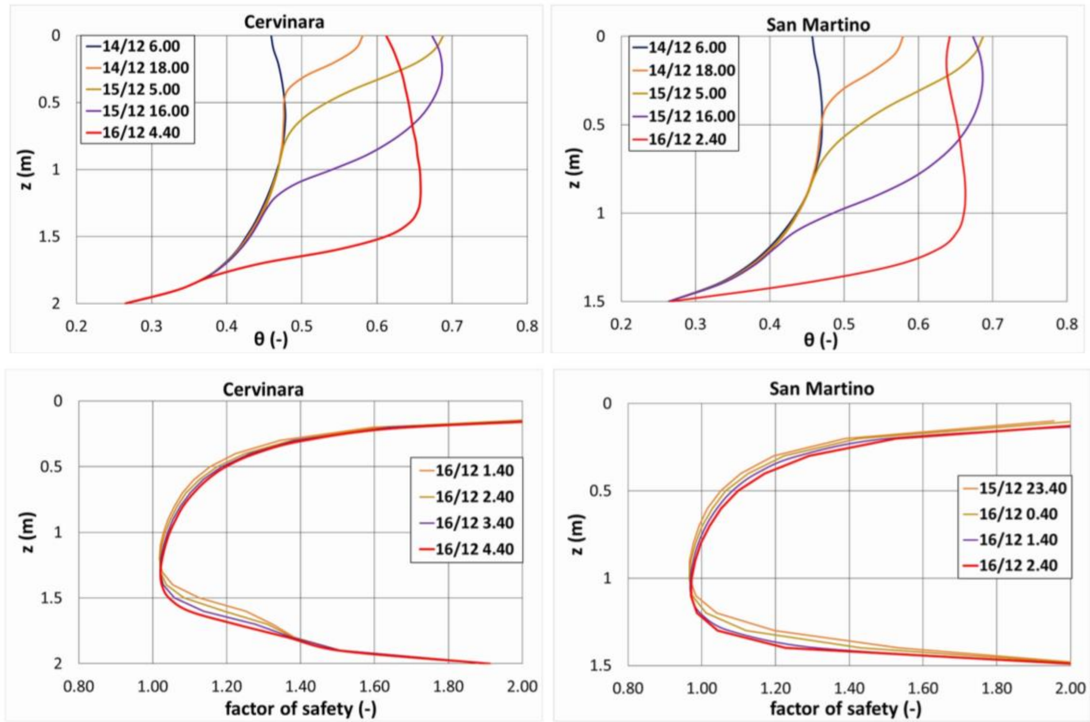

During the rain event of 15 December 1999, both the slopes experienced critical conditions ($FS \cong 1.0$ at Cervinara, and $FS < 1.0$ at S. Martino), as confirmed by the diffuse landsliding in the whole area.

Simulation of the landslide of 2019

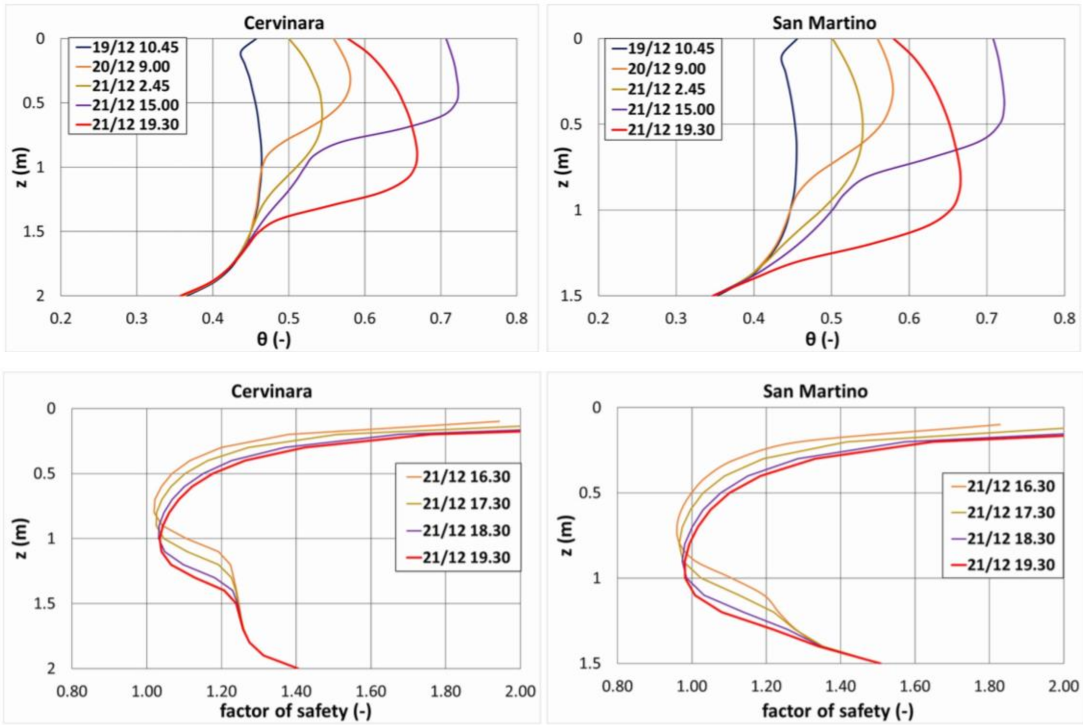

During the event of 21 December 2019, only the slope of S. Martino attained critical conditions (*FS* < 1.0), while at Cervinara, in the depth range where the failure surface occurs (around 0.5m above the bedrock), *FS* remained > 1.0.

Hydrometeorological thresholds for landslide early warning

Empirical thresholds for landslide initiation, to be implemented in early warning systems, are usually defined with an empirical statistical approach.
Based on the values of two (or more) suitable variables, the threshold is drawn as a line (which aims at) separating **positives** (dots corresponding to landslide occurrence) from **negatives** (dots without landslides).

Whatever the variables representing the characteristics of the event, this approach requires a rich dataset, with both negatives and positives, rarely available.
The issue of data scarcity is often addressed enlarging the area where the data are collected. The drawback is that data from heterogeneous geomorphological contexts are mixed.
An alternative way may be the recourse to the generation of **synthetic datasets**.

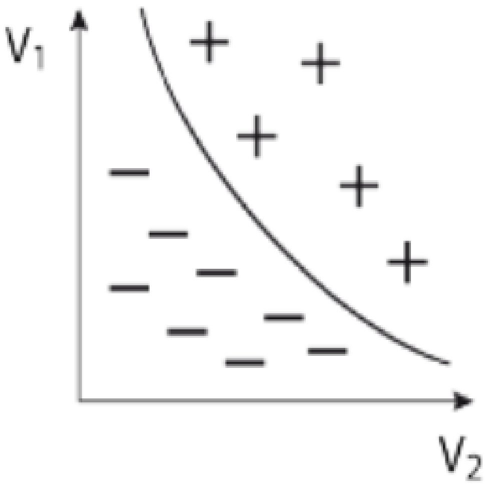

Marino et al., Landslides 2020

Hydrometeorological thresholds for landslide early warning

The Neyman-Scott Rectangular Pulse stochastic model of precipitation, calibrated based on a 17 years-long rainfall record at 10 min resolution, has been used to generate a 1000 years long synthetic series of rainfall at hourly resolution.

It randomly generates the initiation of rainfall events, the number of rain cells in an event, the duration of the event and thus, the rainfall intensity.

1. STOCHASTIC RAINFALL GENERATION
2. PHYSICALLY-BASED MATHEMATIC MODELLING
3. RAINFALL-TRIGGERED LANDSLIDE DEFINITION
4. SYNTHETIC DATASET

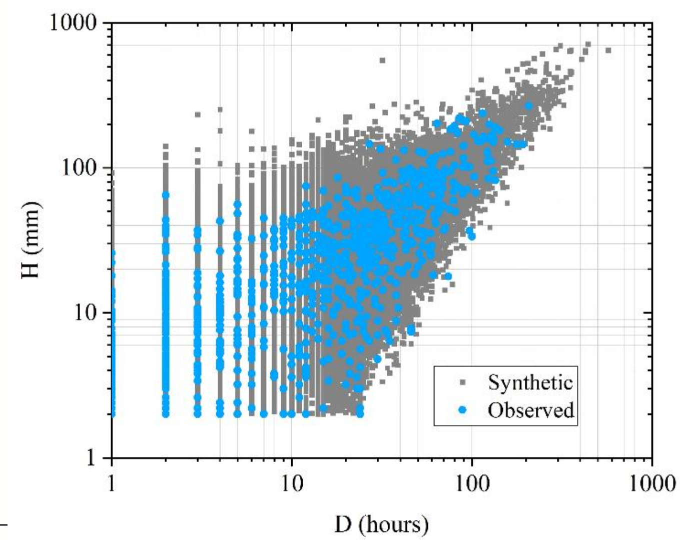

Marino et al., Landslides 2020
Romàn Quintero et al., Egusphere 2023

Hydrometeorological thresholds for landslide early warning

The physically based model, calibrated based on field monitoring data, has been run with this precipitation input, so to obtain a **1000 years long synthetic series** of slope response to weather forcing.

1. STOCHASTIC RAINFALL GENERATION
2. PHYSICALLY-BASED MATHEMATIC MODELLING
3. RAINFALL-TRIGGERED LANDSLIDE DEFINITION
4. SYNTHETIC DATASET

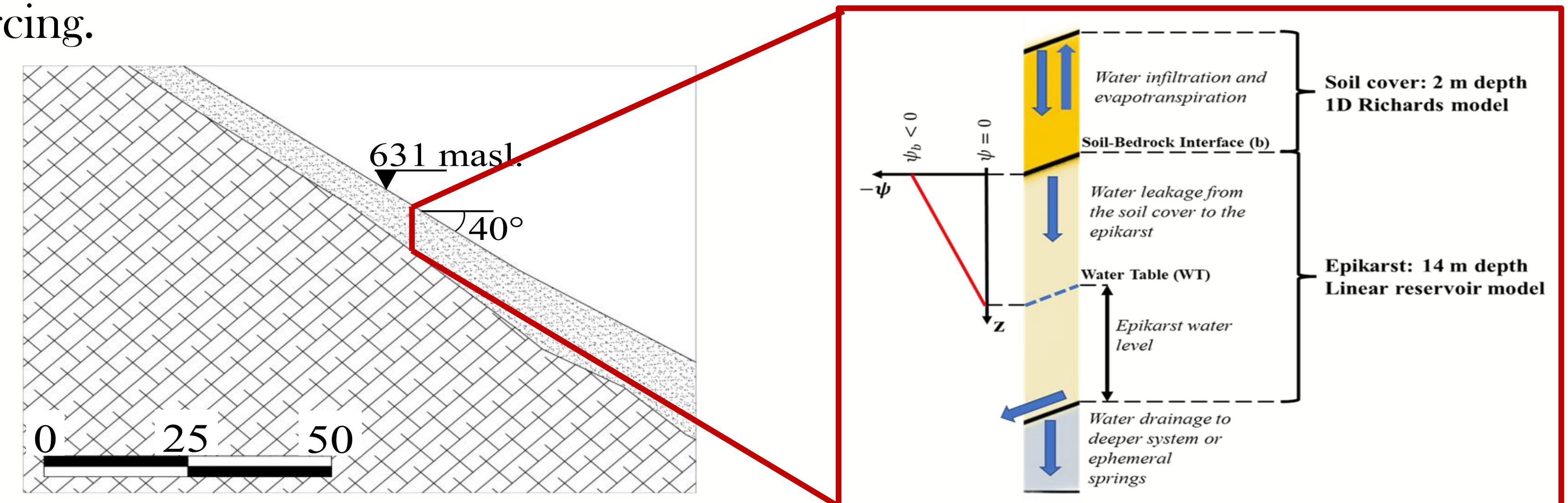

Hydrometeorological thresholds for landslide early warning

1. STOCHASTIC RAINFALL GENERATION
2. PHYSICALLY-BASED MATHEMATIC MODELLING
3. RAINFALL-TRIGGERED LANDSLIDE DEFINITION
4. SYNTHETIC DATASET

The slope equilibrium is analysed under the infinite slope assumption.
42 landslides within the 1000 years dataset (Factor of safety (FS) < 1.1).

- Soil effective cohesion: $c' = 0$ kPa
- Soil effective shear strength angle: $\phi' = 37°$
- Slope inclination angle: $\beta = 40°$
- Soil suction: s
- Unit weight of wet soil: γ
- Depth to failure surface: d
- Unit weight of water: γ_w
- Bishop's effective stress parameter: χ

$$\mathrm{FS} = \frac{c' + \gamma d \cos^2 \beta \tan \phi' - \chi \gamma_w s \tan \phi'}{\gamma d \sin \beta \cos \beta}$$

Marino et al., Landslides 2020
Romàn Quintero et al., EGUsphere 2023

Hydrometeorological thresholds for landslide early warning

The synthetic series consists of soil suction and water content at various depths throughout the soil cover, leakage through the soil-bedrock interface, groundwater level in the perched aquifer.

Assuming a separation interval of at least 24 hours with less than 2 mm rain, 53061 rainfall events are obtained, with durations ranging between 1 and 570 hours, and total rainfall depth between 2 and 710 mm.

1. STOCHASTIC RAINFALL GENERATION
2. PHYSICALLY-BASED MATHEMATIC MODELLING
3. RAINFALL-TRIGGERED LANDSLIDE DEFINITION
4. SYNTHETIC DATASET

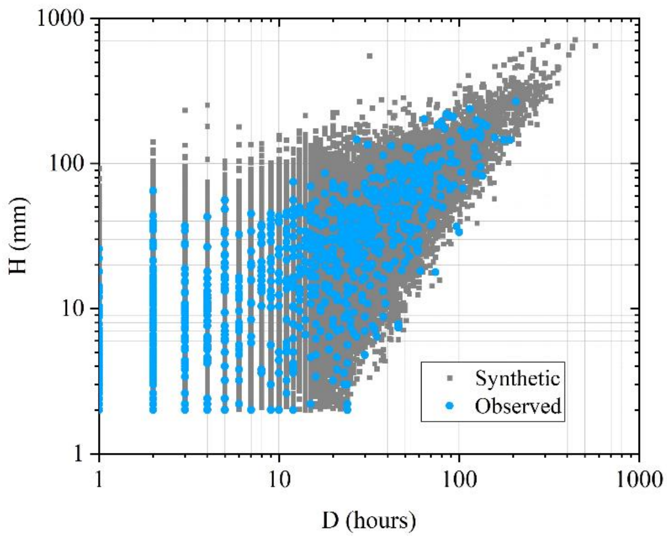

Marino et al., Landslides 2020
Romàn Quintero et al., EGUsphere 2023

Hydrometeorological thresholds for landslide early warning

1. STOCHASTIC RAINFALL GENERATION
2. PHYSICALLY-BASED MATHEMATIC MODELLING
3. RAINFALL-TRIGGERED LANDSLIDE DEFINITION
4. SYNTHETIC DATASET

Rain events are associated to landslides to obtain the subsets of positives (events triggering landslides) and negatives (events without landslides).

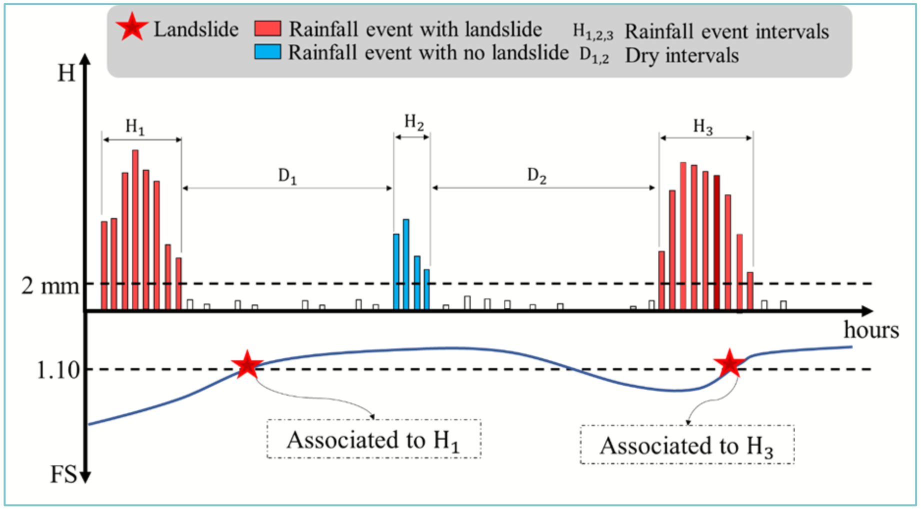

Marino et al., Landslides 2020
Romàn Quintero et al., EGUsphere 2023

Hydrometeorological thresholds for landslide early warning

The antecedent conditions of the slope before each rain event are assessed by means of aquifer level, h_a, and root zone soil moisture, θ, one hour before the onset of the rain event.

1. STOCHASTIC RAINFALL GENERATION
2. PHYSICALLY-BASED MATHEMATIC MODELLING
3. RAINFALL-TRIGGERED LANDSLIDE DEFINITION
4. SYNTHETIC DATASET

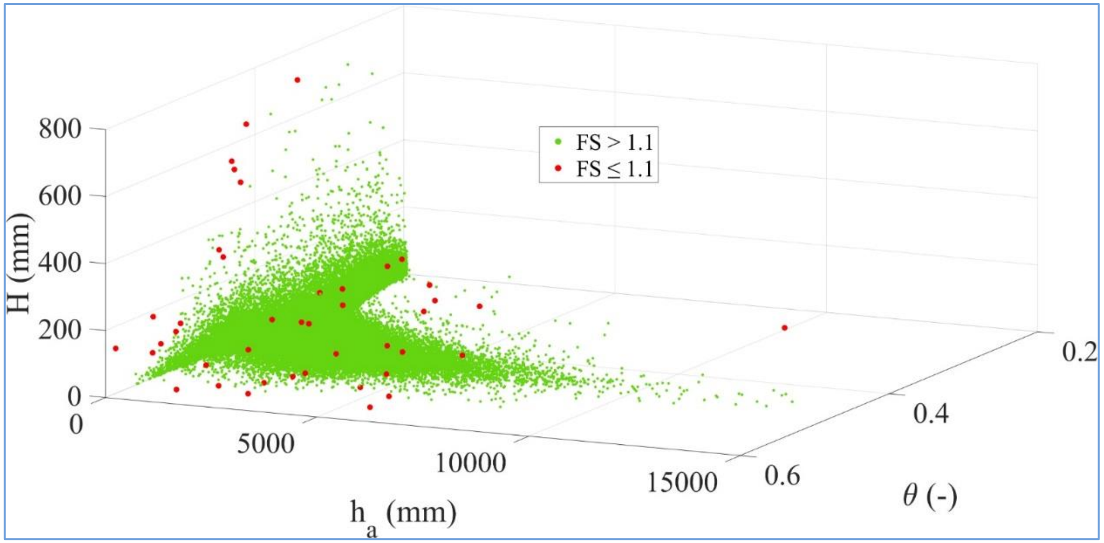

Marino et al., Landslides 2020

Hydrometeorological thresholds for landslide early warning

The thresholds are identified by maximizing the true skill statistic, *TSS*.

$$TSS = 1 - \frac{M}{P} - \frac{F}{N}$$

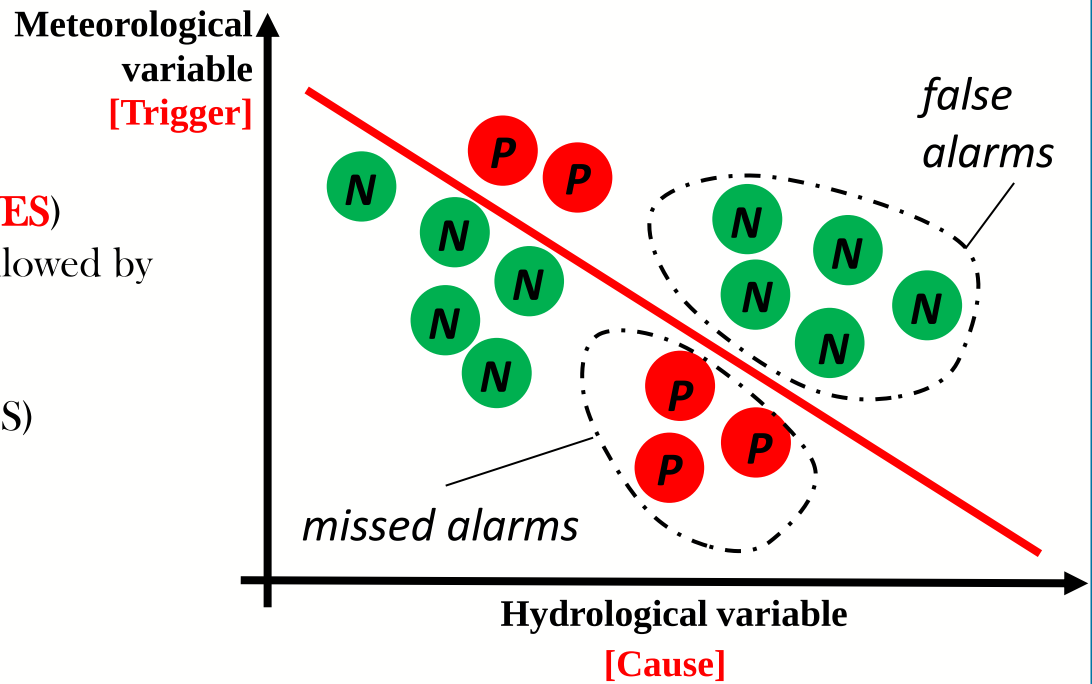

P = total number of landslides (POSITIVES)
N = total number of rainfall events not followed by any landslide (NEGATIVES)
F = false alarms (FALSE POSITIVES)
M = missed alarms (FALSE NEGATIVES)

$\boldsymbol{TSS = 1}$ →

$\boldsymbol{TSS = -1}$ →

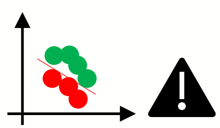

Hydrometeorological thresholds for landslide early warning

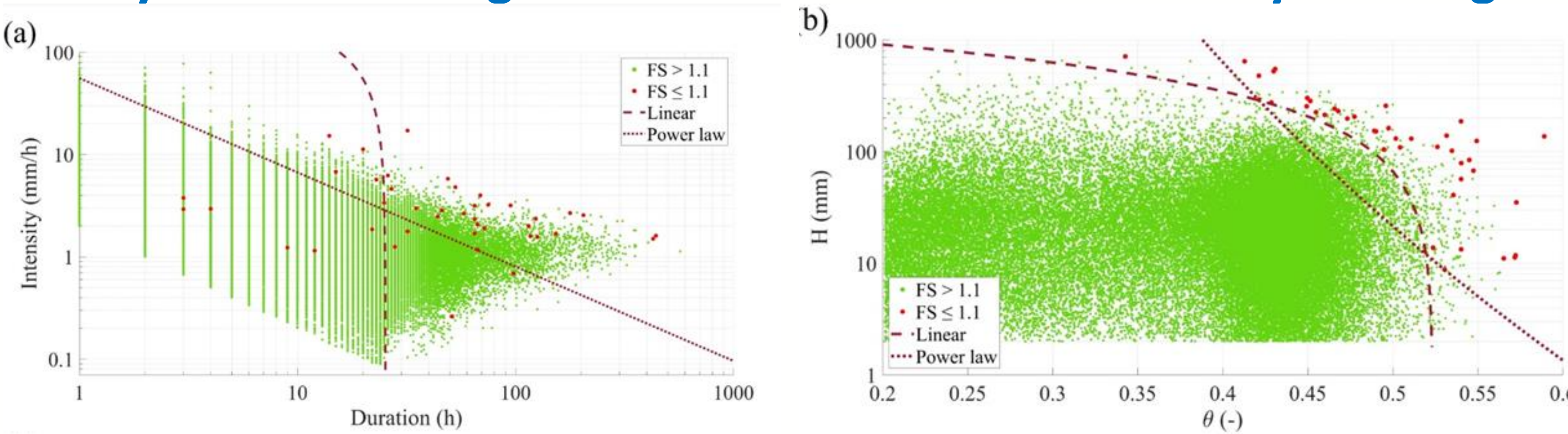

The 2D hydrometeorological thresholds, based on antecedent root-zone soil moisture, largely outperform the purely meteorological ones.

Threshold type	Missed alarms	False alarms	TSS
Meteorological linear	10	12484	0.526
Meteorologicalpower-law	10	3655	0.693
Hydrometeteorological linear	0	274	0.995
Hydrometeorological power-law	1	1346	0.951

Hydrometeorological thresholds for landslide early warning

A 3D hydrometeorological thresholds, based on antecedent root-zone soil moisture and aquifer level, further improves the predictive skill.

Equation	a	b	h_x (m)	TSS	Missed alarms	False alarms
$H_1 = a_1\theta + b_1$, with $h_a < h_x$	-2519	1331	2.3	0.997	0	130
$H_2 = a_2\theta + b_2$, with $h_a \geq h_x$	-2300	1281				

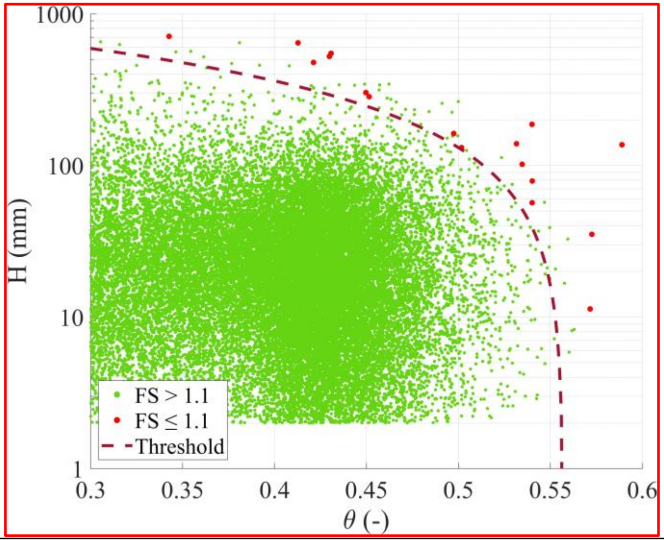

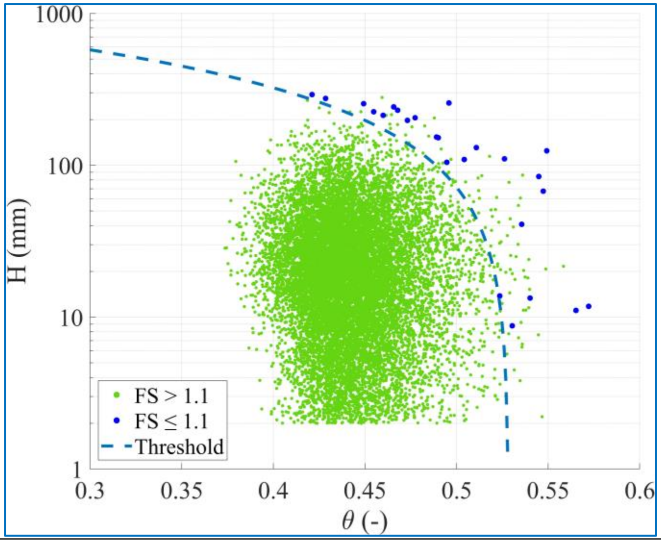

Understanding the processes leading to landslides

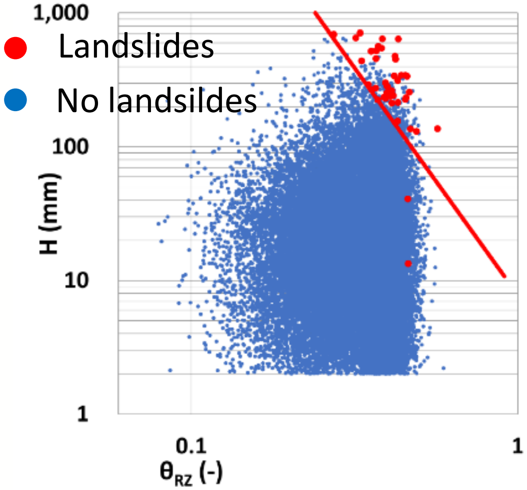

- Landslides triggered by saturation from the bottom (leakage impeded)
- Landslides triggered by saturation from the top
- No landslides

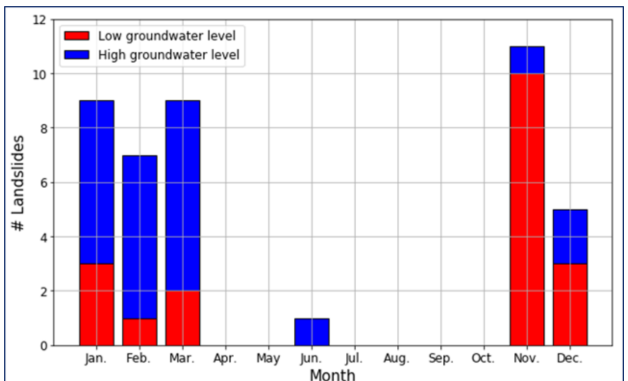

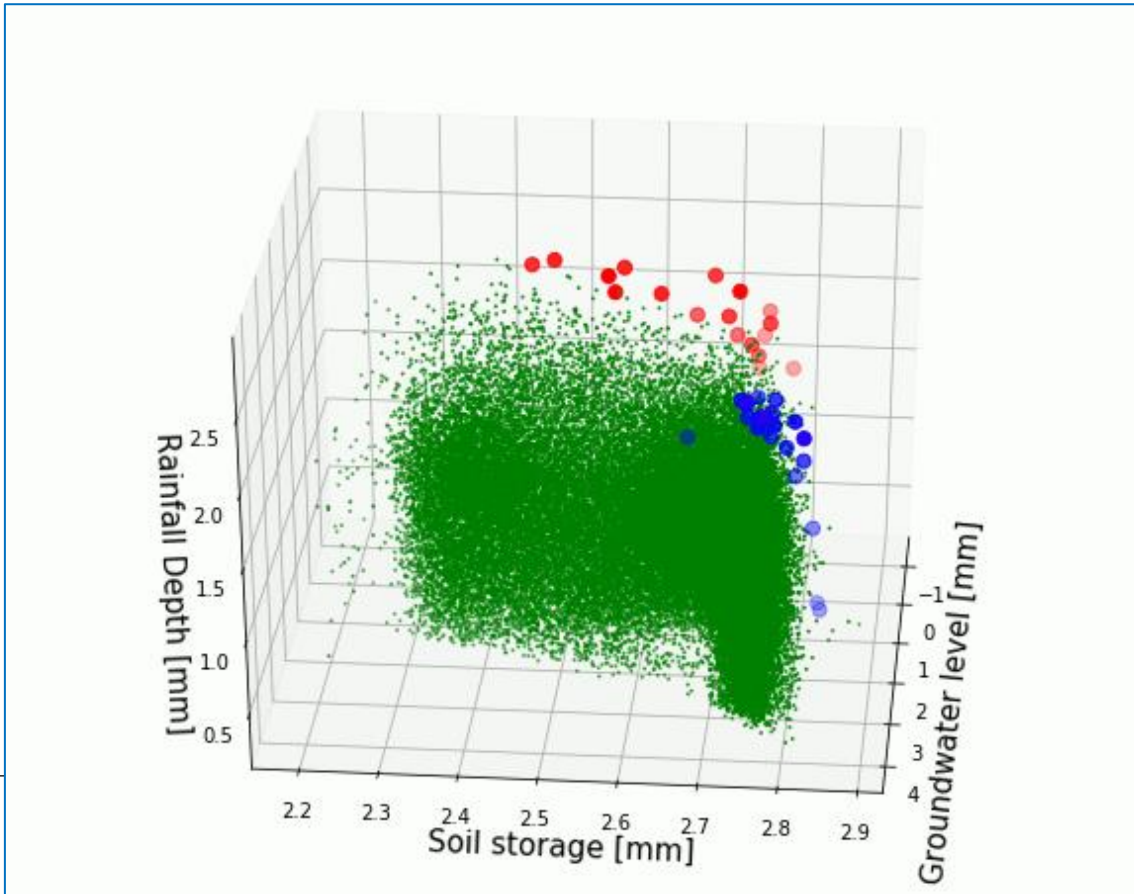

Università
degli Studi
della Campania
Luigi Vanvitelli

References

Allocca V, Manna F, De Vita P (2014). Estimating annual groundwater recharge coefficient for karst aquifers of the southern Apennines (Italy), Hydrol Earth Syst Sci 18: 803-817.

Bogaard TA, Greco R (2016). Landslide hydrology: from hydrology to pore pressure. WIREs Water 3(3): 439-459.

Bogaard TA, Greco R (2018). Invited perspectives: Hydrological perspectives on precipitation intensity-duration thresholds for landslide initiation: proposing hydro-meteorological thresholds. Nat Haz Earth Syst Sci 18(1): 31-39.

Børgesen CD, Jacobsen OH, Hansen S, Schaap MG (2006). Soil hydraulic properties near saturation, an improved conductivity model. J Hydrol 324: 40-50.

Cascini L, Cuomo S, Guida D (2008). Typical source areas of May 1998 flow-like mass movements in the Campania region, Southern Italy, Eng Geol, 96: 107-125.

Celico F, Naclerio G, Bucci A, Nerone V, Capuano P, Carcione M, Allocca V, Celico P (2010). Influence of pyroclastic soil on epikarst formation: a test study in southern Italy. Terra Nova, 22: 110-115.

Thank you for your attention!

References (continued)

Damiano E, Olivares L, Picarelli L (2013). Steep-slope monitoring in unsaturated pyroclastic soils. Eng Geo 137-138: 1-12.

Feddes RA, Kowalik P, Kolinska-Malinka K, Zaradny H (1976). Simulation of fieldwater uptake by plants using a soil water dependent root extraction function. J Hydrol 31(1): 13-26.

Greco R, Comegna L, Damiano E, Guida A, Olivares L, Picarelli L (2013). Hydrological modelling of a slope covered with shallow pyroclastic deposits from field monitoring data. Hydrol Earth Syst Sci 17: 4001-4013.

Greco R, Comegna L, Damiano E, Marino P, Olivares L, Santonastaso GF (2021). Recurrent rainfall-induced landslides on the slopes with pyroclastic cover of Partenio Mountains (Campania, Italy): Comparison of 1999 and 2019 events. Eng Geo 288: 106160.

Greco R, Marino P, Santonastaso GF, Damiano E (2018). Interaction between perched epikarst aquifer and unsaturated soil cover in the initiation of shallow landslides in pyroclastic soils. Water, 10(7): 948.

References (continued)

Guzzetti F, Peruccacci S, Rossi M, Stark CP (2007). Rainfall thresholds for the initiation of landslides in central and southern Europe, Meteorol Atmos Phys 98: 239–267.

Hartmann A, Goldscheider N, Wagener T, Lange J, Weiler M (2014). Karst water resources in a changing world: Review of hydrological modeling approaches. Rev Geophys 52: 218-242.

Hendrickx JMH, Flury M (2001). Uniform and preferential flow mechanisms in the vadose zone. In: Conceptual Models of Flow and Transport in the Fractured Vadose Zone. Washington, DC: National Academy Press; 149–187.

Marino P, Comegna L, Damiano E, Olivares L, Greco R (2020). Monitoring the hydrological balance of a landslide-prone slope covered by pyroclastic deposits over limestone fractured bedrock. Water 12: 3309.

Marino, P., Peres, D.J., Cancelliere, A., Greco, R., Bogaard, T.A. (2020). Soil moisture information can improve shallow landslide forecasting using the hydrometeorological threshold approach. Landslides 17: 2041-2054.

Thank you for your attention!

References (continued)

Marino P, Santonastaso GF, Fan X, Greco R (2021). Prediction of shallow landslides in pyroclastic-covered slopes by coupled modeling of unsaturated and saturated groundwater flow, Landslides 18,: 31-41.

Meixner T, Manning AH, Stonestrom DA, Allen DM, Ajami H, Blasch KW, Brookfield AE, Castro CL, Clark JF, Gochis DJ, Flint AL, Neff KL, Niraula R, Rodell M, Scanlon BR, Singham K, Walvoord MA (2016). Implications of projected climate change for groundwater recharge in the western United States. J Hydrol, 534: 124-138.

Mirus B, Morphew M, Smith J (2018) Developing Hydro-Meteorological Thresholds for Shallow Landslide Initiation and Early Warning. Water, 10: 1274.

Romàn Quintero D, Marino P, Santonastaso GF, Greco R (2023) Understanding hydrologic controls of sloping soil response to precipitation through Machine Learning analysis applied to synthetic data. EGUsphere, https://doi.org/10.5194/egusphere-2022-1078 (preprint).

Thank you for your attention!

References (continued)

Sidle RC, Tsuboyama Y, Noguchi S, Hosoda I, Fujieda M, Shimizu T (2000). Stormflow generation in steep forested head-waters: a linked hydrogeomorphic paradigm. Hydrol Proc, 14: 369-385

Tromp-van Meerveld HJ, McDonnell JJ (2006). Threshold relations in subsurface stormflow: 2. The fill and spill hypothesis. Water Resour Res, 42: W02411.

Twarakavi NKC, Sakai M, Simunek J (2009). An objective analysis of the dynamic nature of field capacity. Water Resour Res, 45: W10410.

Zhao B, Dai Q, Han D, et al (2019) Probabilistic thresholds for landslides warning by integrating soil moisture conditions with rainfall thresholds. J Hydrol, 574: 276-287.

Thank you for your attention!

Water in soil

Saturated soil (two-phase medium)

Unsaturated soil (three-phase medium)

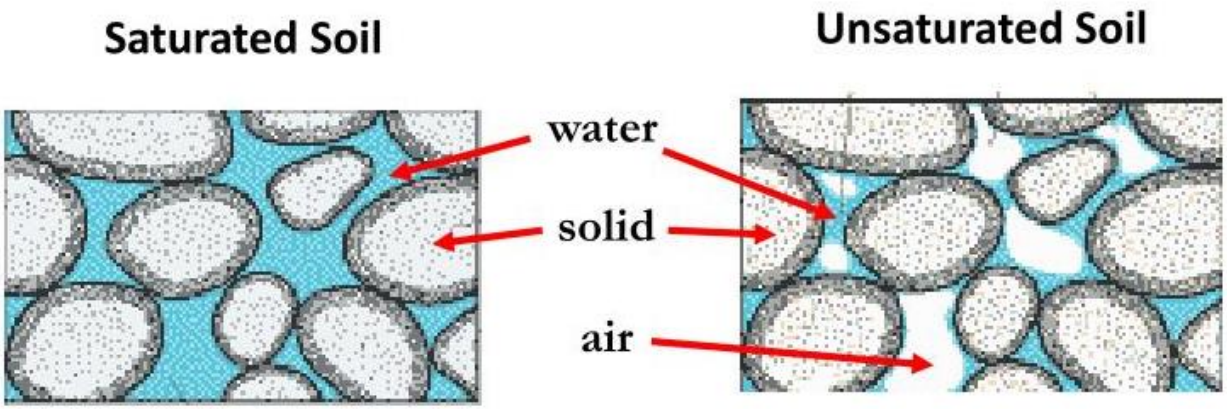

The homogeneous model of soil

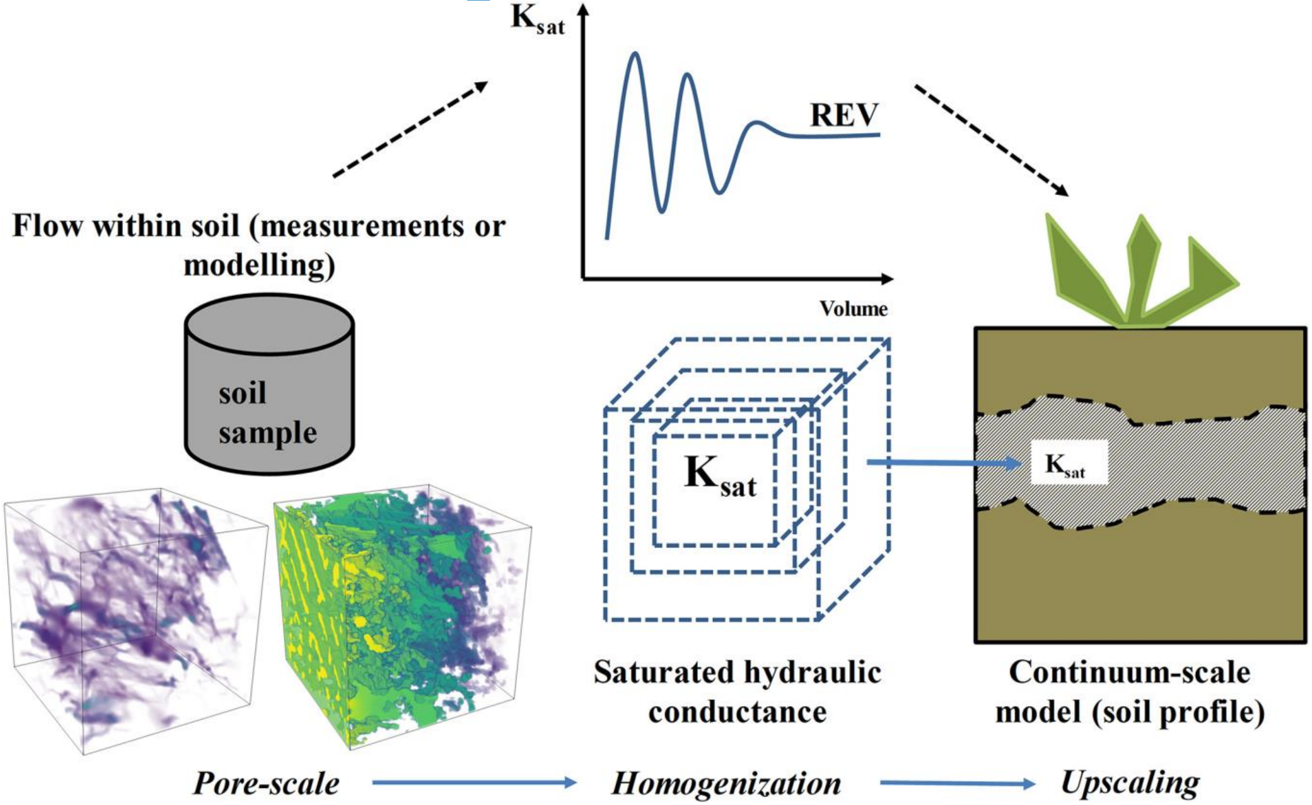

Any soil property refers to a Reference Elementary Volume (REV), over which soil properties are homogenized

The homogeneous model of soil

Saturated soil

At any point the two phases coexist, sharing the space according to soil porosity:

$$n = \frac{Volume\ of\ voids\ in\ REV}{Total\ volume\ of\ REV}$$

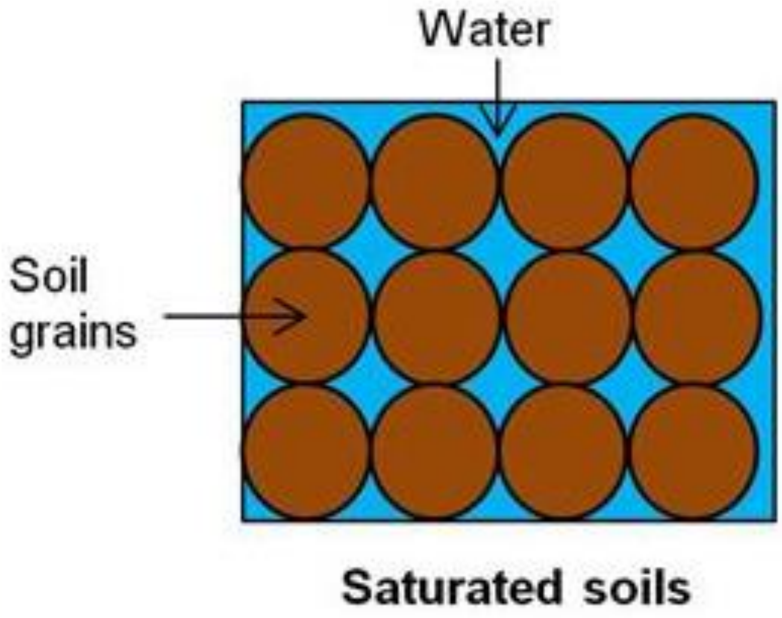

All variables are **continuum and derivable** in space and time.

The homogeneous model of soil

Unsaturated soil

At any point the three phases coexist, sharing the space according to soil porosity

$$n = \frac{Volume\ of\ voids\ in\ REV}{Total\ volume\ of\ REV}$$

and soil volumetric water content

$$\theta = \frac{Volume\ of\ water\ in\ REV}{Total\ volume\ of\ REV}$$

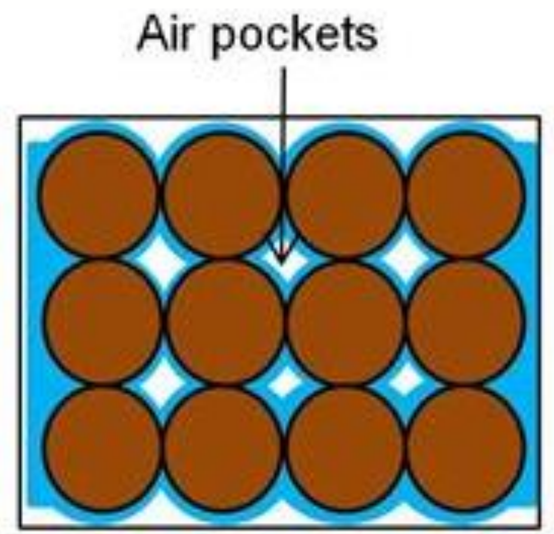

Unsaturated soils

All variables are **continuum and derivable** in space and time.

Potential energy of water in soil

Saturated soil

$$H = z + \frac{p_{wat} - p_{air}}{\gamma} = z + h$$

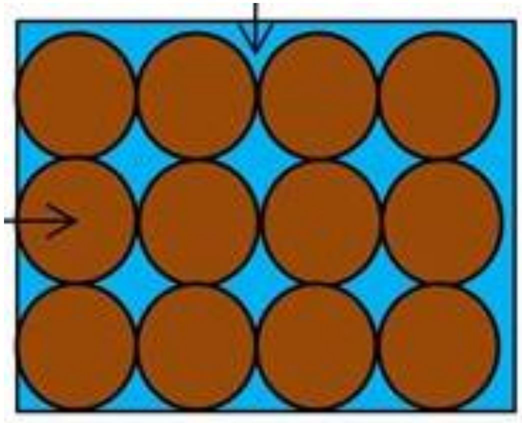

Unsaturated soil

$$H = z + \frac{p_c}{\gamma} = z + \psi$$

capillary pressure

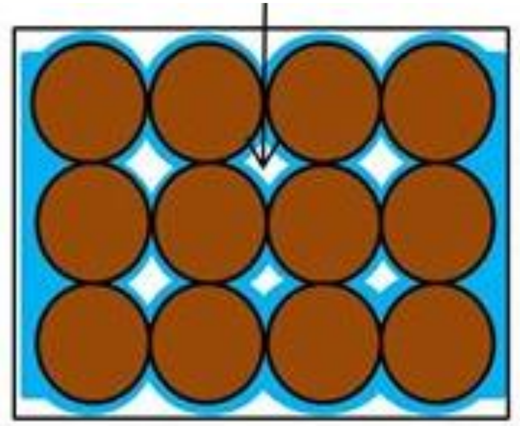

Capillarity in unsaturated soil

surface tension

$$\vec{F} = 2\pi\vec{T} \qquad \overrightarrow{S_{air}} = p_{air}\pi r^2\vec{k} \qquad \overrightarrow{S_{wat}} = p_{wat}\pi r^2\vec{k}$$

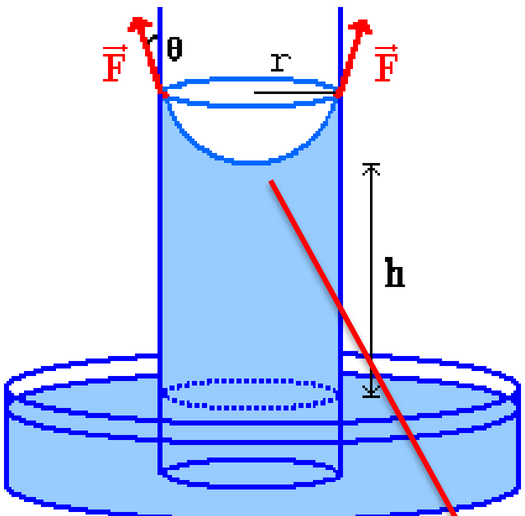

$$p_c = p_{air} - p_{wat} = \frac{2T\cos\vartheta}{r}$$

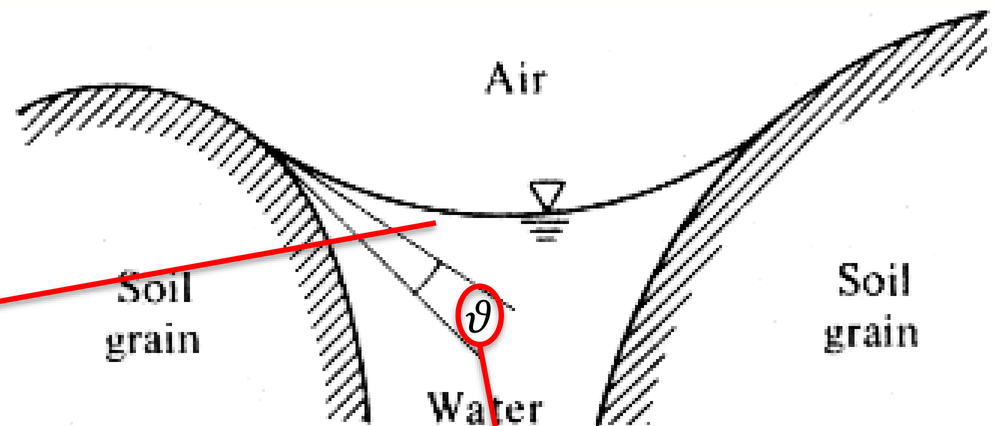

Equilibrium of a meniscus in a capillary tube and in a pore

contact angle due to water adhesion to solid surfaces

Water flow in soil

Saturated soil

saturated conductivity

$$\vec{\boldsymbol{q}} = k_{sat}\vec{\boldsymbol{\nabla}}H = k_{sat}\vec{\nabla}(z+h)$$

specific discharge

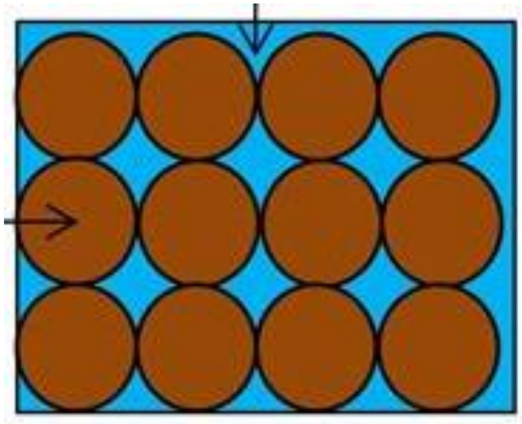

Unsaturated soil

$$\vec{\boldsymbol{q}} = k(\psi)\vec{\boldsymbol{\nabla}}H = k(\psi)\vec{\nabla}(z+\psi)$$

unsaturated conductivity

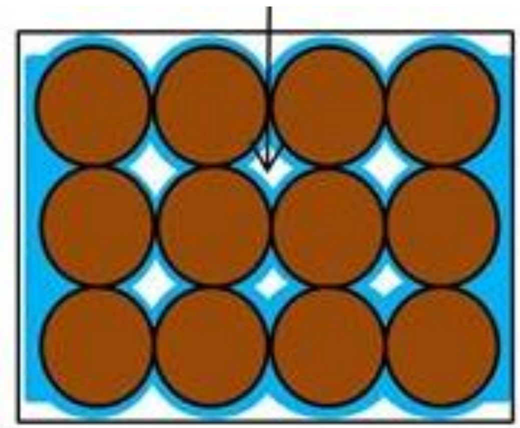

Water flow in unsaturated soil

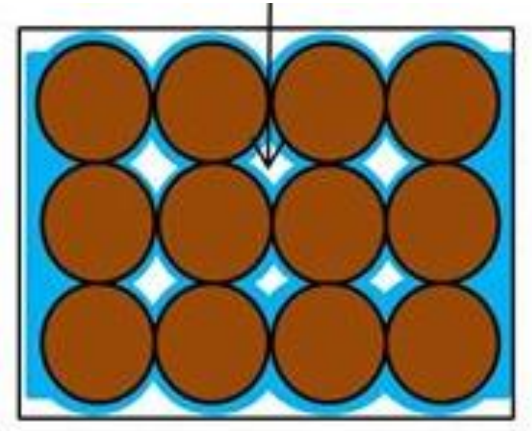

Flow equation:

$$\vec{\boldsymbol{q}} = k(\psi)\vec{\boldsymbol{\nabla}}H = k(\psi)\vec{\boldsymbol{\nabla}}(z+\psi)$$

Continuity equation:

$$\frac{\partial\theta}{\partial t} = \vec{\boldsymbol{\nabla}} \cdot \vec{\boldsymbol{q}}$$

$$\frac{\partial\theta}{\partial t} = \vec{\boldsymbol{\nabla}} \cdot \left[k(\psi)\vec{\boldsymbol{\nabla}}(z+\psi)\right]$$

Richards' equation

Hydraulic characteristic curves of unsaturated soil

$$\frac{\partial \theta}{\partial t} = \vec{\boldsymbol{\nabla}} \cdot \left[k(\psi) \vec{\boldsymbol{\nabla}} (z + \psi) \right]$$

Soil Water Retention Curve (SWRC)

$$\vartheta(\psi)$$

Hydraulic Conductivity Function (HCF)

$$k(\vartheta) \longrightarrow k(\psi)$$

Soil Water Retention Curve

Soil pores, with their variable shapes and dimensions, can be conceptually regarded as capillary tubes with different radii.

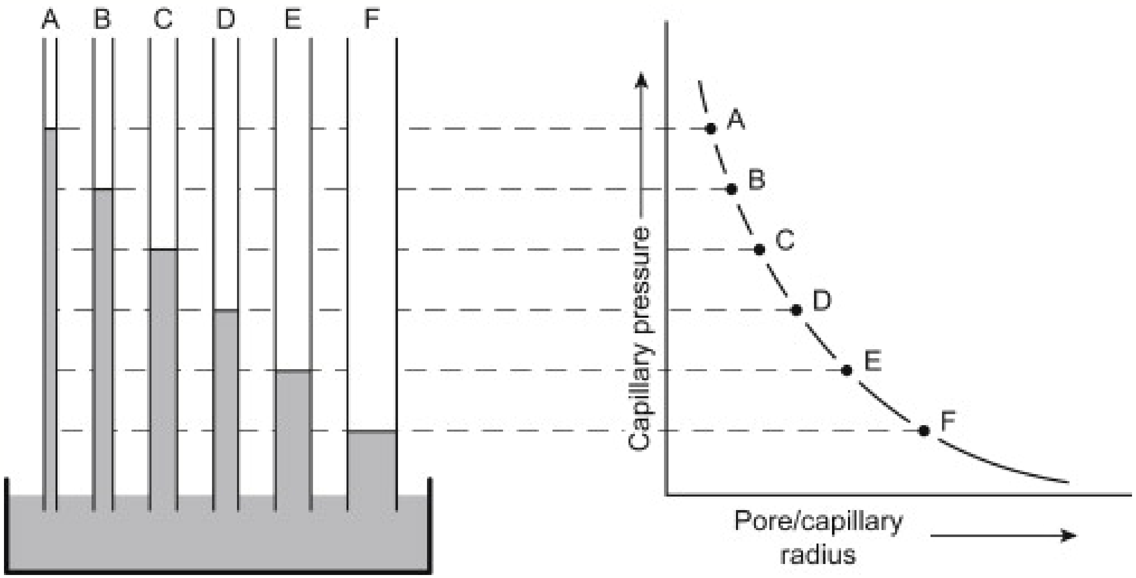

At a given capillary pressure, the equilibrium of menisci is possible only in pores of the corresponding dimension.

Soil Water Retention Curve

Consequently, the shape of the WRC of a soil is related to the distribution of dimensions (and shapes) of its pores.

Most soils exhibit a **residual water content**, due to a water retention mechanism, differnt from capillarity, called **adsorption**.

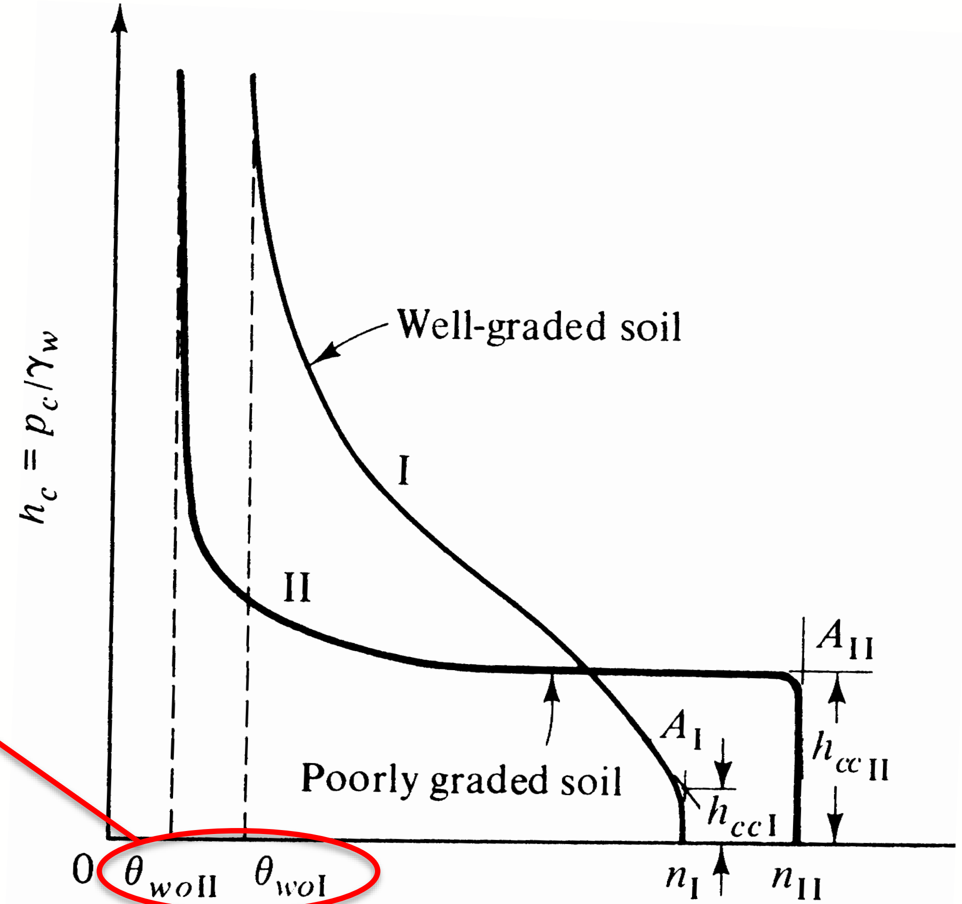

Soil Water Retention Curve

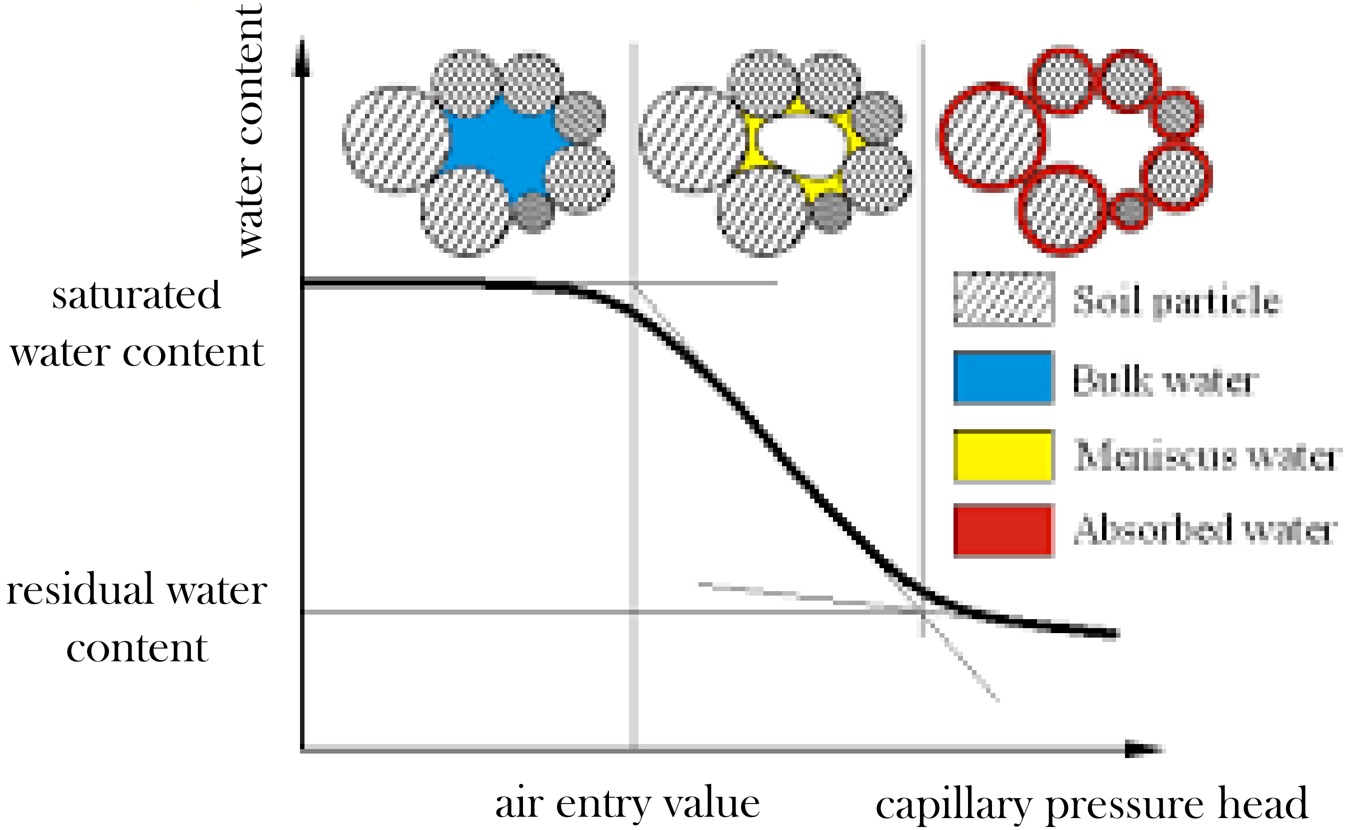

Different mechanisms of water retention in an unsaturated soil

Soil Water Retention Curve

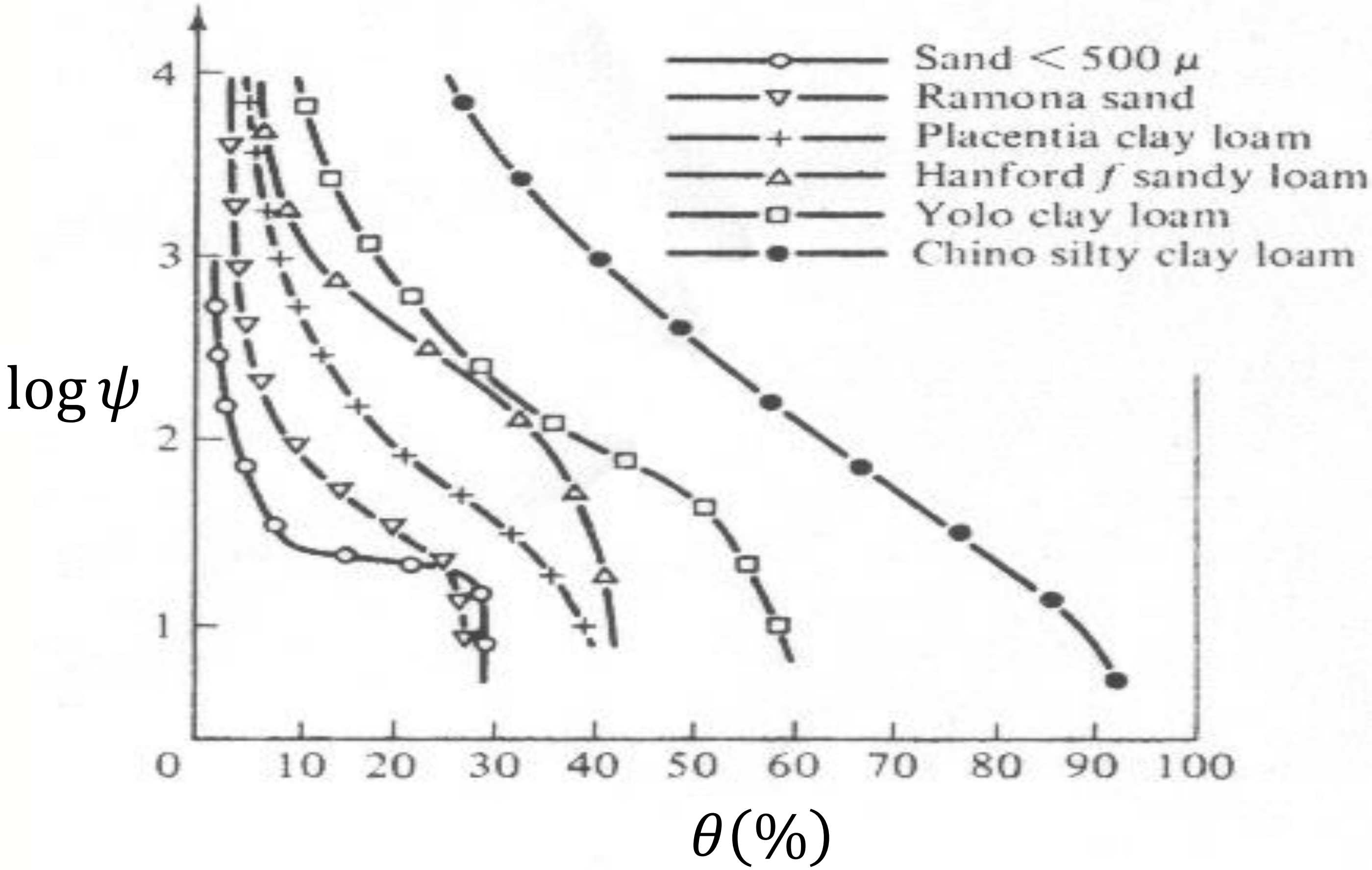

Hydraulic conductivity function

Water flow through soil pores follows narrow and tortuous paths

In an unsaturated soil, the presence of air makes the available paths narrower and more tortuous.

$$k_{sat} \gg k(\theta < \theta_{sat})$$

Hydraulic conductivity function

$k(\theta)$ HCF of different soils present similar shapes

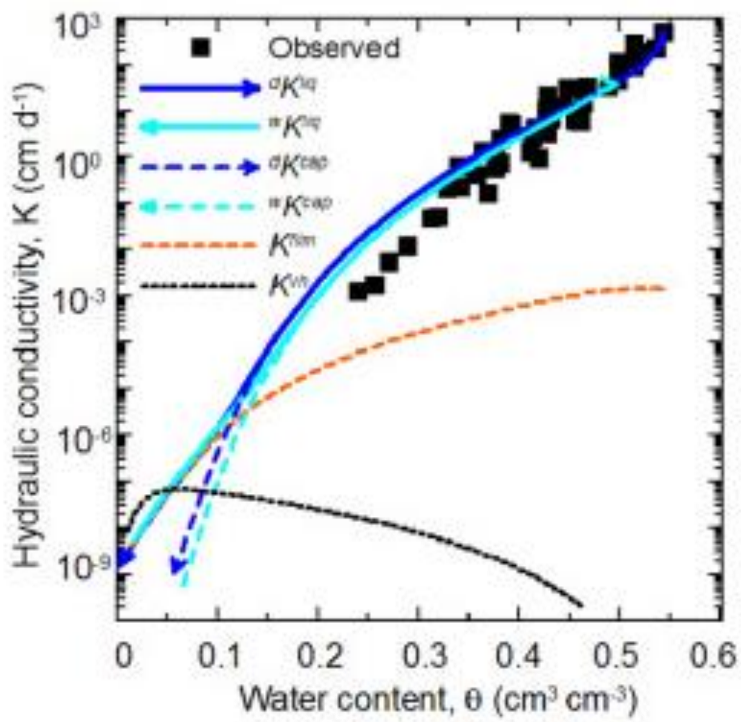

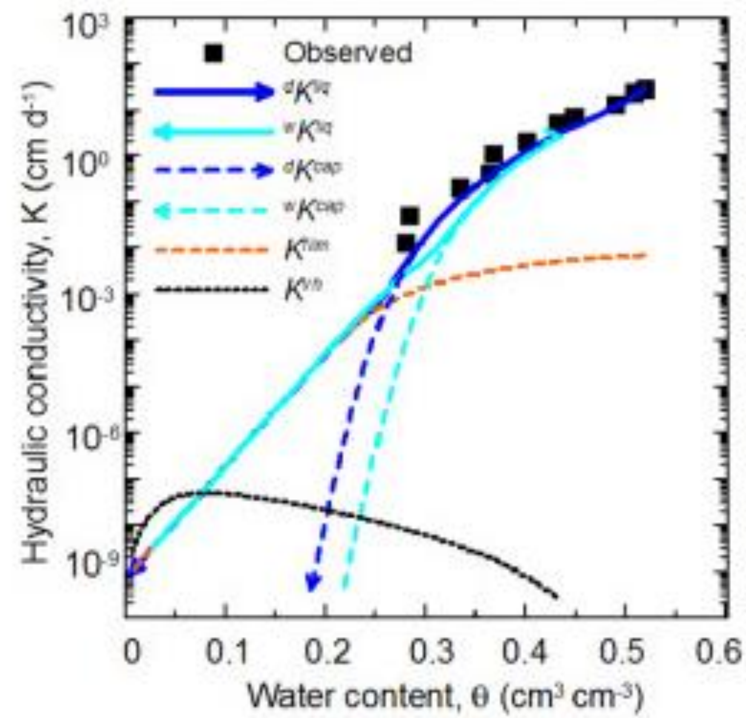

Hydraulic conductivity function

$k(\psi)$ HCF of different soils present quite different shape, according to the pore size distribution of the soil

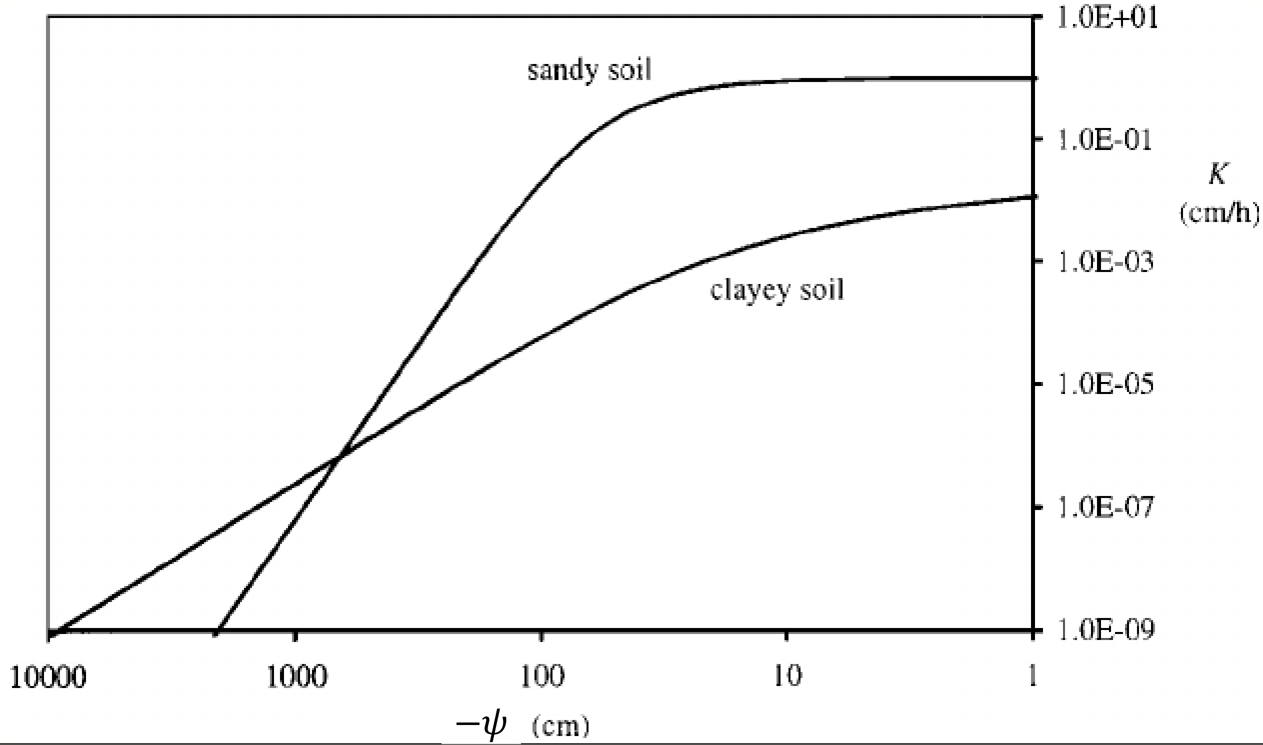

Models of soil hydraulic characteristic curves

Van Genuchten – Mualem model

SWRC
$$S_e(\psi) = \frac{1}{[1 + (\alpha|\psi|)^n]^m}$$

HCF
$$k(S_e) = k_{sat} S_e^{1/2} \left[1 - \left(1 - S_e^{1/m}\right)^m\right]^2$$

with
$$S_e = \frac{\theta - \theta_{res}}{\theta_{sat} - \theta_{res}} \qquad m = 1 - \frac{1}{n}$$

Soil water flow in the field

Even in homogeneous soil, **preferential flow** is the rule and not the exception

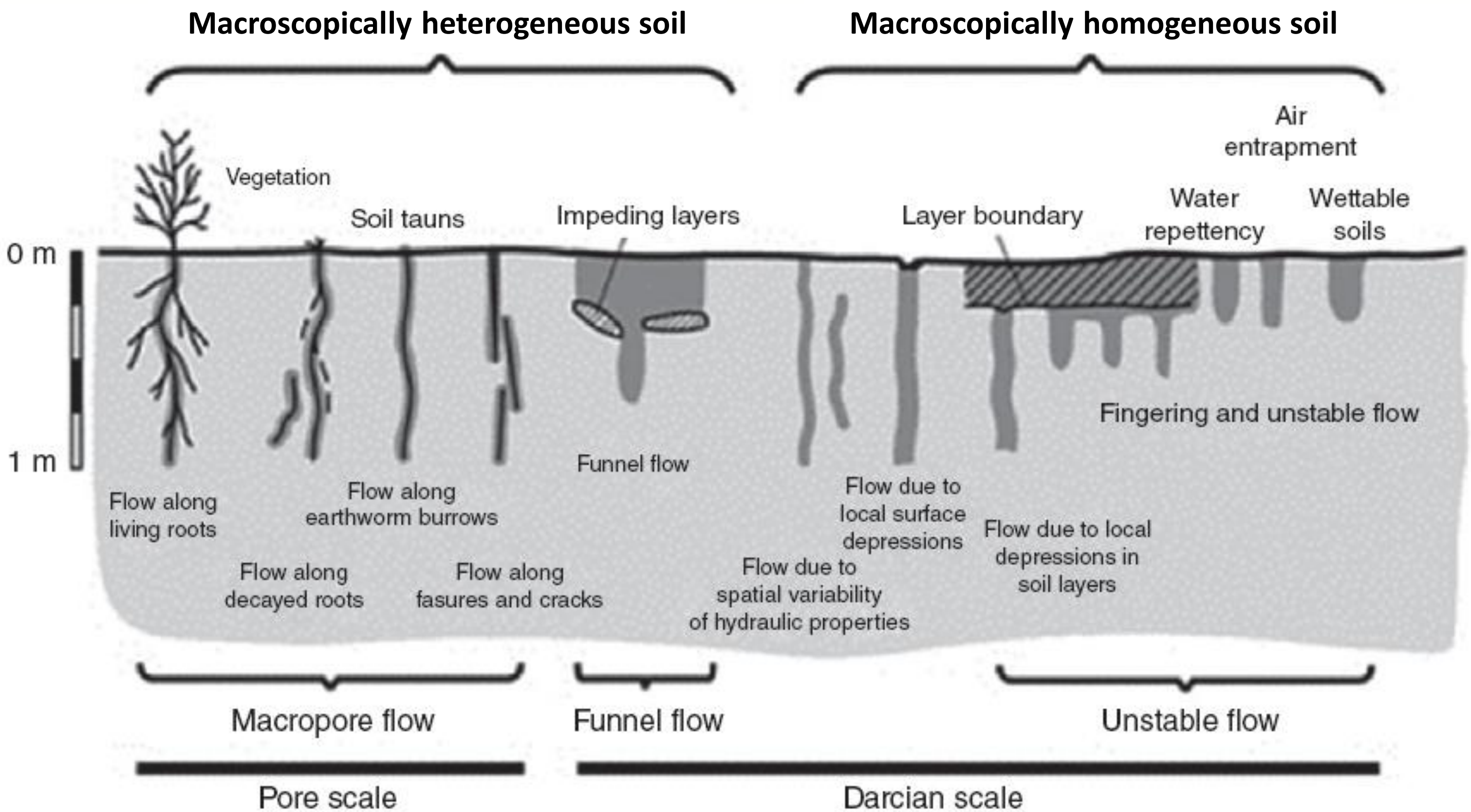

Hendricks and Flury, 2001

Preferential flow

Dye tracers allow visualizing preferential flow paths in the soil

Macropore flow

Fingered flow

Funneled flow

Soil hydraulic functions in the field

Macropores strongly affect soil hydraulic properties near saturation

> One Order of Magnitude

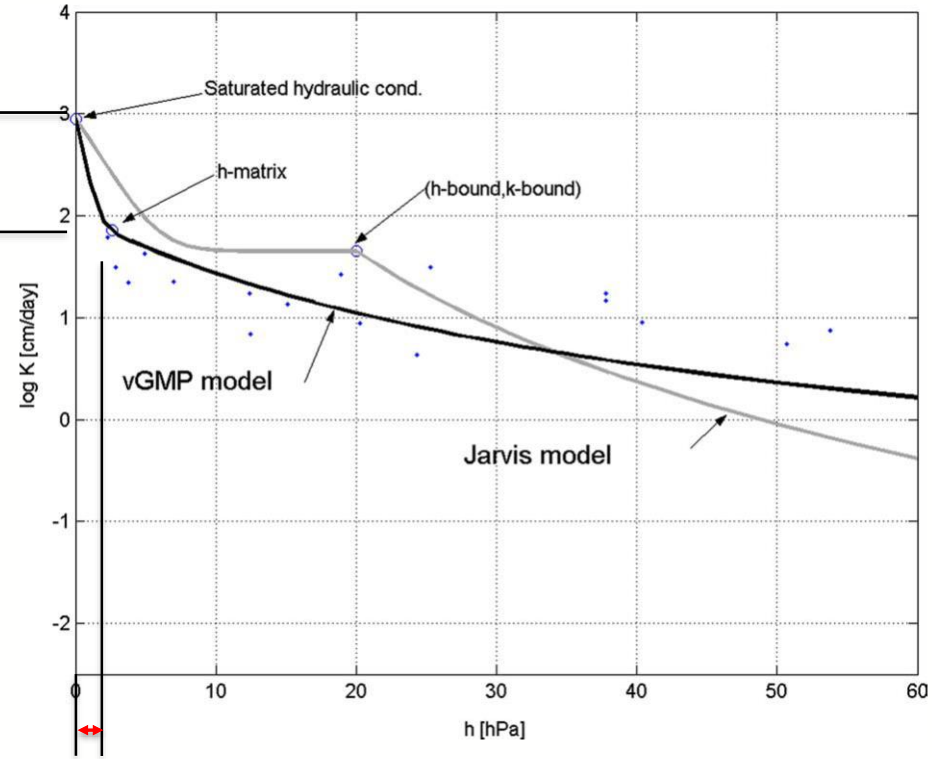

≈ 0.2 kPa

The REV is much larger!

Measurements must be taken on soil specimens much larger than usually adopted in the lab, depending on the kind of macropores.

Retention and conductivity models must be adapted

Børgesen et al., J Hydrol 2006

Empirical landslide hazard assessment for early warning

Based on the values of two (or more) suitable variables, ientification of a threshold as a line separating positives (dots corresponding to landslide occurrence) from negatives (dots without landslides).

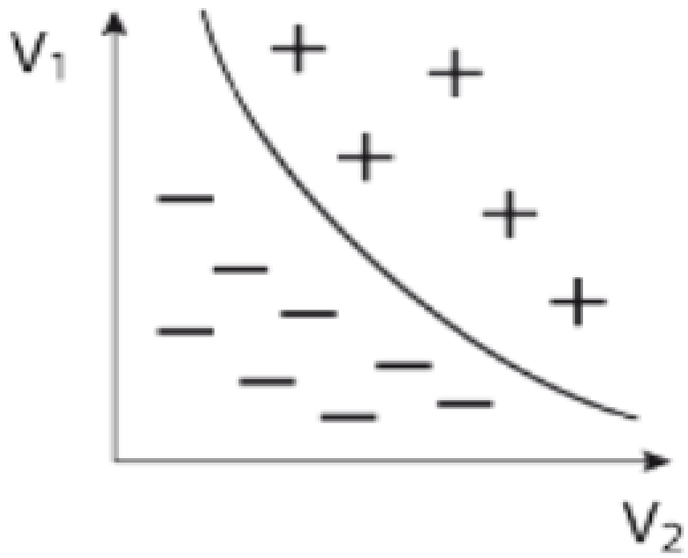

Empirical landslide hazard assessment for early warning

The complexity of factors and processes leading to landslides often results in a transition zone from negatives to positives, making uneasy the identification of the threshold line.

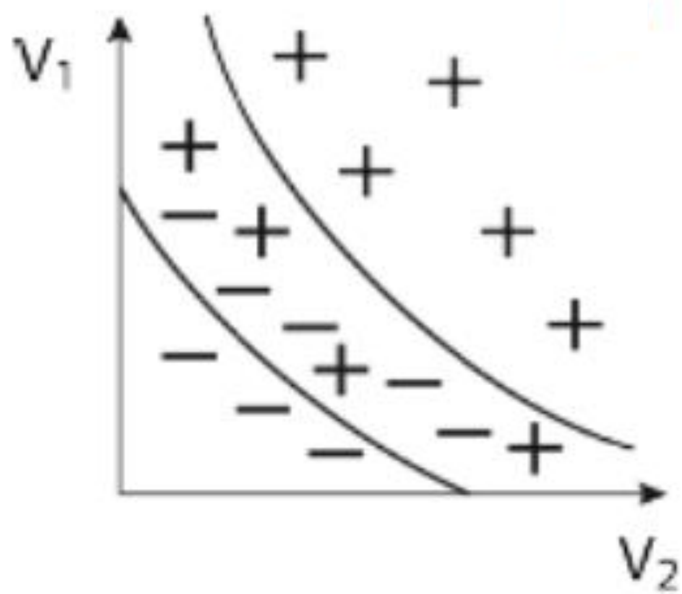

Empirical landslide hazard assessment for early warning

An effective threshold for hazard assessment should reduce as much as possible **missed alarms** and false alarms.

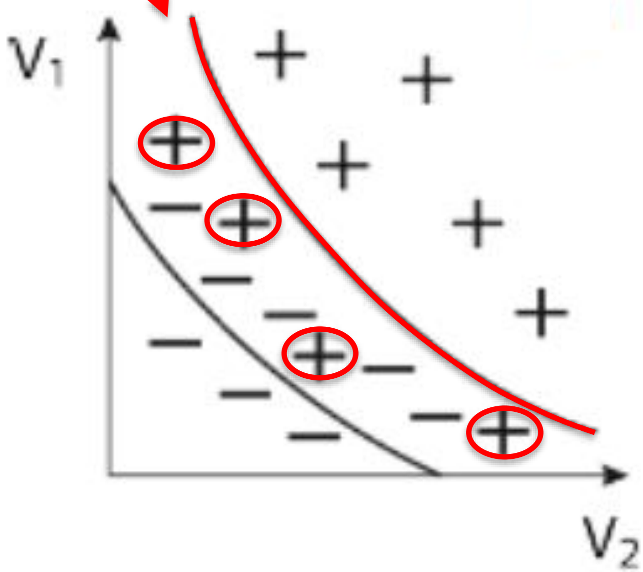

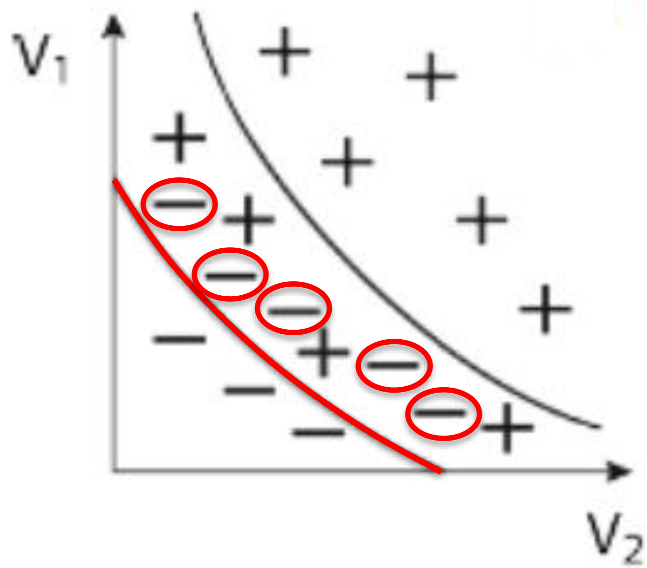

Empirical landslide hazard assessment for early warning

An effective threshold for hazard assessment should reduce as much as possible missed alarms and **false alarms**.

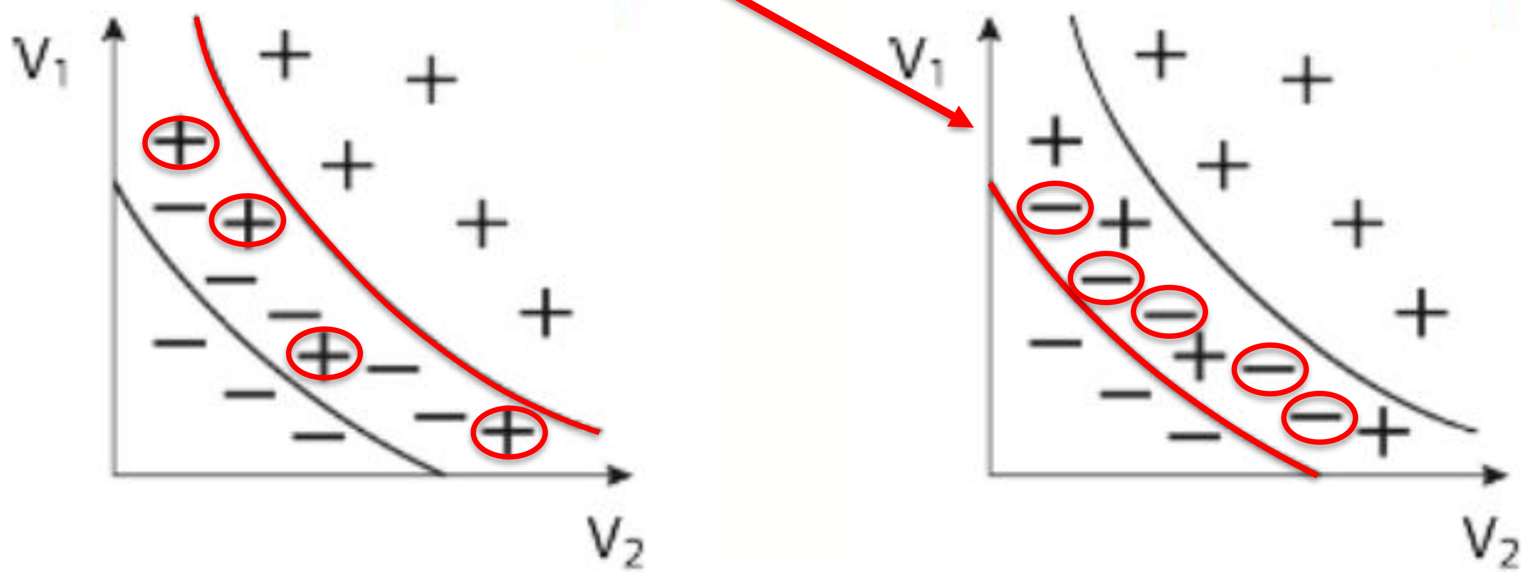

Empirical landslide hazard assessment for early warning

Owing to easy availability of rainfall data, landslide hazard assessment is frequently **based on precipitation (only)**, linking inventoried landslides with:

- Rainfall depth / intensity
- Rainfall duration or antecedent precipitation

These purely meteorological thresholds completely neglect the physical mechanism of landslide triggering, thus resulting in poor predictive performance.

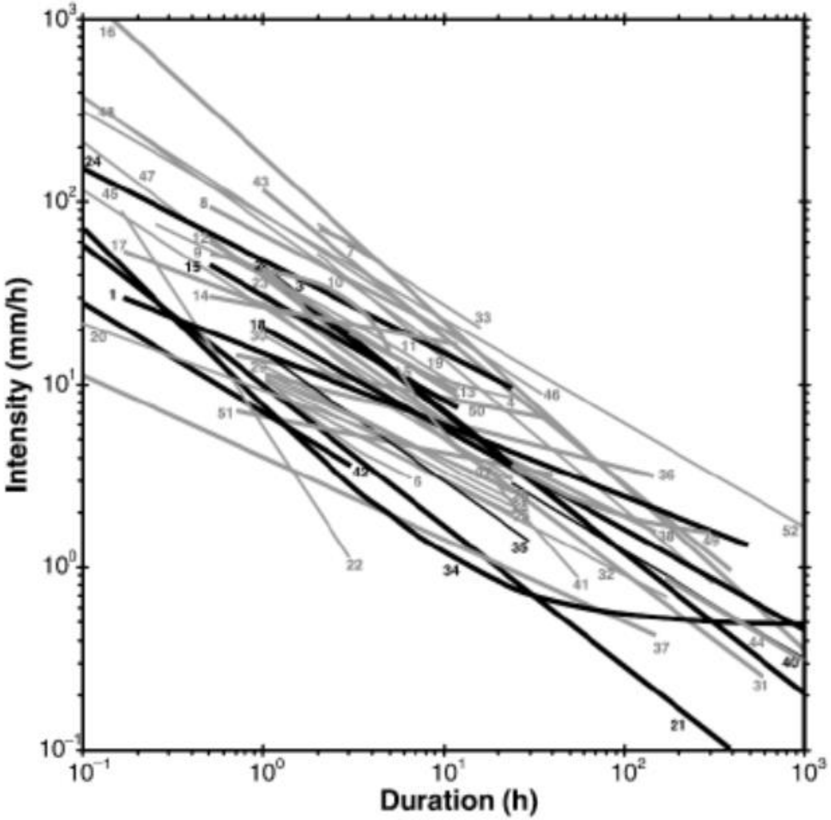

Modified after *Guzzetti et al, 2007*

Empirical landslide hazard assessment for early warning

Hydrometerological thresholds include variables suitable to quantify conditions predisposing the slopes to landslides, leading to reliable thresholds.

For shallow landslides, soil moisture has been successfully introduced together with event precipitation. Soil moisture can be estimated from:

- Field measurements
- Satellite products
- Hydrological modelling

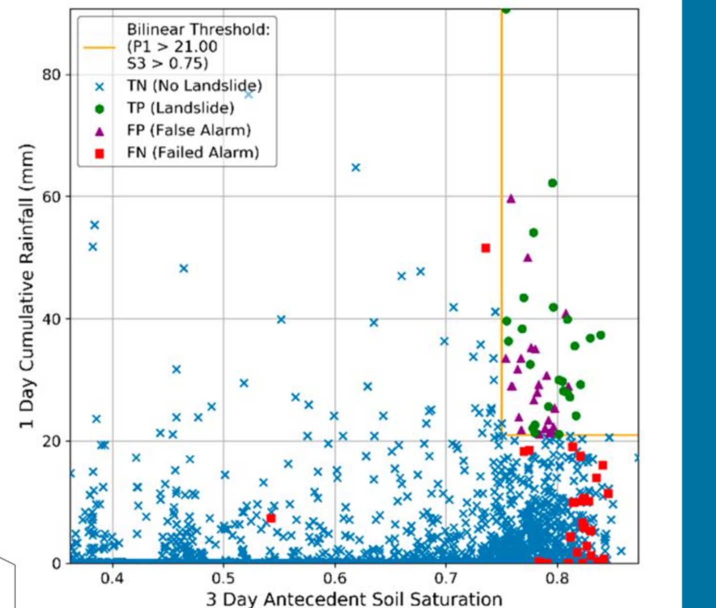

(a)

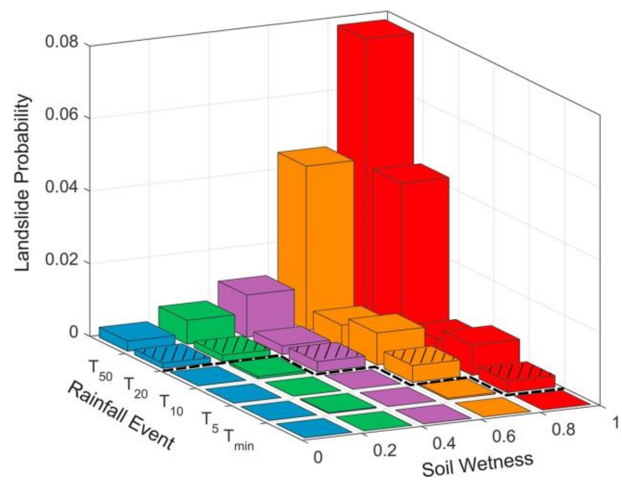

Università
degli Studi
della Campania
Luigi Vanvitelli

BACK!

Mirus et al., Water 2018
Zhao et al., J Hydrol 2019

Soil-atmosphere interaction

Soil water is transferred to atmosphere by direct evaporation and by plants through transpiration (evapotranspiration).

Solar radiation is the source of energy for evapotranspiration.

It is mostly SW (wavelength between 0.3 and 3.0 μm).

Earth surface also radiates as LW (w.l. up to 100 μm).

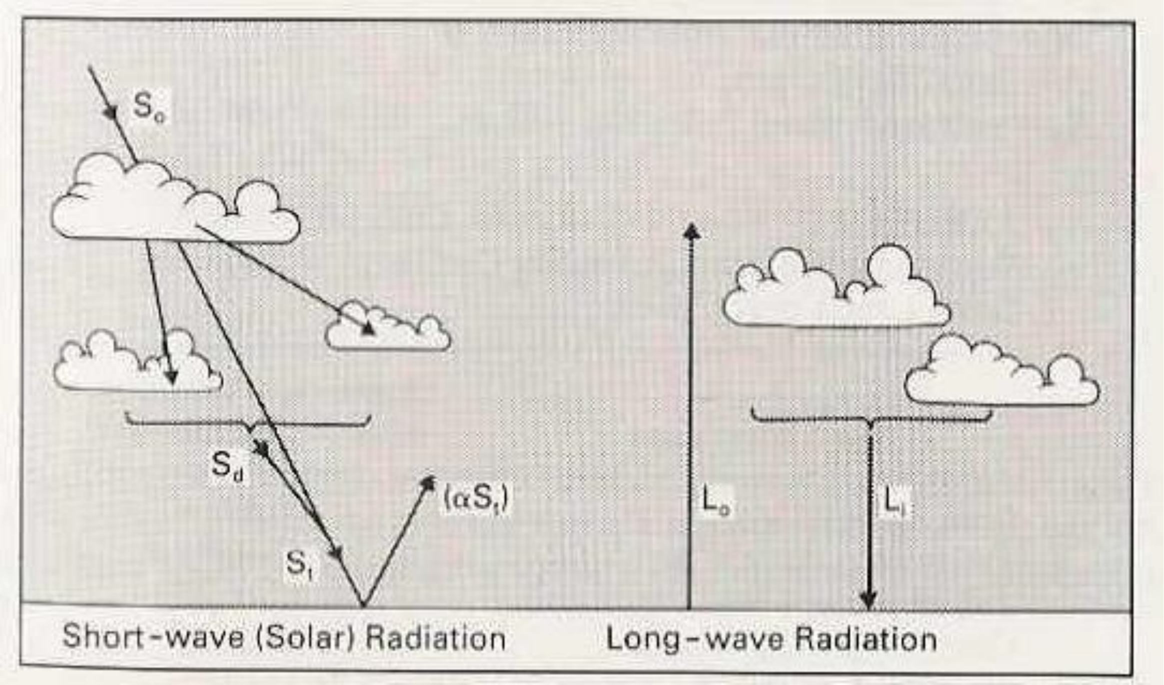

Soil-atmosphere interaction

Net short wave radiation at ground (the coefficient α, called **albedo**, depends on the characteristics of the reflecting surface):

$$S_n = S_t(1-\alpha)$$

Incoming short-wave solar radiation

$$S_t = S_0\left(a_s + b_s\frac{n}{24}\right)$$

Extraterrestrial SW solar radiation

$$S_0 \cong 240\,W/m^2$$

n is the daily number of hours with clear sky

$a_s = 0.25$ $b_s = 0.50$

Land cover class	Short-wave radiation reflection coefficient α
Open water	0.08
Tall forest	0.11–0.16
Tall farm crops (e.g., sugarcane)	0.15–0.20
Cereal crops (e.g., wheat)	0.20–0.26
Short farm crops (e.g., sugar beet)	0.20–0.26
Grass and pasture	0.20–0.26
Bare soil	0.10 (wet)–0.35 (dry)
Snow and ice	0.20 (old)–0.80 (new)

Note: Albedo can vary widely with time of day, season, latitude, and cloud cover.

In the absence of knowledge on crop cover the value $\alpha = 0.23$ is recommended.

Soil-atmosphere interaction

Net long wave radiation at ground (difference between greenhouse effect and earth's emission:

$$L_n = L_i - L_0 = -f\,\varepsilon'\sigma(T_a + 273.2)^4$$

f cloud cover factor

$$f = a_c \frac{\left(a_s + b_s \frac{n}{24}\right)}{(a_s + b_s)} + b_c$$

arid climate:

$a_c = 1.35 \quad b_c = -0.35$

humid climate:

$a_c = 1.00 \quad b_c = 0.00$

σ is the Stefan-Boltzmann constant (4.903×10^{-9} MJm^{-2}d^{-1})

ε' net earth-atmosphere emissivity

$$\varepsilon' = a_e + b_e\sqrt{p_v}$$

$$0.34 \le a_e \le 0.44$$
$$-0.25 \le b_e \le -0.14$$

Soil-atmosphere interaction

Energy balance at ground:

$$S_n + L_n - G - S - P - A_d = \lambda E + H$$

G (conductive exchange with soil) can reach 1% of $S_n + L_n$ only on daily basis, otherwise negligible.

Energy for biochemical processes:

$$P \cong 0.02(S_n + L_n)$$

Energy temporarily stored in the control volume:

$$S \cong 0$$

Energy subtracted by wind: $A_d \cong 0$

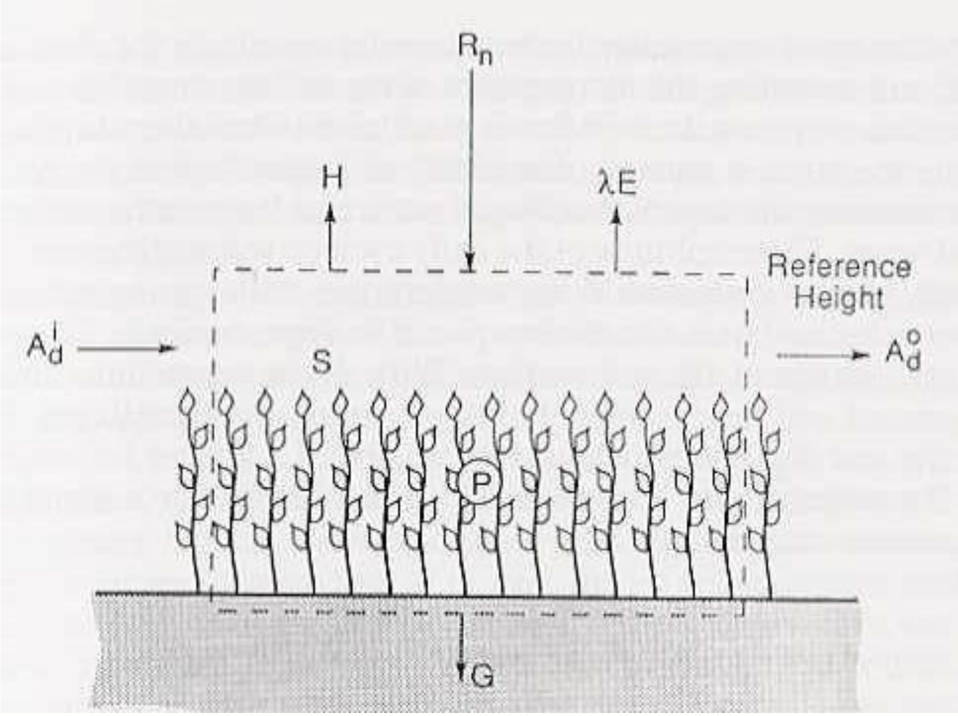

Soil-atmosphere interaction

Energy absorbed by evapotranspiration:

$$\lambda E \cong \kappa(S_n + L_n) - H \qquad (0.96 \le \kappa \le 0.98)$$

Sensible heat flux (energy absorbed to heat the atmosphere)

The partitioning of the available energy between evapotranspiration and sensible heat flux is modelled with a **network of resistances**

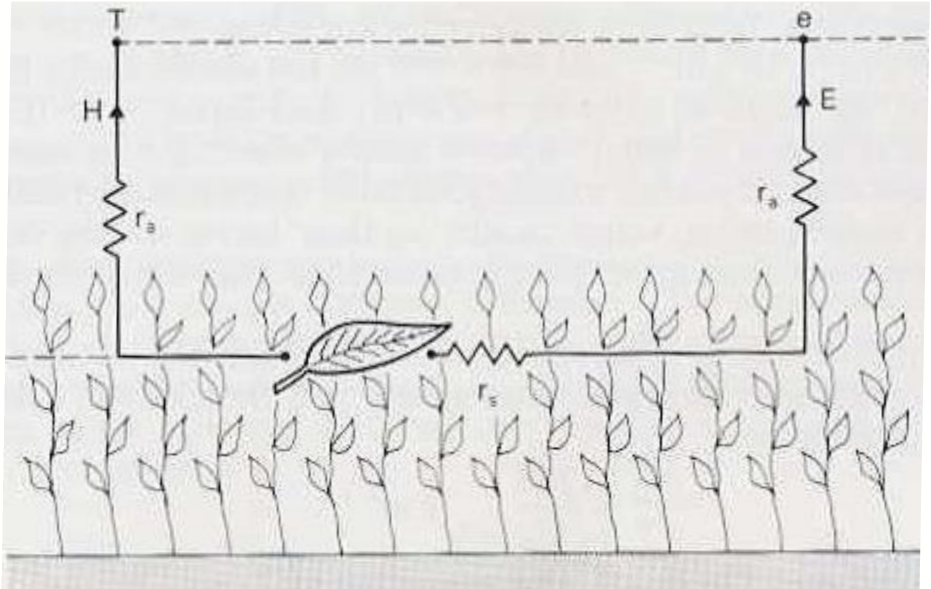

Soil-atmosphere interaction

λE and H are proportional to the vertical gradients of air **relative humidity** and air **temperature**, respectively, according to the values of aerodynamic resistance and stomatal resistance.

The first one controls the upward turbulent diffusion of vapour.

The second is mainly represented by the resistance of leaf stomata to vapour molecular diffusion.

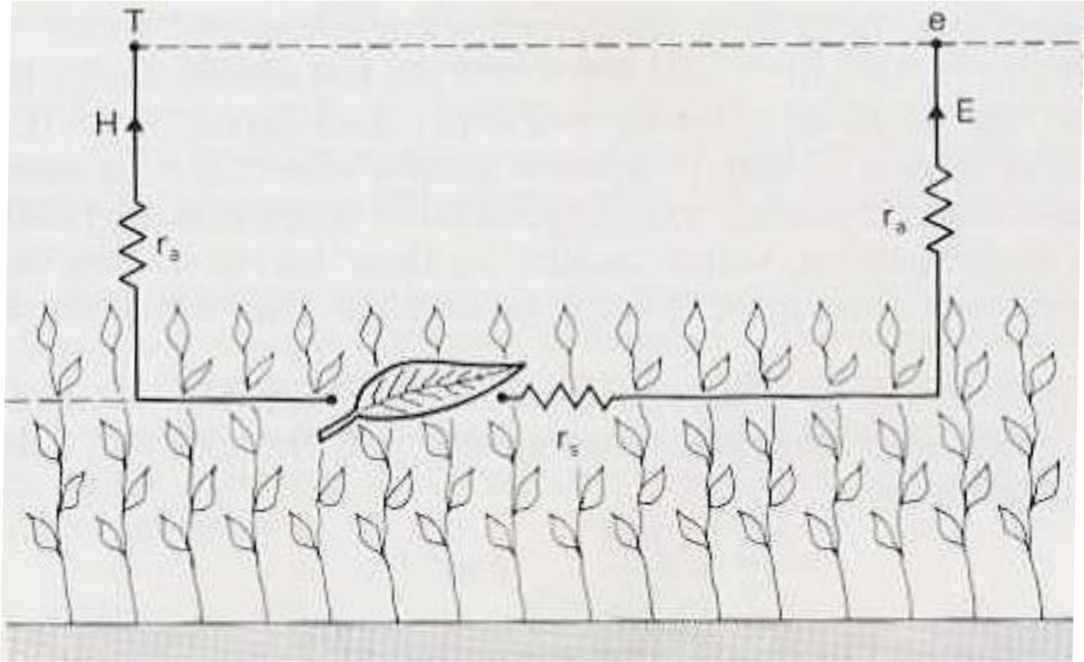

Soil-atmosphere interaction

λE and H are proportional to the vertical gradients of air **relative humidity** and air **temperature**, respectively, according to the values of **aerodynamic resistance** and **stomatal resistance**.

Aerodynamic resistance:

$$r_a = \frac{\ln\left[\frac{(z_u - 0.67\,h_c)}{0.123\,h_c}\right]^2}{0.41^2\,U_z}$$

U_z is wind speed at z_u elevation.

h_c is mean vegetation height.

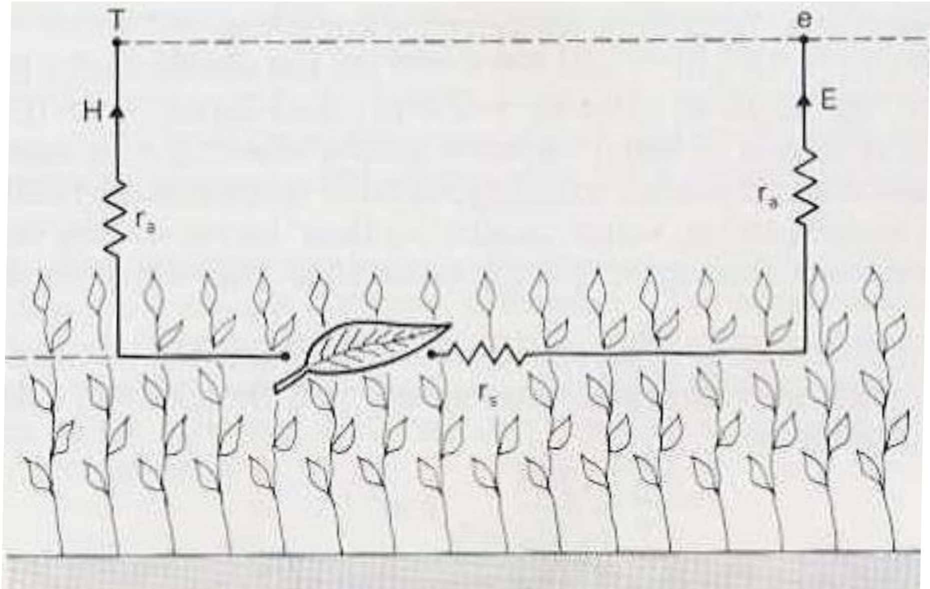

Soil-atmosphere interaction

λE and H are proportional to the vertical gradients of air **relative humidity** and air **temperature**, respectively, according to the values of **aerodynamic resistance** and **stomatal resistance**.

Stomatal resistance:

$$r_s = \frac{200}{L} \quad \mathrm{s\,m^{-1}}$$

L is the **leaf area index**:, which depends on the kind of vegetation.

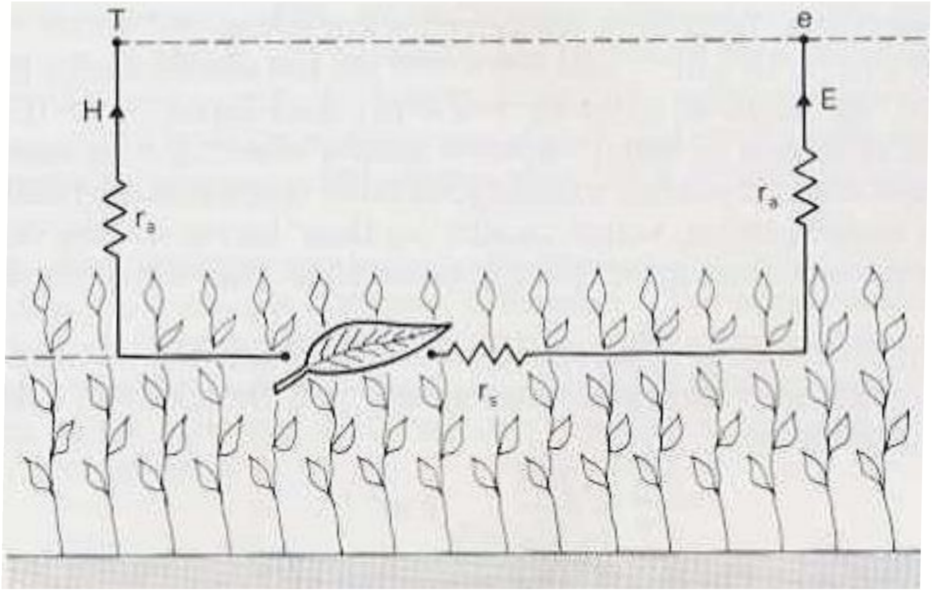

Soil-atmosphere interaction

The application of the model of the network of resistances to the energy balance equation leads to the **Penman-Monteith equation** for the evaluation of the evapotranspiration:

$$\lambda E = \frac{\Delta(S_n + L_n) + \rho_a c_p \dfrac{p_s(1 - RH)}{r_a}}{\Delta + \gamma\left(1 + \dfrac{r_s}{r_a}\right)}$$

Δ, λ , ρ_a , c_p , p_s and γ are known parameters of moist air, either constant or depending on its temperature and pressure.

The applicationof PM equation requires the knowledge of many meteorological variables, hence other simplified empirical expressions have been also proposed in the literature.

Soil-atmosphere interaction

The Penman-Monteith equation, applied introducing the meteorological variables at a site and the parameters representative of the local vegetation, provides an estimate of the potential evapotranspiration (E_0).

To obtain the actual evapotranspiration (E), the actual avaliability of water in soil has to be introduced. This is often made by introducing a **stress factor**:

$$E = k_s E_0$$

The stress factor expresses to what extent the plant roots are capable of extracting water from soil according to its moisture.

Soil-atmosphere interaction

Root water uptake is introduced in the Richards' equation of unsaturated soil.

$$\frac{\partial \theta}{\partial t} = \vec{\nabla} \cdot \left[k(\psi) \vec{\nabla}(z + \psi) \right] - a_r \qquad a_r(z) = \lambda(\psi) d_r(z) E_0$$

The **root distribution** with depth $d_r(z)$ and a **stress function** $\lambda(\psi)$ allow calculating $a_r(z)$.

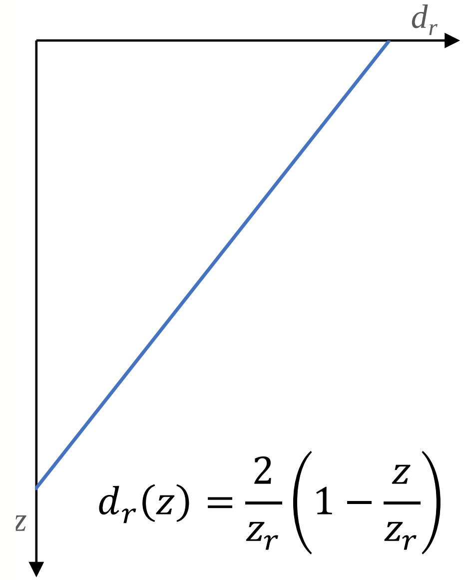

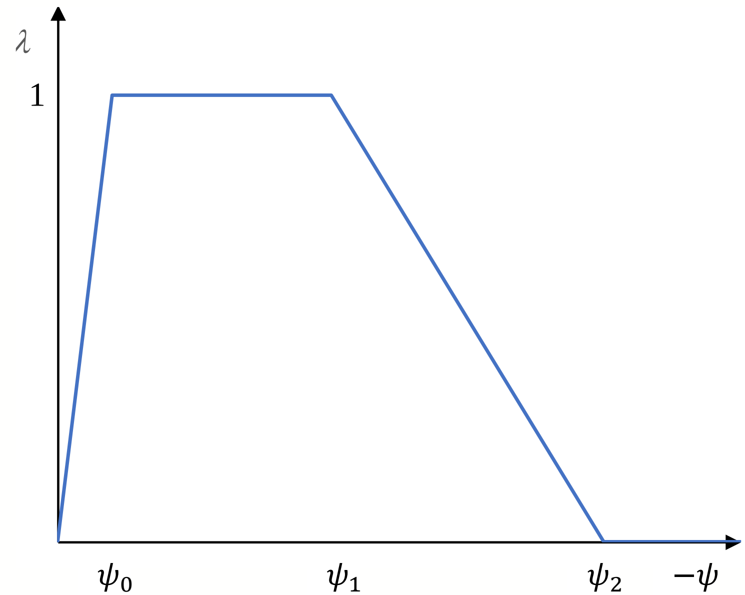

Soil-atmosphere interaction

Evaluating the evapotranspiration with the Penman-Monteith equation requires detailed information about soil, vegetation and climate forcing, rarely available and only for site specific studies.

Empirical expressions allow reliable estimates of potential evapotranspiration based only on meteorological data.

$$E_0 = 16\left(\frac{10\overline{T}_i}{I}\right)^{\alpha} \qquad I = \sum_{i=1}^{12}\left(\frac{\overline{T}_i}{5}\right)^{1.514}$$

$$\alpha = (6.75 \times 10^{-7})I^3 - (7.71 \times 10^{-5})I^2 + (1.79 \times 10^{-2})I + 0.49$$

Thornthwaite formula, based on mean monthly temperatures, gves the monthly potential evapotranspiration in mm.

Soil-atmosphere interaction

Empirical expressions allow reliable estimates of potential evapotranspiration based only on meteorological data.

$$E_0 = 0.0023(T_{mean} + 17.8)(T_{max} - T_{min})^{0.5} R_\alpha$$

$$R_\alpha = \frac{24 \times 60}{\pi} R_n [w_s \sin\varphi \sin\delta + \cos\varphi \sin\delta \sin w_s]$$

Hargreaves formula, based on monthly temperatures, local latitude and solar declination and angle at sunset, gives the daily potential evapotranspiration in mm.

Feddes et al., J Hydrol 1976

Soil-atmosphere interaction

When potential evapotranspiration (E_0) is estimated with empirical formulas based only on local temperature and radiation data, to calculate the actual evapotranspiration (E), beside the stress factor, also a **crop factor** must be introduced:

$$E = k_s k_c E_0$$

The crop factor depends on the kind of vegetation, the amount of canopy and leaves, and can be as small as 0 (dormant vegetation, i.e. deciduous trees in winter).

Deep percolation and groundwater recharge

Various mechanisms of groundwater recharge exsist.

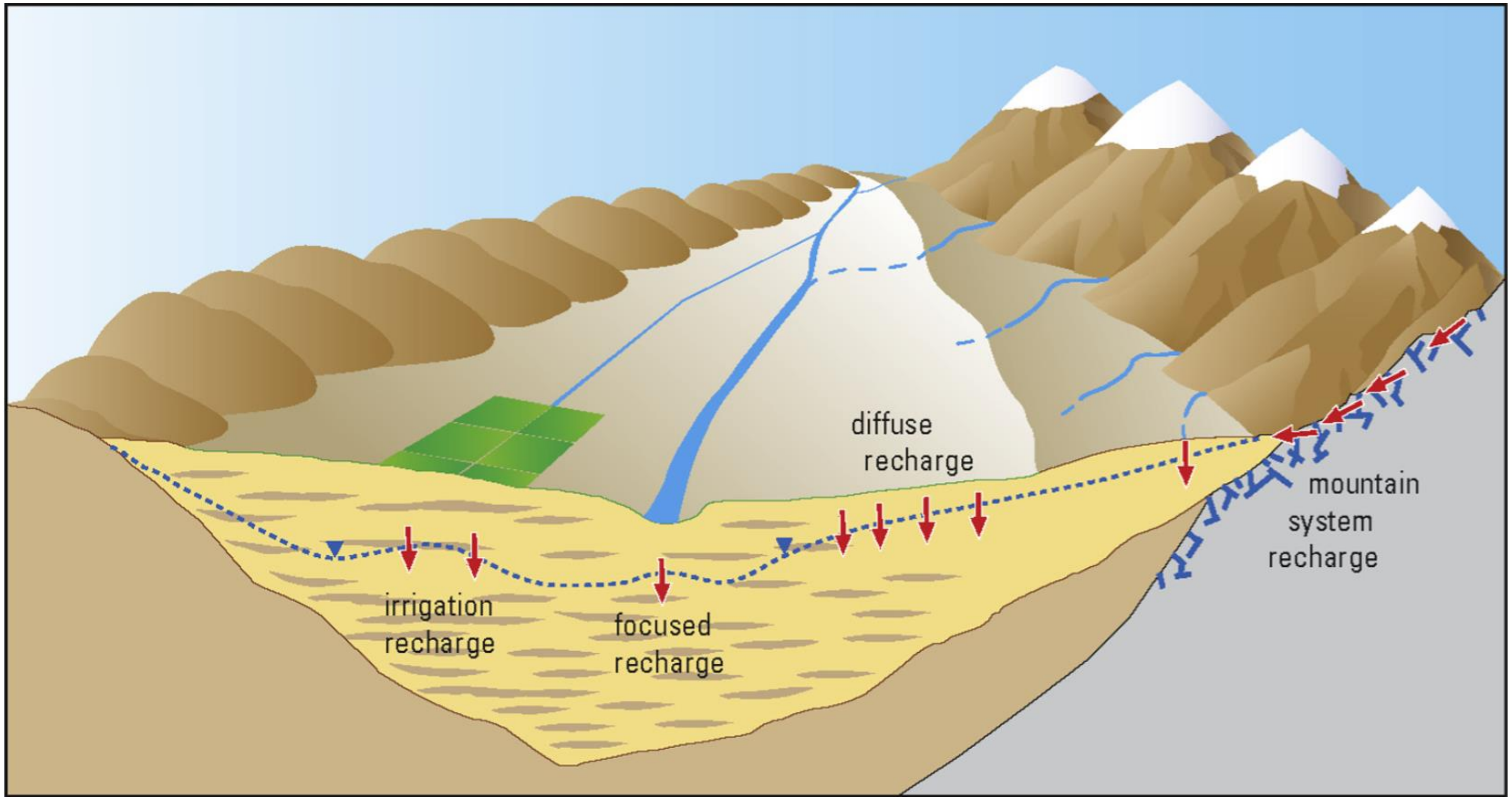

Meixner et al., J Hydrol 2016

Deep percolation and groundwater recharge

Along hillslopes, it occurs through the fractured bedrock.

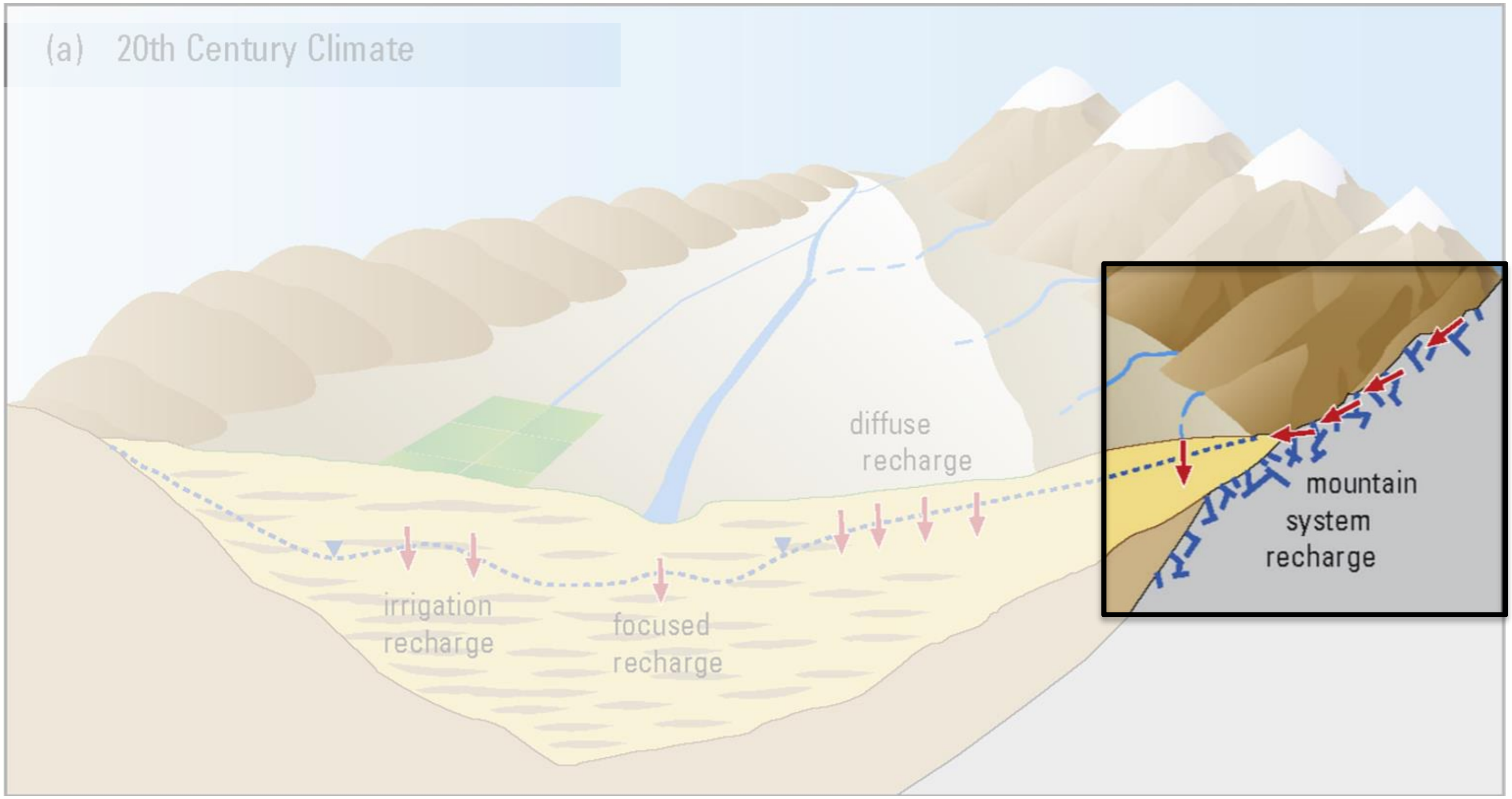

Meixner et al., J Hydrol 2016

Deep percolation and groundwater recharge

Along hillslopes, it occurs through the fractured bedrock.

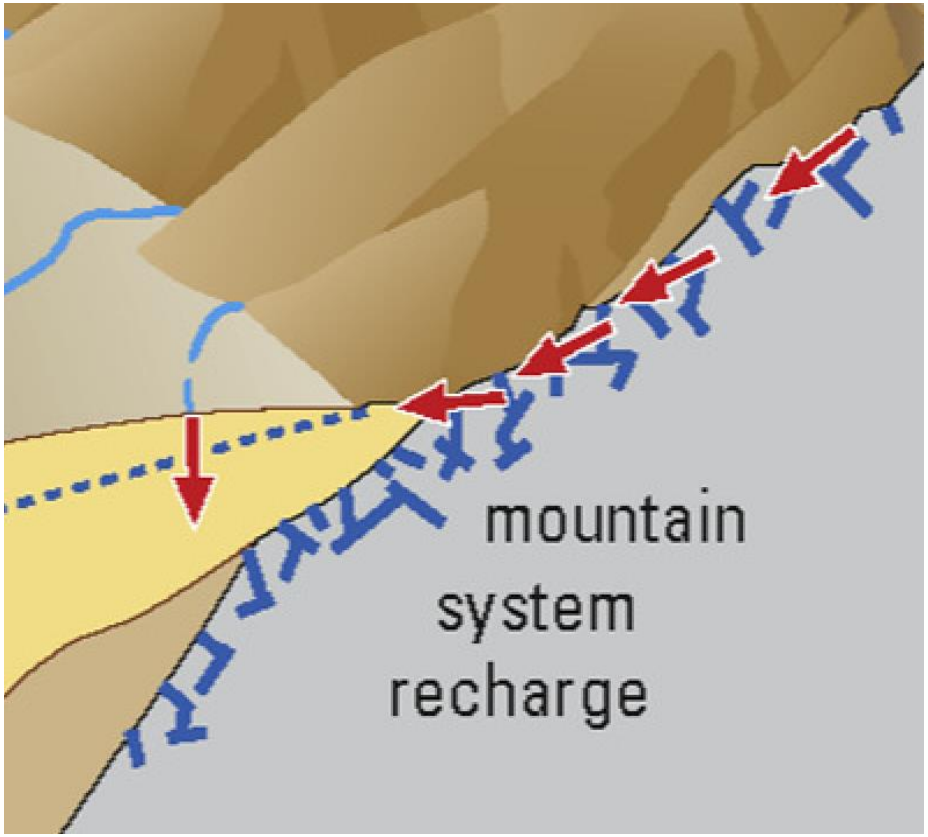

Meixner et al., J Hydrol 2016

Deep percolation and groundwater recharge

Recharge mechanisms can be quite complex.

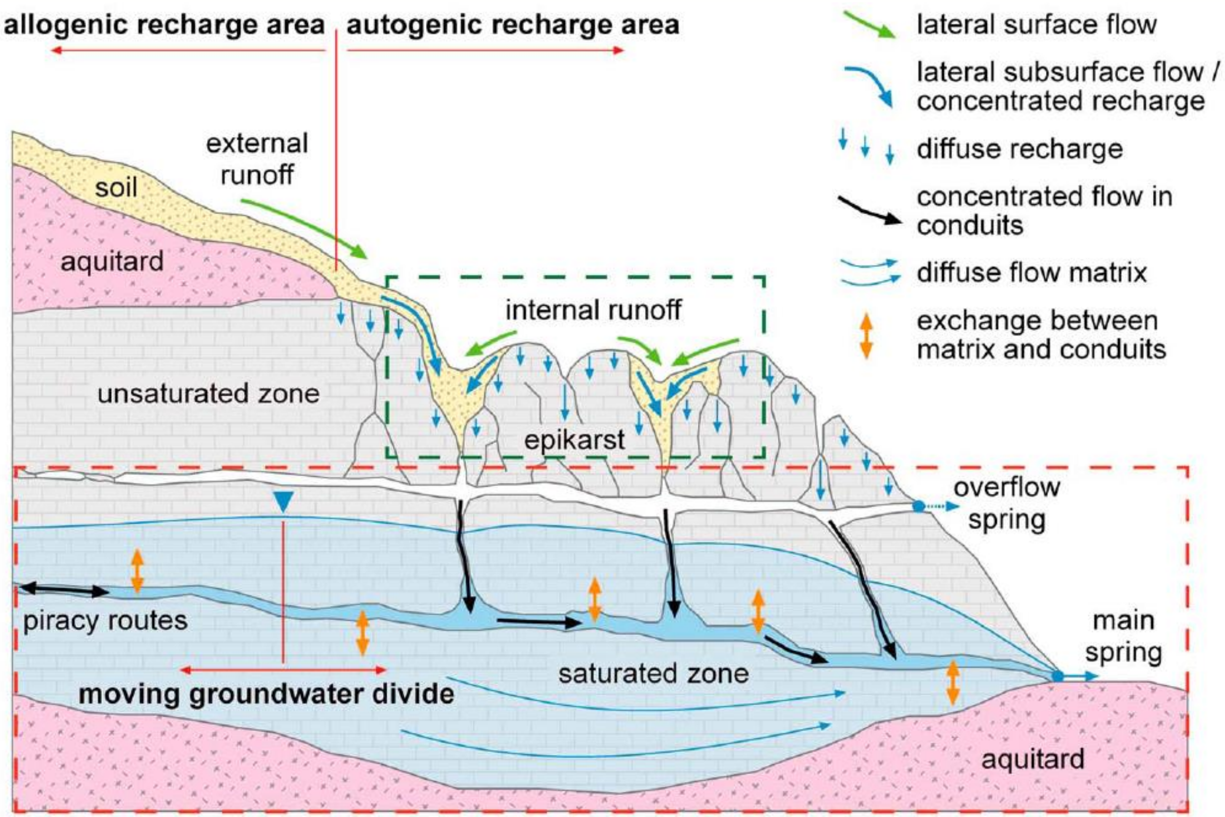

Hartmann et al., Rev Geophys 2014

Deep percolation and groundwater recharge

For the deep percolation to take place, the soil must be wetter than the field capacity.

It is the moisture held in the soil after excess water has drained downward, usually **2–3 days after rain in pervious soils.**

Conventionally defined as the soil water content at −33 kPa.

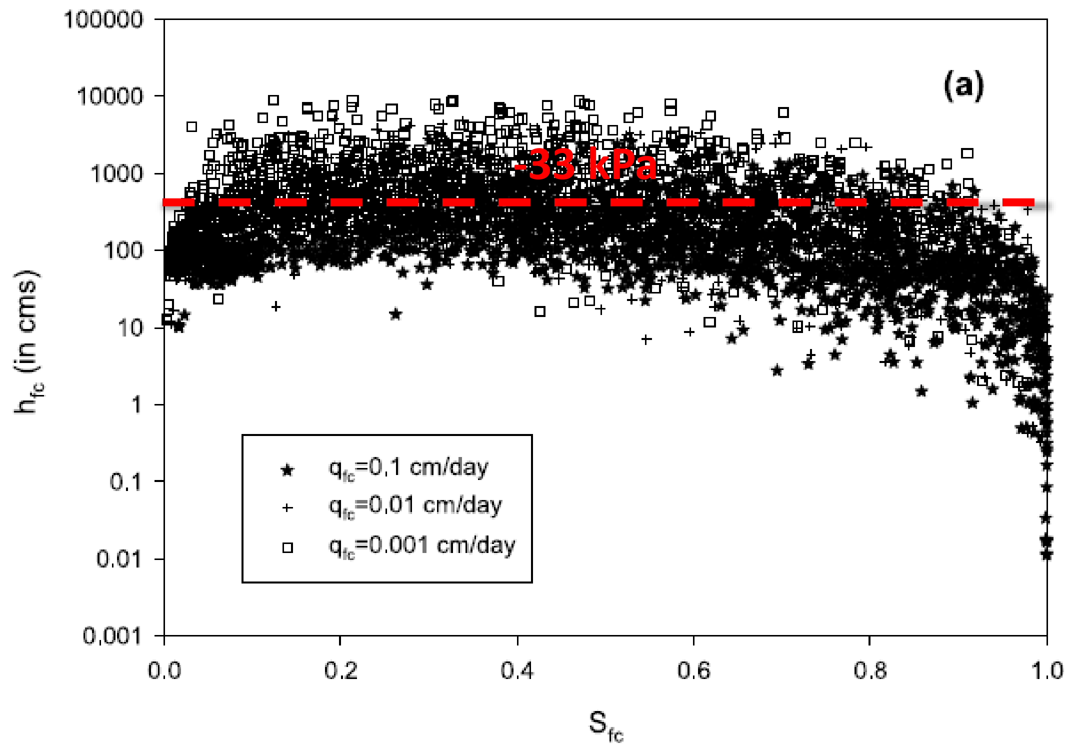

Twarakavi et al., Water Resour Res 2009

Deep percolation and groundwater recharge

Unambiguously quantifying the actual field capacity for a given soil is challenging.

A good estimate can be obtained based on the shape parameter *n* of van Genuchten's water retention curve and k_{sat} (in cm/d):

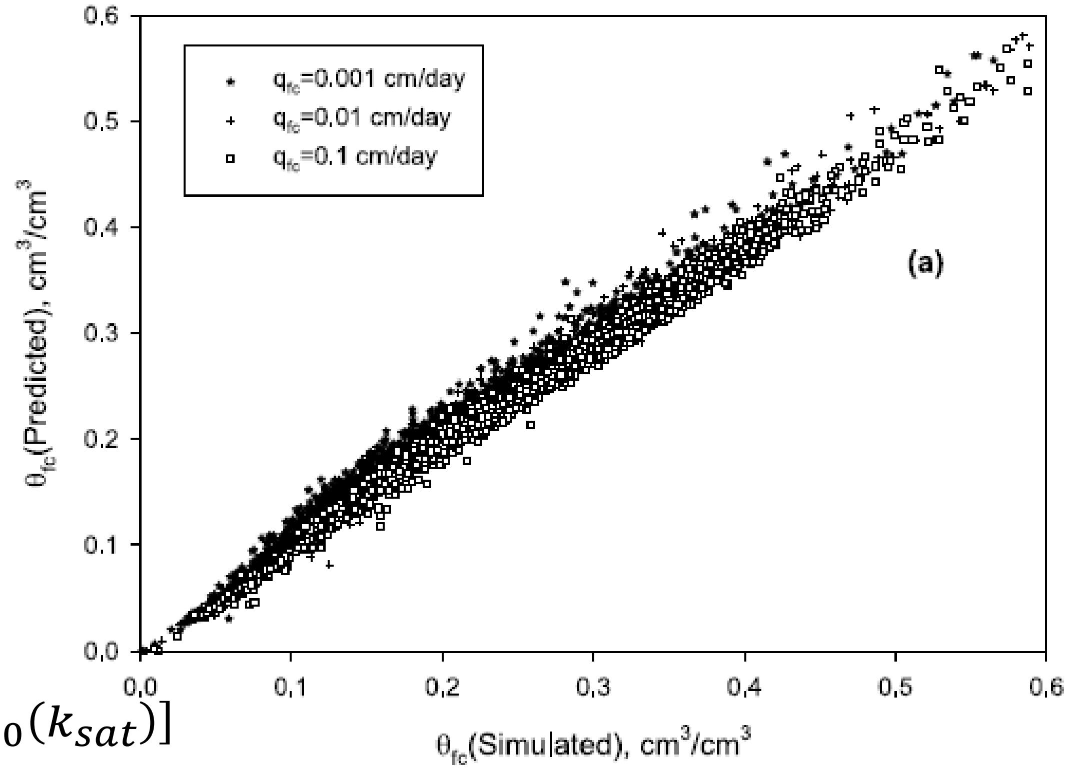

$$\frac{\theta_{fc}-\theta_{res}}{\theta_{sat}-\theta_{res}} = n^{-0.6[2+\log_{10}(k_{sat})]}$$

Twarakavi et al., Water Resour Res 2009